Western Washington University
Western CEDAR

WWU Graduate School Collection

WWU Graduate and Undergraduate Scholarship

Spring 2019

Synthesis of an Archazolid Based Enzyme Inhibitor

Cooper A. Vincent
Western Washington University, cvincent5@gmail.com

Follow this and additional works at: https://cedar.wwu.edu/wwuet

Part of the Chemistry Commons

Recommended Citation

Vincent, Cooper A., "Synthesis of an Archazolid Based Enzyme Inhibitor" (2019). *WWU Graduate School Collection*. 876.
https://cedar.wwu.edu/wwuet/876

This Masters Thesis is brought to you for free and open access by the WWU Graduate and Undergraduate Scholarship at Western CEDAR. It has been accepted for inclusion in WWU Graduate School Collection by an authorized administrator of Western CEDAR. For more information, please contact westerncedar@wwu.edu.

Synthesis of an Archazolid Based Enzyme Inhibitor

By

Cooper Vincent

Accepted in Partial Completion
Of the Requirements for the Degree
Master of Science

ADVISORY COMMITTEE

Chair, Dr. Gregory O'Neil

Dr. James Vyvyan

Dr. John Antos

GRADUATE SCHOOL

Kathleen L. Kitto, Acting Dean

Master's Thesis

In presenting this thesis in partial fulfillment of the requirements for a master's degree at Western Washington University, I grant to Western Washington University the non-exclusive royalty-free right to archive, reproduce, distribute, and display the thesis in any and all forms, including electronic format, via any digital library mechanisms maintained by WWU.

I represent and warrant this is my original work, and does not infringe or violate any rights of others. I warrant that I have obtained written permissions from the owner of any third party copyrighted material included in these files.

I acknowledge that I retain ownership rights to the copyright of this work, including but not limited to the right to use all or part of this work in future works, such as articles or books.

Library users are granted permission for individual, research and non-commercial reproduction of this work for educational purposes only. Any further digital posting of this document requires specific permission from the author.

Any copying or publication of this thesis for commercial purposes, or for financial gain, is not allowed without my written permission

Cooper Vincent

5/30/2019

Synthesis of an Archazolid Based Enzyme Inhibitor

A Thesis
Presented to
The Faculty of
Western Washington University

In Partial Completion
Of the Requirements for the Degree
Master of Science

By
Cooper A. Vincent
May 2019

Abstract

The archazolids are a family of natural products that display powerful growth inhibitory activity against a number of human cancer cell lines. This activity has been linked to inhibition of the vacuolar-type ATPase (V-ATPase) and more recently cyclooxygenase (COX) enzymes. Using the archazolid structure as a starting point, several simplified analogues have been prepared and assayed for their V-ATPase and COX inhibitory activity. These simplified analogues were prepared using a novel Suzuki coupling with yields over 80%. They were assayed to investigate both their V-ATPase and COX inhibitory activity. In our assays there was no COX inhibition, while there was measurable V-ATPase inhibition. The V-ATPase inhibition showed an important difference between the natural product triene (*ZZE*) and an isomer (*ZEE* triene) that were synthesized.

Acknowledgements

Research Advisor: Dr. Gregory W. O’Neil

Thesis Committee Members: Dr. James Vyvyan
Dr. John Antos

Project Contributors: Evan Long, Holly Jones, Dr. Jeff Young, Dr. P. Clint Spiegel

Research Group Members: Evan Long, Holly Jones, Michael Leitch, Diego Acevedo, Elliot Tan, Lauren Baker, Dylan Turner, Amanda Gale, Chris Meyers, Paul Spaltenstein

Instrument Technicians: Dr. Hla Win-Piazza
Sam Danforth

Financial Support: National Institutes of Health, Western Washington University Spring Graduate Enhancement Fund

Western Washington University Department of Chemistry

Table of Contents

I. **Abstract** iv
II. **Acknowledgements** v
III. **List of Schemes** vii
IV. **List of Tables and Figures** x
V. **List of Abbreviations** xii
1. **Introduction** 1
  1. Isolation and Structural Determination of the Archazolid Natural Products 1
  2. Biological Importance of the Archazolids: V-ATPase Inhibition 3
2. **Previous Syntheses of the Archazolids** 8
  1. Synthesis of Archazolid A 8
  2. Synthesis of Archazolid B 13
  3. Modular Synthesis of Archazolid A and B 18
  4. Highly Stereo- and regioselective approach to the C_9-C_{12} fragment of the archazolids 22
  5. Previous Syntheses by the O’Neil Group 23
3. **Synthetic Plan and Work towards Proposed COX-2 Inhibitor Fragment 1 (2-103)** 36
  1. Suzuki Coupling 36
  2. Synthetic Route Changes 46
  3. Boron-Wittig Chemistry 51
4. **Future Work** 70
5. **Experimental** 71
6. **Spectral Data** 89
7. **References** 108

List of Schemes

Scheme 2-1. Menche's retrosynthetic approach to archazolid A. 8

Scheme 2-2. Synthesis of fragment **2-2**. 9

Scheme 2-3. Synthesis of fragment **2-3**. 10

Scheme 2-4. Synthesis of fragment **2-4**. 11

Scheme 2-5. Completion of the archazolid A (**2-1**) synthesis. 12

Scheme 2-6. Trauner's retrosynthetic approach to archazolid B (**2-27**). 13

Scheme 2-7. Synthesis of fragment **2-29**. 14

Scheme 2-8. Synthesis of fragment **2-28**. 15

Scheme 2-9. Trauner's synthesis of fragment **2-4**. 16

Scheme 2-10. Synthesis of fragment **2-44**. 16

Scheme 2-11. Synthesis of fragment **2-45**. 17

Scheme 2-12. Completion of the archazolid B (**2-27**) synthesis. 17

Scheme 2-13. Menche's modular retrosynthesis of archazolid A (**2-1**) and B (**2-27**). 18

Scheme 2-14. Revised strategy for synthesis of **2-21**. 19

Scheme 2-15. Revised strategy for the synthesis of fragment **2-2**. 19

Scheme 2-16. Completion of the synthesis of archazolid B (**2-27**). 21

Scheme 2-17. Negishi and Huang's synthesis of the C_9-C_{12} triene fragment of the archazolids. 23

Scheme 2-18. O'Neil group's planned retrosynthesis of dihydroarchazolid B. 24

Scheme 2-19. Completion of the eastern fragment, EZZE-triene **2-60**. 25

Scheme 2-20. Completion of the western fragment **2-61**. 26

Scheme 2-21. Thiazole fragment coupling to the western fragment **2-61**. 27

Scheme 2-22. Esterification of the eastern and western fragments **2-60** and **2-83**. 27

Scheme 2-23. Attempted coupling of the triene through RCM. 28

Scheme 2-24. Synthesis of the cis-homodimer **2-85**. 29

Scheme 2-25. Coupling of the cis-homodimer **2-85** with the eastern fragment **2-60**. 29

Scheme 2-26. Synthesis of the revised organostannane western fragment **2-96**. 30

Scheme 2-27. Synthesis of the revised eastern fragment **2-92**. 31

Scheme 2-28. Synthesis of revised coupling partners 2-96 and 2-97 as well as Stille coupling to synthesize 2-98. 31

Scheme 3-1. Two examples illustrating different boron groups used for Suzuki coupling. 40

Scheme 3-2. Three examples of different palladium sources used in Suzuki couplings. 42

Scheme 3-3. Three examples of different bases used in Suzuki couplings. 43

Scheme 3-4. An example of microwave assisted Suzuki coupling improving yields as well as shortening the time of reaction. 44

Scheme 3-5. An example of greener Suzuki couplings occurring within water. 45

Scheme 3-6. Examples of sp^3-sp^2 hybridized carbon Suzuki reactions. 45

Scheme 3-7. Suzuki coupling within the synthesis of the complex polyene polyketide etnangien by Menche et al. 46

Scheme 3-8. The updated eastern fragment **3-4** for Suzuki Coupling. 47

Scheme 3-9. The difficult to purify phosphonates and their corresponding olefination products. 47

Scheme 3-10. Shortened eastern fragment synthesis through the use of phosphonate **3-13**. 48

Scheme 3-11. Formation of diene **3-15** through the E2 mechanism. 49

Scheme 3-12. Proposed pathway to synthesize vinyl iodide **3-18** from lactone **3-14**. 51

Scheme 3-13. Proposed pathway from lactol **3-16** to vinyl boronate **3-19** through a boron-wittig reaction. 51

Scheme 3-14. General reaction boron-Wittig reaction scheme proposed by Endo et al. 52

Scheme 3-15. Stereospecific synthesis of trisubstituted vinyl boronates proposed by Morken et al. 54

Scheme 3-16. Variety of substrates shown by Morken at al. demonstrating substrate selectivity based on boronic ester. 55

Scheme 3-17. Synthesis of ethyl bis(boronate)s **3-27** and **3-28**. 56

Scheme 3-18. Boron-Wittig reaction forming the undesired E isomer with the lactol. 59

Scheme 3-19. Boron-Wittig reaction forming the undesired E isomer with the aldehyde. 60

Scheme 3-20. Fischer projections displaying the steric clash of the Boron-Wittig reaction for the formation of both the Z and E isomers. 61

Scheme 3-21. Proposed retrosynthesis of Reker et al.'s fragment 1. 62

Scheme 3-22. Synthesis of vinyl iodide **3-31**. 63

Scheme 3-23. Initial Suzuki coupling reaction. 65

Scheme 3-24. Updated and final Suzuki coupling reaction. 66

Scheme 3-25. The deprotection of **3-39** and **3-40** to **3-41** and **3-42** respectively. 67

Scheme 4-1. The proposed synthesis of the carboxylic acid derivative from our starting compound **3-40**. 69

List of Tables and Figures

Table 1-1. IC50 values for the archazolid natural products against murine cell line L-929. 3

Table 3-1. The variable conditions of natural product synthesis utilizing Suzuki couplings, as detailed in by Koshvandi et al. 39

Table 3-2. An example of the wide variety of boron groups as well as benefits and attributes. 41

Table 3-3. Optimization of intramolecular HWE reaction of **3-8** to produce lactone **3-14**. 50

Table 3-4. Variety of 1,1-diboronates and their yields, and selectivity. 52

Table 3-5. Variety of ketones and their corresponding yields and selectivity. 53

Table 3-6. Resolution data for alcohol **3-35.**

Figure 1-1. Archazolid family of natural products. 2

Figure 1-2. The V-ATPase. 4

Figure 1-3. Plecomacrolide natural products bafilomycin and cocanamycin. 5

Figure 1-4. Binding sites of the archazolids (blue stars) and the plecomacrolides (red stars) on the V-ATPase c subunits. 6

Figure 2-1. Positions C_7-C_8 and C_{16}-C_{17} were prone to elimination under mild reaction conditions. 20

Figure 2-2. Comparison between archazolid B and archazolid F as a basis for the simplified archazolid, dihydroarchazolid B. 24

Figure 2-3. The compounds that were used in an Arabidopsis-based V-ATPase assay. 32

Figure 2-4. Demonstration of pharmacophore effects in **2-102**. 33

Figure 2-5. *Arabidopsis*-based V-ATPase inhibition of compound **2-102** and cocanamycin A 34

Figure 2-6. Reker et Al. predicted potent COX-2 inhibitor fragment 1. 34

Figure 2-7. Structural overlay of arachidonic acid and archazolid A. 35

Figure 3-1. General Suzuki coupling mechanism. 36

Figure 3-2. Documents containing reports of Suzuki couplings versus the year. 37

Figure 3-3. Two figures showing the asymptotic increase of Suzuki coupling reactions published as the reaction was discovered and utilized. 38

Figure 3-4. Demonstration of NOE spatial relationship between proton and methyl group on the (E)-alkene. 57

Figure 3-5. Demonstration of no NOE spatial relationship between proton and methyl group on the (Z)-alkene. 58

Figure 3-6. Comparison of structures for the COX assay, our synthesized compound, Reker's proposed COX-inhibitor, and the native COX substrate, arachidonic acid. 68

Figure 3-7. *Arabidopsis*-based V-ATPase assay data showing the inhibited growth of the *Arabidopsis* seeds due to V-ATPase inhibition. 69

List of Abbreviations

Ac	Acyl
Aq.	Aqueous
Boc	Di-tert-butyl-carboxylate
BOP	(Benzotriazol-1-yloxy)tris(dimethylamino)phosphonium hexafluorophosphate
Bu	Butyl
Bz	Benzyl
CBS	Corey-Bakshi-Shibata
CDI	Carbonyl diimidazole
*c*Hex	Cyclohexane
CM	Cross metathesis
COSY	Correlation spectroscopy
Cp	Cyclopentyl
DBU	1,8-Diazabicyclo[5.4.0]undec-7-ene
DCM	Dichloromethane
DIBAl-H	Diisobutyl aluminum hydride
DMAP	4-dimethylaminopyridine
DMP	Dess-Martin periodinane
dr	Diastereomeric ratio
er	Entantiomeric ratio
Et	Ethyl
Et_2O	Diethyl ether
EtO	Ethoxy

EtOAc	Ethyl acetate
GH	Grubb’s Hoveyda
GI	Grubb’s first generation
GII	Grubb’s second generation
HMQC	Heteronuclear multiple-quantum correlation
HWE	Horner-Wadsworth-Emmons PMB
Hz	Hertz
IC_{50}	50% inhibitory concentration
*i*Pr	isopropyl
IR	infrared
KHMDS	Potassium hexamethyldisilazide
L-929	Murine leukemia cell line 929
LiHMD	Lithium hexamethyldisilazide
Me	Methyl
MeLi	Methyl lithium
MeMgBr	Methyl magnesium bromide
MHz	Megahertz
Mmol	Millimole
MTBE	Methyl-tert-butyl-ether
n-BuLi	*n*-Butyllithium
NEt3	Triethyl amine
NHC	N-heterocyclic carbine
NMR	Nuclear magnetic resonance

Ph	Phenyl
PhCH3	Toluene
ppm	parts per million
RCM	Ring closing metathesis
RRCM	Relay ring-opening metathesis
rt	Room temperature
SAR	Structure activity relationship
Sat.	Saturated
TBACl	Tetrabutylammonium chloride
TBDPS	tert-Butyldiphenylsilyl
TBS	tert-Butyldimethyl silyl
*t*BuOH	tert-Butyl alcohol
TES	Triethylsilyl
Tf	Triflate
THF	Tetrahydrofuran
TIPS	Triisopropylsilyl
TLC	Thin layer chromatography

Chapter 1. Introduction

1.1 Isolation and Structural Determination of the Archazolid Natural Products

Archazolids are a family of natural products comprised of six (A-F) chemically distinct yet structurally related members (Figure 1-1). The first of the archazolids were discovered in 1993 when Sasse et al. were testing for biologically active metabolites from myxobacteria in a screening assay with L929 mouse fibroblasts. Sasse et al. found a strain of *Archangium gephyra* whose extracts showed high cytotoxic activity (Table 1-1). Ultimately this activity was determined to arise from two structurally related compounds deemed to be archazolid A and B (Figure 1-1).[1] As the study of these natural products continued, the general structures of both archazolids A and B were determined by Höfle and Steinmetz in 2003 by the use of ^{1}H and ^{13}C NMR, COSY, NOE, and HMQC data. In confirmation of the spectral assignments, the analysis of a ^{13}C-labeled sample of archazolid A was procured by feeding a sample of ^{13}C-enriched acetate and methionine to *Archangium gephyra*.[2] In 2006 the absolute and relative stereochemistry of both archazolid A and B were determined by Menche et al. through the use of high field NMR studies along with molecular modeling and derivatization. It was determined that the unique structure of archazolid A and B possesses a 24-membered lactone ring with a thiazole side chain, seven alkenes (2*E*, 5*E*, 9*Z*, 11*Z*, 13*E*, 18*E*, 20*E*), as well as a complex sequence of eight methyl- and hydroxyl- bearing stereocenters.[3] This was followed by Menche et al. publishing the first total synthesis of archazolid A and Trauner et al. publishing the first total synthesis of archazolid B, both in 2007.[4,5] *A. gephyra* is the source for archazolid A, B, and F, while another myxobacterial strain, *Cystobacter violaceus,* produces the glycosylated archazolids C, D, and E.[6,7,8] Although archazolids are structurally complex, they are attractive synthetic targets due to their nanomolar inhibitory activity of vacuolar-type ATPases (V-ATPases) which are important therapeutic targets (*vide infra*), and low availability from the natural sources (roughly 200 mg from 350 L fermentation for archazolid A).

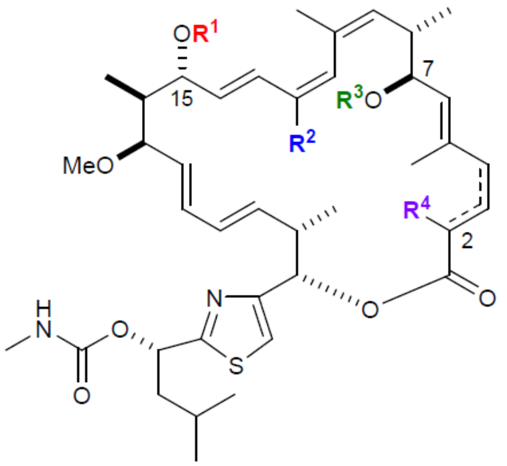

A (R^1 = H, R^2 = Me, R^3 = H, R^4 = Me), $\Delta^{2,3}$
B (R^1 = H, R^2 =Me, R^3 = H, R^4 = H), $\Delta^{2,3}$
C (R^1 = H, R^2 = Me, R^3 = ß-glucoside, R^4 = Me), $\Delta^{2,3}$
D (R^1 = H, R^2 = CH_2OH, R^3 = ß-glucoside, R^4 = Me), $\Delta^{2,3}$
E (R^1 = ß-glucoside,R^2 = Me, R^3 = H, R^4 = Me), $\Delta^{2,3}$
F (R^1 = H, R^2 =Me, R^3 = H, R^4 = H), $\Delta^{3,4}$

Figure 1-1. Archazolid family of natural products.

Table 1-1. IC_{50} values for the archazolid natural products against murine cell line L-929.

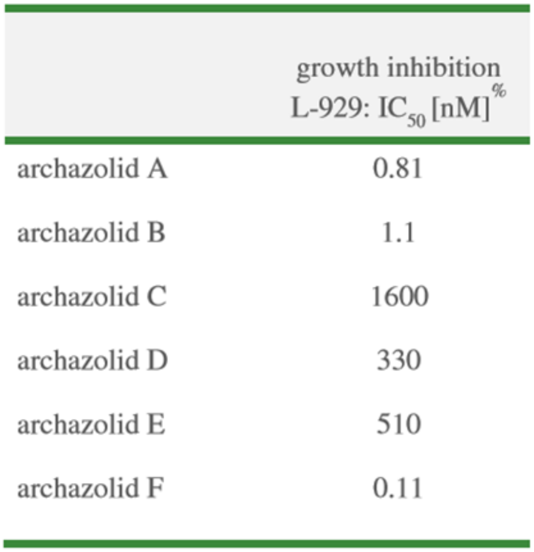

	growth inhibition L-929: IC_{50} [nM]$^{\%}$
archazolid A	0.81
archazolid B	1.1
archazolid C	1600
archazolid D	330
archazolid E	510
archazolid F	0.11

1.2 Biological Importance of the Archazolids: V-ATPase Inhibition

Vacuolar-type ATPases, or V-ATPases, are ATP-dependent proton pumps that control pH by shuttling protons in various endomembrane systems. They are commonly found in intracellular organelles as well as the plasma membrane. The V-ATPase is comprised of two domains that are made up of a total of 21 to 22 subunits. The V_1 and V_0 domains are responsible for ATP-hydrolysis to ADP and transporting protons, respectively. The V_1 domain resides in the cytoplasm and is made up of a total of 8 subunits, A-H (Figure 1-2). Within this domain, there are a total of 13 to 14 units with three A and B subunits, a single C, D, E, and F subunit, along with two G subunits and one to two H subunits. The V_0 domain is bound to the membrane and is comprised of subunits a, d, e and six c subunits labelled as 2c, 2c', 2c''. These six c subunits form a rotor like domain that binds protons and transports them from the cytoplasm to the endosomal lumen or the extracellular space.[9]

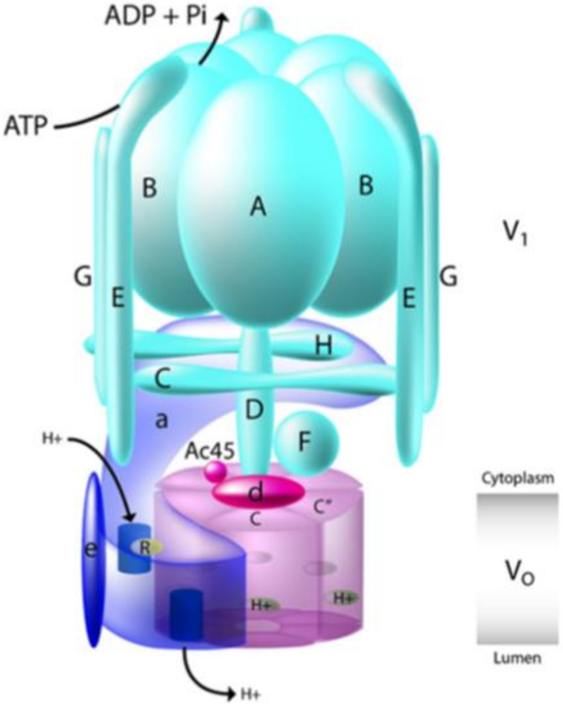

Figure 1-2. The V-ATPase.

Due to their ability to control the pH, V-ATPases are hypothesized to create an acidic pericellular microenvironment that promotes the activity of invasive proteases, such as Cathepsin B.[10] It has also been seen that a phenotype of invasive of cancer cells correlates to upregulated V-ATPase activity and expression.[11] This upregulated activity along with acidified microenvironment allow for survival and growth of cancer cells. The V-ATPase is therefore a promising molecular target for inhibition as a cancer therepeutic.[12]

Currently there are two well-known and studied inhibitors of V-ATPase, concanamycin and bafilomycin (Figure 1-3). These are both members of the plecomacrolide family of natural products. Plecomacrolides are a subset of the polyketides, where “pleco” describes their secondary structure, 1-fold, formed by the polyketide chain that is pendant to the macrolactone core.[13]

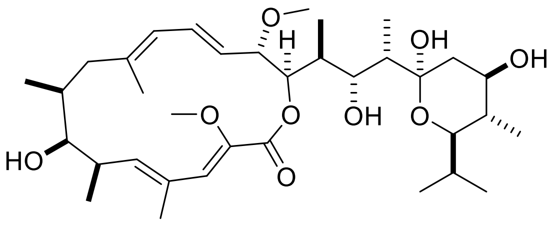

bafilomycin A_1

L-929 IC_{50} = 3.2 nM

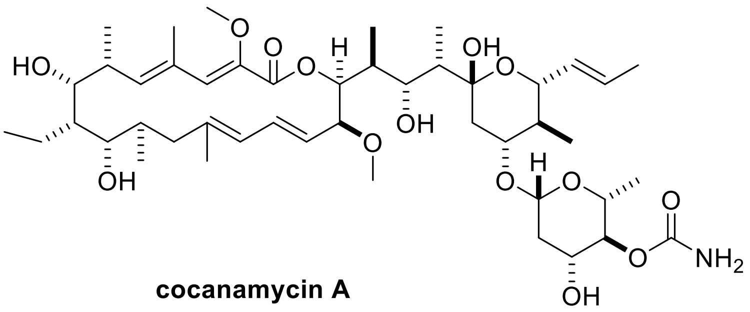

cocanamycin A

L-929 IC_{50} = 0.23 nM

Figure 1-3. Plecomacrolide natural products bafilomycin and cocanamycin.

While both concanamycin and bafilomycin are potent V-ATPase inhibitors with IC_{50} values in the nanomolar range, information from studies using these compounds on the signaling pathways affected by V-ATPase inhibition is limited.[14] This is due in part to concanamycin and bafilomycin also interacting with phosphorylation ATPases (P-ATPases) at concentrations in the micromolar range. Both archazolid A and B have been shown to be highly potent inhibitors of the V-ATPase, however they do not inhibit P-ATPases like bafilomycin and concanamycin. This difference is attributed to differences in the mechanism of action between the two classes of inhibitors. The plecomacrolides bind between two c subunits within the V_0 domain whereas the archazolids bind only within a single c subunit within the V_0 domain (Figure 1-4).[15]

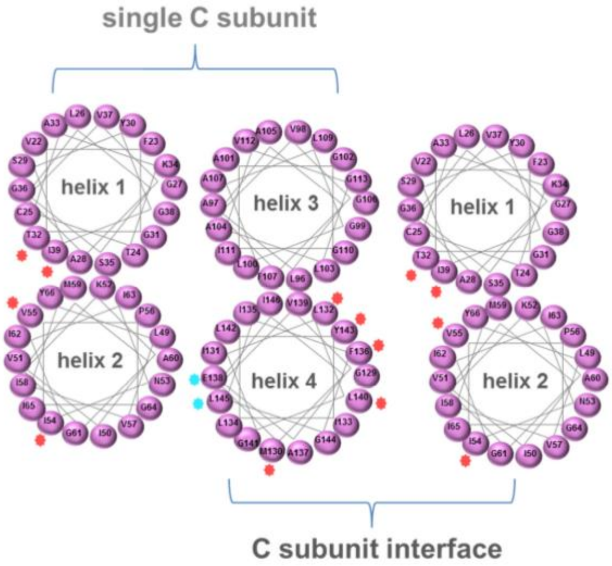

Figure 1-4. Binding sites of the archazolids (blue stars) and the plecomacrolides (red stars) on the V-ATPase c subunits.

V-ATPases have been increasingly studied as of late due to their upregulation in cancerous cells. In 2017, Merk et al. published a study on the relationship between V-ATPases and tumor initiating cells (TIC).[16] TICs as of late have shown increased resistance to chemotherapeutics that can account for tumor metastasis and reoccurrence. TICs limit most therapeutic success and cause relapses. TIC's ability for self-renewal and invasiveness have been correlated with the epithelial-mesenchymal transition (EMT).[16] EMT confers a mesenchymal stem-like phenotype to cells, which causes cancer cells to become highly malignant and invasive, giving them self-renewal capacity and elevated resistance to therapeutics. EMT causes a change in structural proteins that maintain the cytoskeleton and cell-cell adhesions, and potentially most importantly, the loss of E-cadherin.[16] E-cadherin is responsible for cell-cell contact and, when removed from the cell, this allows mesenchymal cells to be freed and become mobile within the body. Merk et al. discovered that V-ATPase inhibition disturbs the loss of E-cadherin by preventing its internalization and recycling. This then disrupts the process of EMT and makes the TICs less invasive, diminishing their ability for self-renewal as well as decreasing their resistance to therapeutics.[16]

Due to V-ATPases strong correlation with the robustness of cancer cells, especially the TICs, they make interesting inhibition targets for anti-cancer activity drugs. The archazolids represent a potential starting point for further investigation of V-ATPase inhibition and development of new cancer therapeutics. However, before a thorough investigation of this type can begin, there must be efficient access to this class of compounds.

Chapter 2. Previous Syntheses of the Archazolids

2.1 Synthesis of Archazolid A

In 2007, the first synthesis of archazolid A was published by Menche and Hassfield. Their synthesis was based on the combination and assembly of three pieces, which are detailed in the retrosynthetic plan shown in Scheme 2-1.[1]

Scheme 2-1. Menche's retrosynthetic approach to archazolid A.

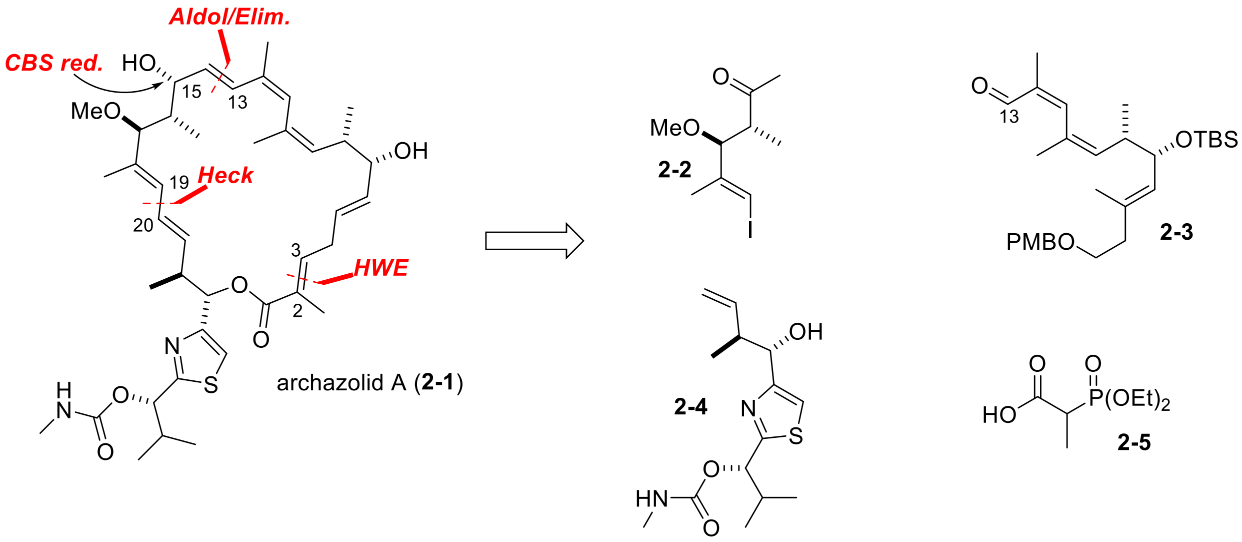
Aldol/Elim.
CBS red.
HO
15
13
MeO
OH
19
Heck
20
3
HWE
2
O
O
N
S
H
N
O
O
archazolid A (2-1)
O
MeO
2-2
I
O
13
OTBS
PMBO
2-3
OH
2-4
N
S
O
HN
O
O
O
HO
P(OEt)2
2-5

The *E*-alkene at C13-C14 was planned to result from an aldol condensation between **2-2** and **2-3**, while the C18-C21 *E*,*E*-diene would result from a Heck coupling between iodide **2-2** and alkene **2-4**. In order to complete the macrocyclic ring, a Horner-Wadsworth-Emmons (HWE) olefination would be employed. This synthesis is flexible in that either the HWE or an esterification can be used for ring closure.

Scheme 2-2. Synthesis of fragment **2-2**.

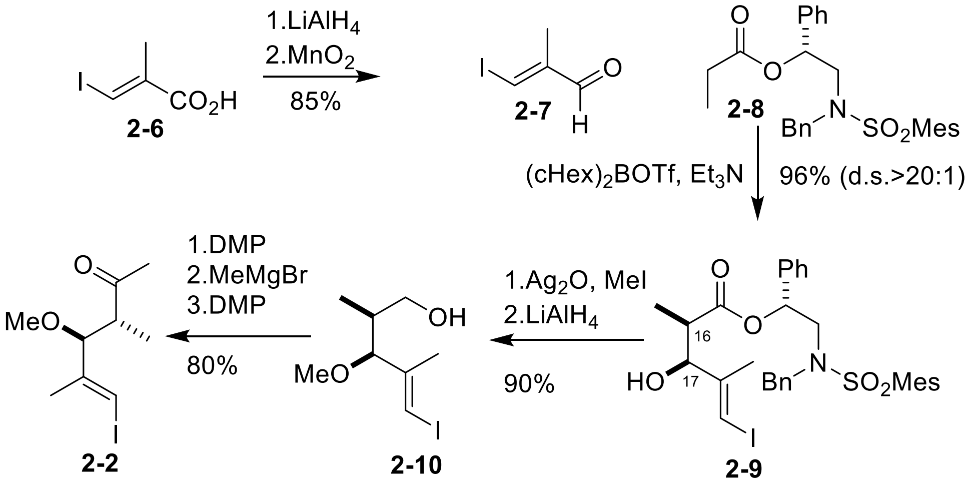

The synthesis of iodide **2-2** (Scheme 2-2) begins with the *E*-vinyliodide **2-6**, which was prepared by a known procedure.[2] The acid in **2-6** was reduced to an alcohol and then oxidized to an aldehyde producing **2-7** in 85% yield over the two steps.[2] Aldehyde **2-7** was then used in an anti-aldol coupling through the use of Masumune's chiral ephedrine-derived ethyl ketone **2-8**. This was done in order to install the methyl and methoxy stereocenters at C16 and C17, respectively, found in the natural product.[3] A 96% yield was obtained for this reaction with a diastereoselectivity of >20:1. The resulting product **2-9** was methylated using Ag_2O/MeI and the ephedrine auxiliary was reductively removed using $LiAlH_4$ to give alcohol **2-10**. Fragment **2-2** was then completed by oxidation of the hydroxyl using Dess-Martin periodinane (DMP), methyl Grignard (MeMgBr) addition, and then oxidation again by DMP to afford ketone **2-5** (Scheme 2-2).

As shown in Scheme 2-3, the synthesis of C3-C11 fragment **2-3** uses a boron-mediated Paterson aldol reaction of the lactate derived ethyl-ketone **2-11** and aldehyde **2-12**.[4] This aldol reaction resulted in the anti-aldol product **2-13** with high diastereoselectivity (>20:1) and yield (88%). The free hydroxyl was protected using TBS and aldehyde **2-14** was afforded in 85% yield through a sequence of reduction and periodate cleavage. Aldehyde **2-14** was then subjected to a Still-Gennari modified HWE olefination with phosphonate **2-15**.[5] Through the use of both KHMDS as the base and 18-crown-6, the *Z*-enone **2-16** was obtained in an 88% yield. After conversion to the aldehyde through a reduction (DIBAl-H) and oxidation (MnO_2), a Still-Gennari HWE was performed again to achieve the *Z*-enone **2-17** in 80% yield. Reduction with DIBAl-H and oxidation with DMP then gave the completed fragment **2-3** in 90% yield.

Scheme 2-3. Synthesis of fragment **2-3**.

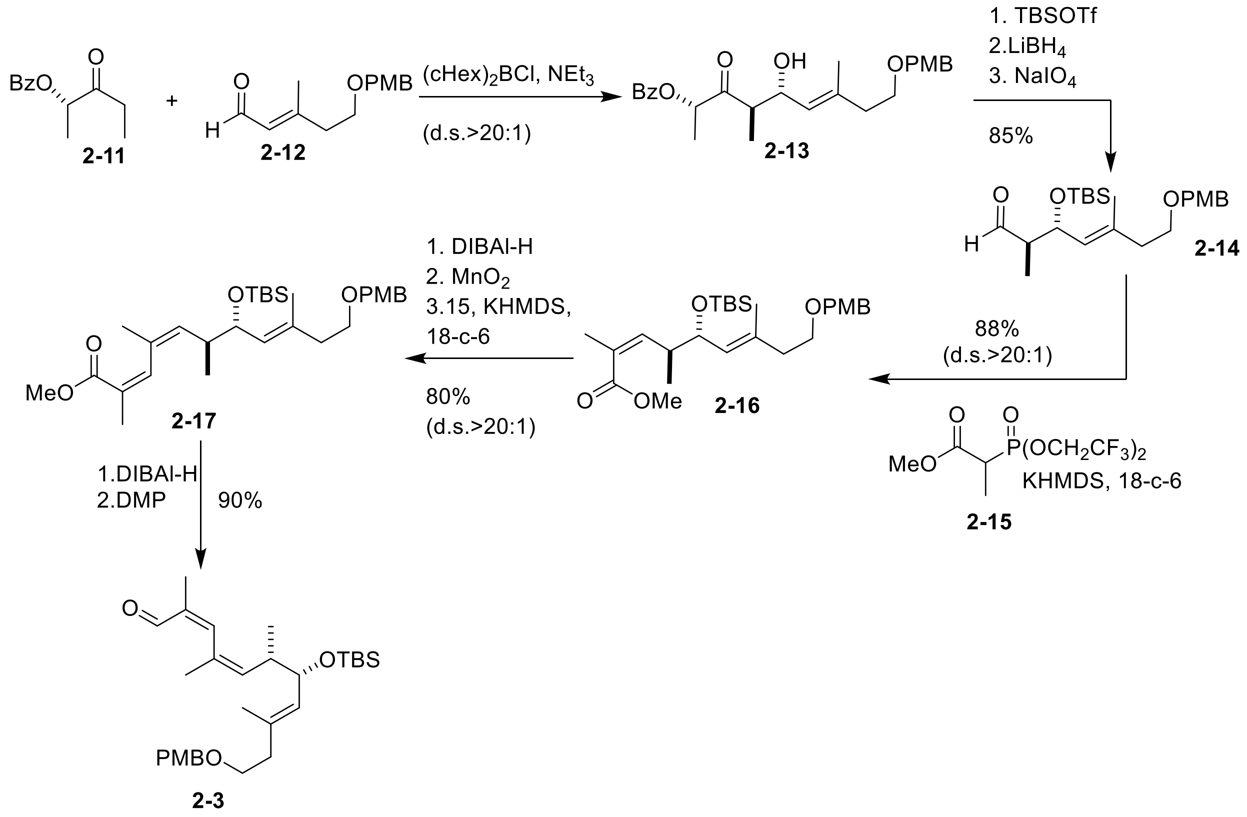
BzO
O
2-11
+
O
H
OPMB
2-12
(cHex)2BCl, NEt3
(d.s.>20:1)
BzO
O
OH
OPMB
2-13
1. TBSOTf
2.LiBH4
3. NaIO4
85%
O
H
OTBS
OPMB
2-14
88%
(d.s.>20:1)
MeO
O
O
P(OCH2CF3)2
KHMDS, 18-c-6
2-15
OTBS
OPMB
O
OMe
2-16
1. DIBAl-H
2. MnO2
3.15, KHMDS,
18-c-6
80%
(d.s.>20:1)
OTBS
OPMB
O
MeO
2-17
1.DIBAl-H
2.DMP
90%
O
OTBS
PMBO
2-3

In Scheme 2-4, the synthesis of fragment **2-4** is described. This synthesis starts with the conversion of alpha-hydroxyacid **2-18** to the thioamide **2-19** in 58% yield over four steps. This was done through an amide formation, hydroxyl protection with TBSCl and the use of the Lawesson reagent. This thioamide was then cyclized through the use of bromo-ester **2-20**.

Deprotection of the TBS-group with TBAF gave **2-21** in 76% yield from **2-19**. The free hydroxyl in **2-21** was then converted to a carbamate through the use of carbonyldiimidazole and trapping of the activated carbamate with methylamine to form **2-22** in 94% yield. After the reduction of ester **2-22** to aldehyde **2-23** through the use of DIBAl-H, the complete fragment **2-4** was prepared using Brown's asymmetric crotylation protocol in a good yield of 65%.[6]

Scheme 2-4. Synthesis of fragment **2-4**.

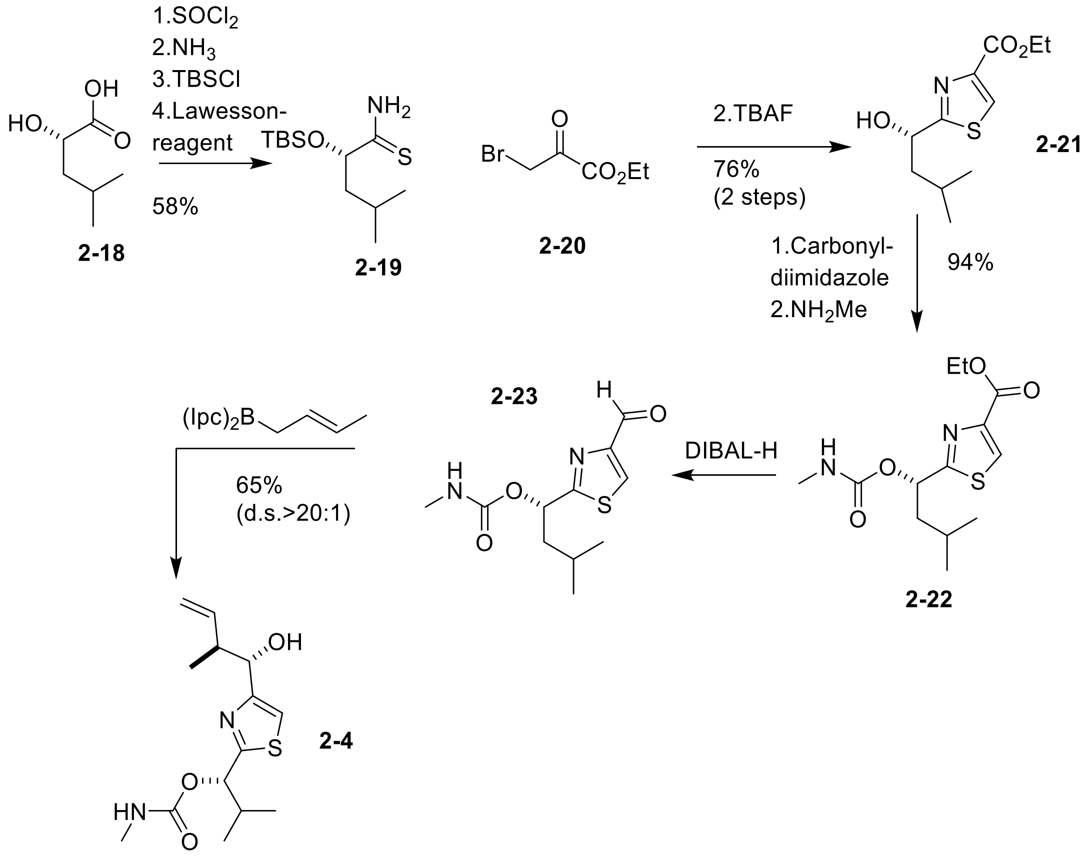

1.SOCl2
2.NH3
3.TBSCl
4.Lawesson-reagent
58%
OH
HO
O
2-18
NH2
TBSO
S
2-19
O
Br
CO2Et
2-20
2.TBAF
76%
(2 steps)
CO2Et
N
HO
S
2-21
1.Carbonyl-diimidazole
2.NH2Me
94%
EtO
O
N
S
H
N
O
O
2-22
DIBAL-H
2-23
H
O
N
S
H
N
O
O
(Ipc)2B
65%
(d.s.>20:1)
OH
N
S
2-4
O
HN
O

In order to complete the synthesis of archazolid A (Scheme 2-5), fragments **2-2** and **2-3** were combined through a boron-mediated aldol reaction followed by a two-step elimination to give **2-24** (94%, 2 steps). Then, **2-24** was reacted with **2-4** in a Heck reaction by heating the mixtutre to 80 °C in the presence of the catalyst $PdCl_2(PPh_3)_2$, along with TBSCl, TEA, and a solution of CH_3CN/H_2O to give **2-25** with 6:1 *E*/*Z* selectivity. Compound **2-26** was obtained from **2-25** through the attachment of the phosphonate **2-5** by use of BOP, oxidative removal of the PMB protecting group, and Swern oxidation to the aldehyde. Macrocyclization of the resulting keto-phosphonate **2-26** was accomplished using NaH as base. After macrocyclization, the C15 ketone was stereoselectively reduced through the use of an oxazaborolidine-assisted borane ((*S*)-CBS) reduction in 73% yield and d.s. >20:1.[7] Finally, deprotection with HF/pyridine in THF gave archazolid A (**2-1**) in 80% yields.[8] Overall, the longest linear sequence of the scheme was 20 steps with a yield of 4%.

Scheme 2-5. Completion of the archazolid A (**2-1**) synthesis.

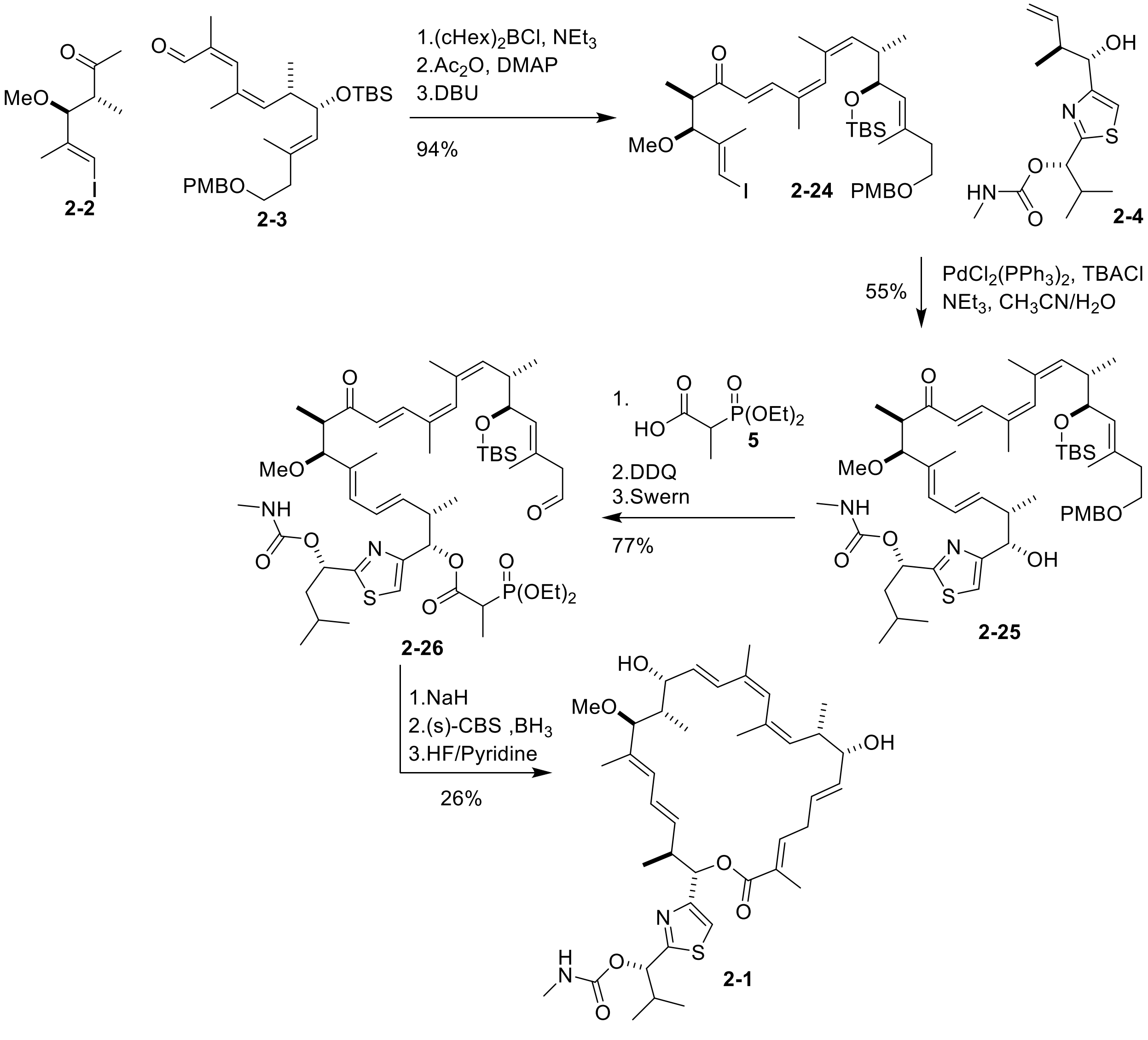
2-2
2-3
1.(cHex)$_2$BCl, NEt$_3$
2.Ac$_2$O, DMAP
3.DBU
94%
2-24
2-4
55%
PdCl$_2$(PPh$_3$)$_2$, TBACl
NEt$_3$, CH$_3$CN/H$_2$O
2-25
1.
5
2.DDQ
3.Swern
77%
2-26
1.NaH
2.(s)-CBS ,BH$_3$
3.HF/Pyridine
26%
2-1

2.2 Synthesis of Archazolid B

Due to the high bioactivity and fascinating structural features, Trauner, Roethle, and Chen pursued the synthesis of archazolid B (**2-27**). Key transformations of their synthesis include a Hoye relay ring-closing methathesis (RRCM), a Stille coupling at C10-C11, and a Kita esterification utilizing three fragments: **2-28**, **2-29**, and, like Menche, **2-4** (Scheme 2-6).[9] Overall, their synthesis had a longest linear sequence of 19 steps and an overall yield of 0.8%.

Scheme 2-6. Trauner's retrosynthetic approach to archazolid B (**2-27**).

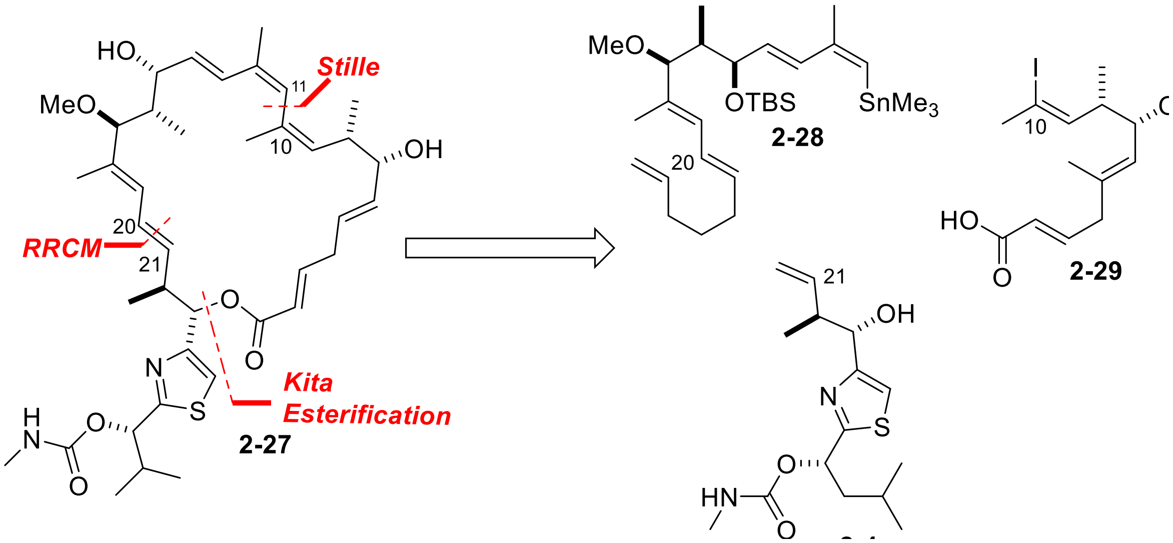

The three fragments **2-28**, **2-29**, and **2-4** were designated by the group as the northwestern, northeastern, and southern fragments respectively based on their location within the molecule as commonly drawn. The northeastern fragment was synthesized by starting with known ynone **2-31** available from the (*S*)-Roche ester **2-30**, as shown in Scheme 2-7.[10] Compound **2-31** was taken through a highly diastereoselective reduction with (*S*)-alpine borane to give a secondary hydroxyl, which was then protected as its triisopropylsilyl (TIPS) ether. Selective deprotection of the TBS-group gave primary alcohol 2-**32** in 80% yield. Oxidation of the primary alcohol through the use of DMP and $NaHCO_3$ led to an aldehyde, which was then subjected to a Cory-Fuchs transformation using triphenylphosphine, potassium bicarbonate, and carbon tetrabromide in order to achieve dibromide **2-33** in 75% yield. Conversion of **2-33** to the (*Z*)-vinyl iodide **2-34** was accomplished using the method developed of Tanino and Miyashita, which involved methyllithium, copper(I) iodide and I_2.[11] This was followed by the exchange of the secondary silyl protecting group (TIPS) for a secondary *tert*-butylcarbonate (Boc) protecting group (76% over two steps). They performed this exchange of protecting groups so that there was the presence of a coordinating carbonate, which encouraged high regioselectivity in the Trost Alder-ene reaction. Compound **2-34** was then subjected to a highly selective Trost Alder-ene reaction with 3-butenol to afford the triene **2-35** in 88% yield, which contained the sensitive skipped diene found in the natural product that has been seen to be prone to isomerization.[12] Compound **2-35** was then oxidized in a two-step process to afford the "northeastern" carboxylic acid **2-29** in nearly quantitative yield for the two steps (Scheme 2-7).

Scheme 2-7. Synthesis of fragment **2-29**.

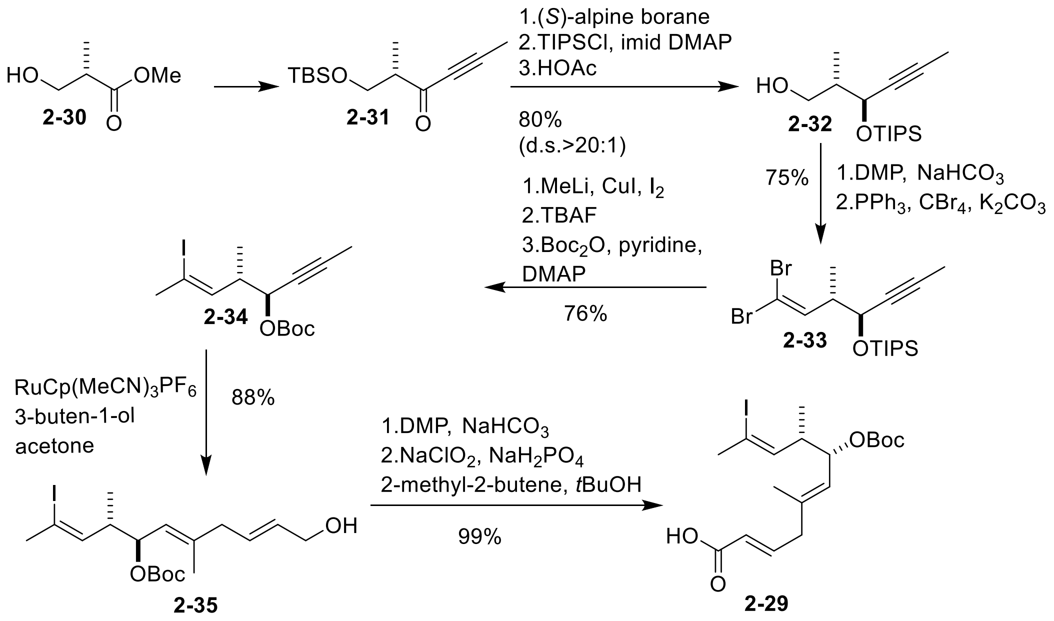
HO
OMe
2-30
O
TBSO
2-31
O
1.(S)-alpine borane
2.TIPSCl, imid DMAP
3.HOAc
80%
(d.s.>20:1)
HO
2-32
OTIPS
75%
1.DMP, NaHCO3
2.PPh3, CBr4, K2CO3
Br
Br
2-33
OTIPS
1.MeLi, CuI, I2
2.TBAF
3.Boc2O, pyridine, DMAP
76%
I
2-34
OBoc
RuCp(MeCN)3PF6
3-buten-1-ol
acetone
88%
I
OH
OBoc
2-35
1.DMP, NaHCO3
2.NaClO2, NaH2PO4
2-methyl-2-butene, tBuOH
99%
I
OBoc
HO
O
2-29

As shown in Scheme 2-8, the synthesis of the northwestern fragment (**2-28**) began with iodoenoate **2-36**, which was obtained in three steps from a propargyl alcohol.[13] Reduction by DIBAl-H followed by an oxidation to the aldehyde with DMP was followed by an efficient Evans *syn*-aldol addition with the boron enolate of benzyl oxazolidinone **2-37** to afford **2-38** in 73% for the three steps. This was then converted into the corresponding Weinreb amide, which was followed by a TBS protection of the secondary free hydroxyl. The Weinreb amide then underwent a phosphonate Claisen reaction to give a beta-keto phosponate **2-39**, with a yield of 68%. This phosphonate was then subjected to a HWE reaction with the enal **2-4** to afford **2-41** in 79% yield. A highly diastereoselective reduction with $NaBH_4$ followed by etherification and an iodine-tin exchange gave the completed northwestern fragment **2-28** in 70% yield over three steps. Trauner et al. did not report confirmation of the stereochemistry from their $NaBH_4$ reduction at this stage, however, they were able to match their final archazolid B NMR to the isolated NMR.

Scheme 2-8. Synthesis of fragment **2-28**.

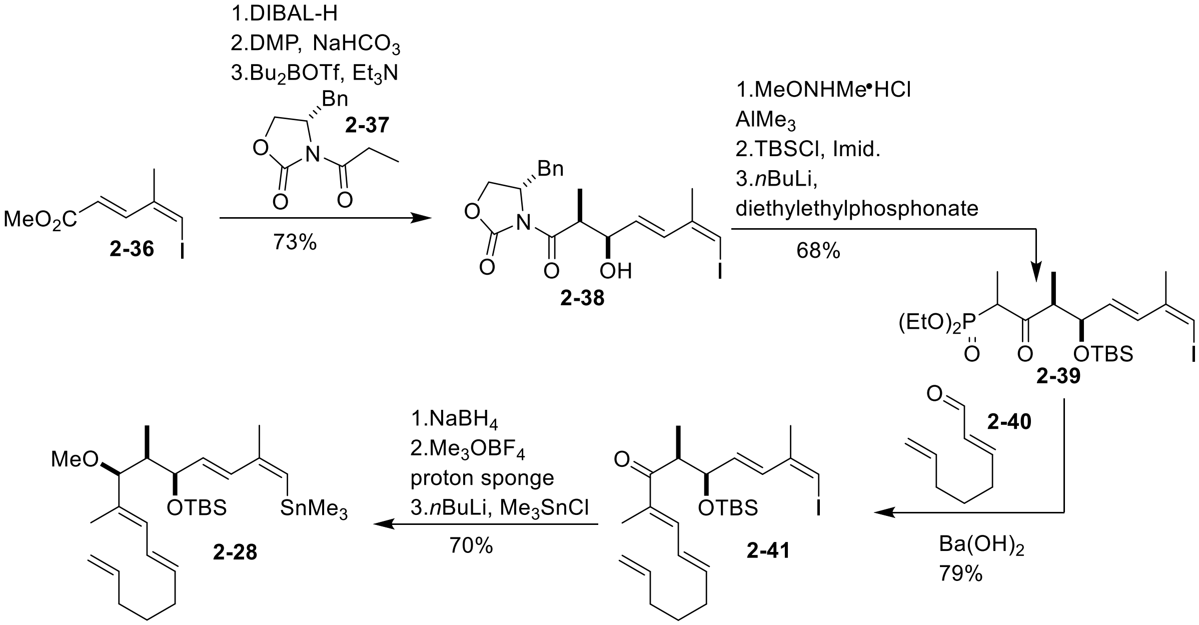

1.DIBAL-H
2.DMP, NaHCO3
3.Bu2BOTf, Et3N
Bn
2-37
O
N
O
O
MeO2C
2-36
I
73%
Bn
O
N
O
O
OH
I
2-38
1.MeONHMe•HCl
AlMe3
2.TBSCl, Imid.
3.nBuLi,
diethylethylphosphonate
68%
(EtO)2P
O
O
OTBS
I
2-39
O
2-40
Ba(OH)2
79%
O
OTBS
I
2-41
1.NaBH4
2.Me3OBF4
proton sponge
3.nBuLi, Me3SnCl
70%
MeO
OTBS
SnMe3
2-28

The synthesis of the southern thiazole fragment **2-4** is shown in Scheme 2-9 and was built upon the known hydroxyalkyl thiazolecarboxylate **2-43**, available in a six step synthesis from leucine **2-42**.[14] Compound **2-43** was then subjected to carbamoylation with carbonyldiimidazole (CDI) and methylamine followed by a chemoselective reduction of the ester and Brown crotylation of the resulting aldehyde.[15] In this way fragment **2-4** was obtained in 9 steps and 30% yield from leucine (Scheme 2-9).

Scheme 2-9. Trauner's synthesis of fragment **2-4**.

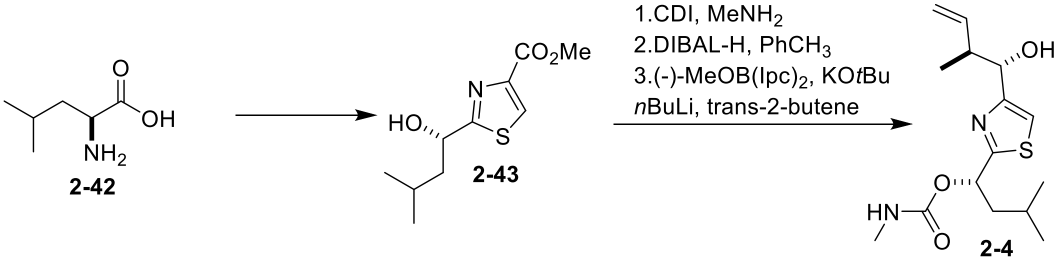

O
OH
NH2
2-42
CO2Me
N
S
HO
2-43
1.CDI, MeNH2
2.DIBAL-H, PhCH3
3.(-)-MeOB(Ipc)2, KOtBu
nBuLi, trans-2-butene
OH
N
S
O
HN
O
2-4

Once the fragments had been synthesized, the southern fragment **2-4** and northeastern fragment **2-29** were combined using a ruthenium catalyzed Kita esterification to form **2-44** (Scheme 2-10).[16] The authors note that this type of esterification was required because "all base-mediated methods led to the migration of the C2-C3-double bond." Due to this isomerization in basic conditions, esterifications such as the Yamaguchi esterification[17] could not be utilized due to their basic additives (e.g. triethylamine/DMAP).

Scheme 2-10. Synthesis of fragment **2-44**.

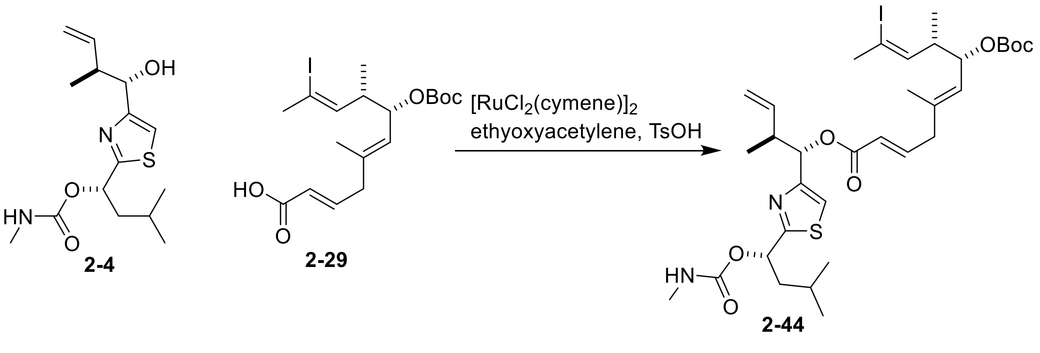

OH
N
S
O
HN
O
2-4
I
OBoc
HO
O
2-29
[RuCl2(cymene)]2
ethyoxyacetylene, TsOH
I
OBoc
O
O
N
S
O
HN
O
2-44

Once esterified, **2-44** was subjected to a thermal deprotection of the Boc group with silica to afford the corresponding free hydroxyl (Scheme 2-11). It could be that the Boc group was removed prior to the coupling because of the instability of the triene, thus once the coupling occurred the triene would decompose during deprotection. This was followed a modified Liebskind coupling with vinyl stannane **2-28** to give the relay ring closing metathesis precursor **2-45** in 21% yield.[18]

Scheme 2-11. Synthesis of fragment **2-45**.

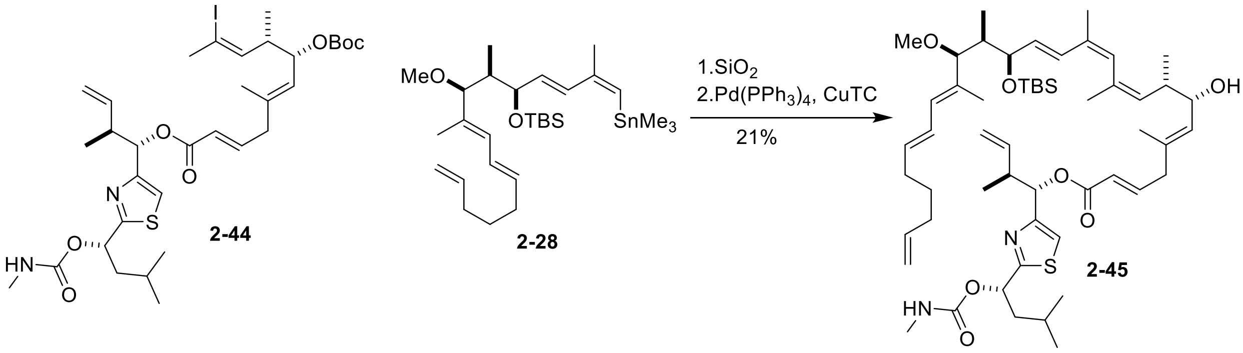
OBoc
I
HN
O
N
S
2-44
MeO
OTBS
SnMe3
2-28
1.SiO2
2.Pd(PPh3)4, CuTC
21%
MeO
OTBS
OH
N
S
2-45
HN
O

The RRCM used a second generation Grubb’s catalyst and afforded a 27% yield of the macrocycle (Scheme 2-12).[18] Deprotection of the TBS group using a solution of formic acid/THF/H_2O in a 3:6:1 ratio then completed their synthesis of archazolid B (**2-27**).

Scheme 2-12. Completion of the archazolid B (**2-27**) synthesis.

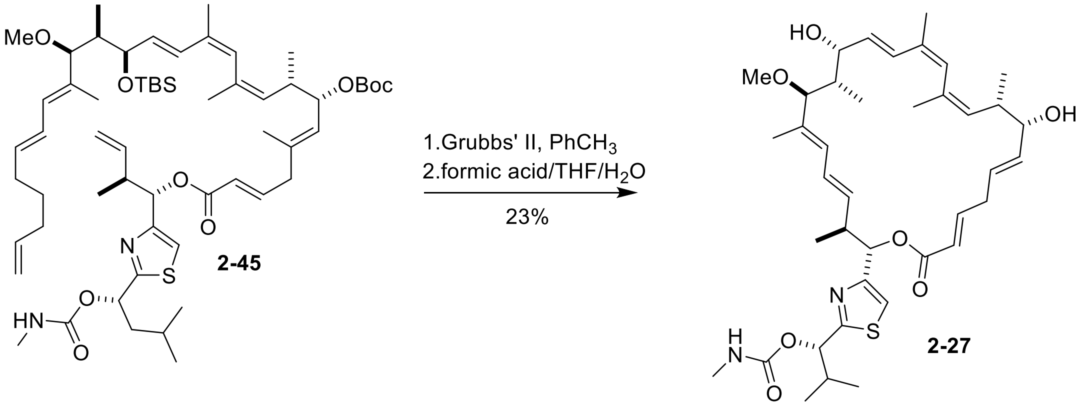
MeO
OTBS
OBoc
N
S
2-45
HN
O
1.Grubbs' II, PhCH3
2.formic acid/THF/H2O
23%
HO
MeO
OH
N
S
H
N
O
2-27

2.3 Modular Synthesis of Archazolid A and B

In 2009, Menche and Hassfeld published a modular total synthesis of archazolid A and B, with the key difference being the use of different phosphonates, **2-5** or **2-46** to access archazolid A and B, respectively (Scheme 2-13).[19] Overall, they improved their previous synthesis of archazolid A by using the same three of four fragments (**2-2** through **2-4**), but they optimized their reaction procedures and investigated alternative fragment coupling sequences. This modular approach allowed the Menche group the freedom to change the order of addition of fragments.

Scheme 2-13. Menche's modular retrosynthesis of archazolid A (**2-1**) and B (**2-27**).

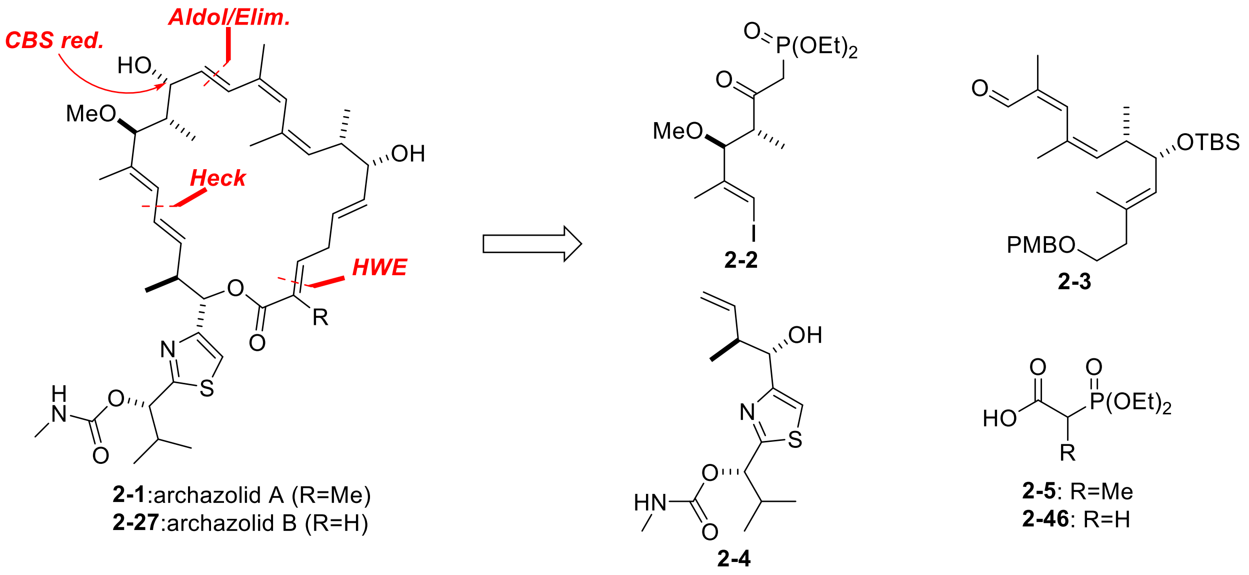
CBS red.
Aldol/Elim.
HO
MeO
OH
Heck
HWE
O
R
O
N
S
H
N
O
O
2-1:archazolid A (R=Me)
2-27:archazolid B (R=H)
O
P(OEt)2
O
MeO
I
2-2
O
OTBS
PMBO
2-3
OH
N
S
O
HN
O
2-4
O
O
HO
P(OEt)2
R
2-5: R=Me
2-46: R=H

From the previously reported synthesis of **2-4**, there were reports that when installing the thiazole ring, epimerization of the free hydroxyl stereocenter occurred. Menche and Hassfeld corrected this by oxidizing that hydroxyl group to the ketone **2-47**, which was followed by a stereoselective reduction with (*R*)-CBS to give the enantiopure **2-21** (Scheme 2-14). This was the only change made to the synthesis of fragment **2-4**.

Scheme 2-14. Revised strategy for synthesis of **2-21**.

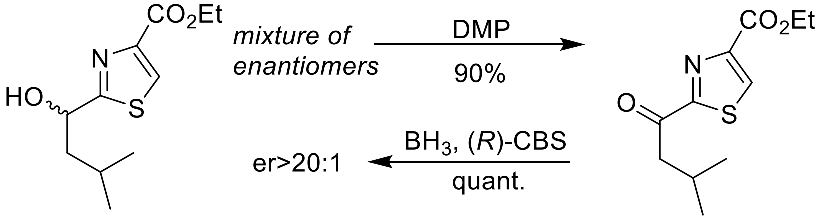
CO2Et
HO
N
S
mixture of enantiomers
DMP
90%
BH3, (R)-CBS
quant.
er>20:1
O

2-21 **2-47**

When attempting to optimize the synthesis of fragment **2-2**, the removal of the Abiki-Masamune auxiliary was investigated due to the multitude of steps outlined in Scheme 2-2. It was found that if the ester carbonyl was activated by coordination to the free hydroxyl using a Lewis acid, promoted the nucleophilic attack of the *N*-(methoxylmethyl)methyl amine **2-48** to give Weinreb amide **2-49** (Scheme 2-15). The highest yields were obtained using *i*-PrMgCl as the coordinating Lewis acid. In this way **2-49** was obtained in 72% and could be transformed to the methyl ketone **2-2** in two steps with a 74% yield.

Scheme 2-15. Revised strategy for the synthesis of fragment **2-2**.

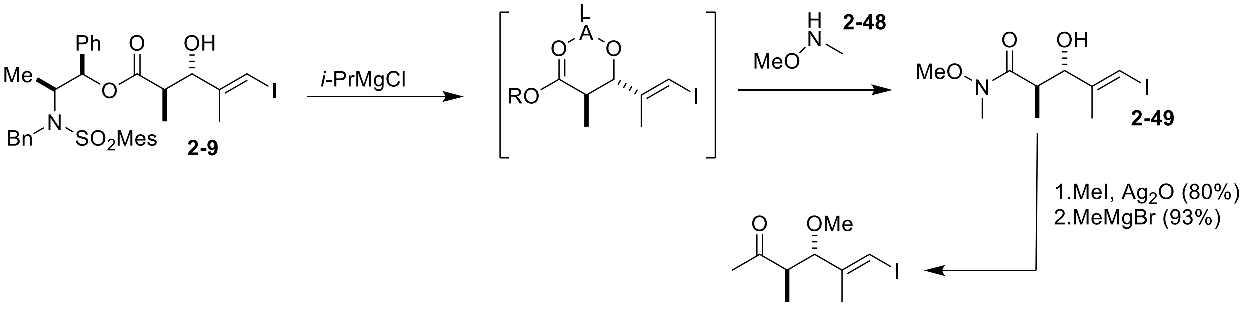
Ph
O
OH
Me
N
Bn
SO2Mes
2-9
i-PrMgCl
L
A
O
O
RO
I
H
2-48
N
MeO
MeO
N
O
OH
2-49
1.MeI, Ag2O (80%)
2.MeMgBr (93%)
O
OMe
I

2-2

Previously unreported, macrocyclization of **2-26** to **2-1** (archazolid A) with a base caused the anti-propionates (C_7/C_8 and C_{16}/C_{17}) to undergo elimination rather than cyclization to achieve archazolid A. The elimination was overcome by the use of molecular sieves. It was theorized that the molecular sieves were important due to their slightly acidic nature (Figure 2-1).

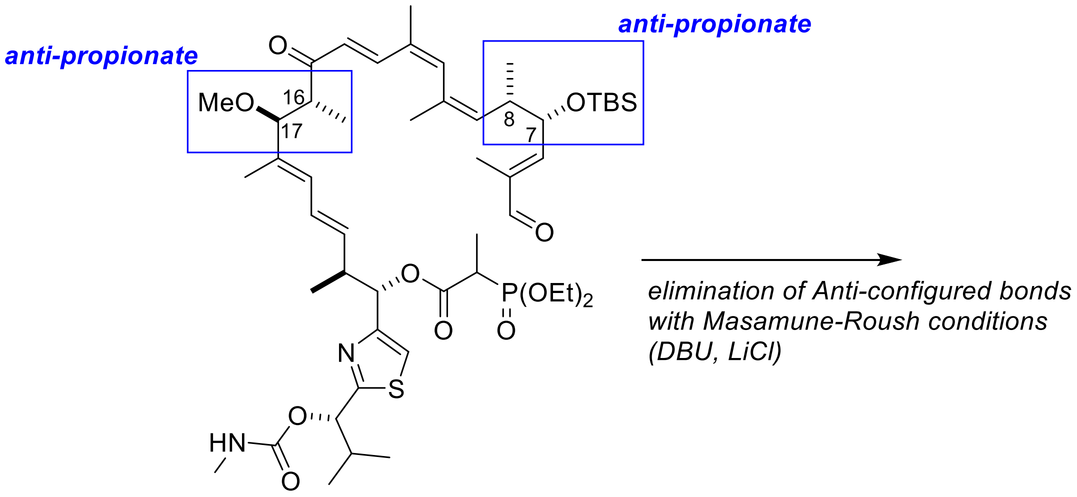

elimination of Anti-configured bonds with Masamune-Roush conditions (DBU, LiCl)

Figure 2-1. Positions C$_7$-C$_8$ and C$_{16}$-C$_{17}$ were prone to elimination under mild reaction conditions.

In order to demonstrate the modularity of their synthetic approach and avoid elimination during HWE cyclization, the synthesis of archazolid B (**2-27**) was investigated using a different order of the fragment coupling process (Scheme 2-16). Phosphonate **2-50** resulted from the addition of phosphonate **2-46** with BOP to fragment **2-4.** Aldehyde **2-51** was afforded from deprotecting the primary PMB group on **2-24** followed by a Swern oxidation. Compounds **2-51** and **2-50** were stitched together through the use of an intermolecular HWE to give **2-52**. After the olefination, an intramolecular Heck macrocyclization was performed, followed by a stereoselective CBS reduction of the ketone to the free hydroxyl. Finally, HF/pyridine was used in the TBS deprotection using to give **2-27** (Scheme 2-16).

Scheme 2-16. Completion of the synthesis of archazolid B (**2-27**).

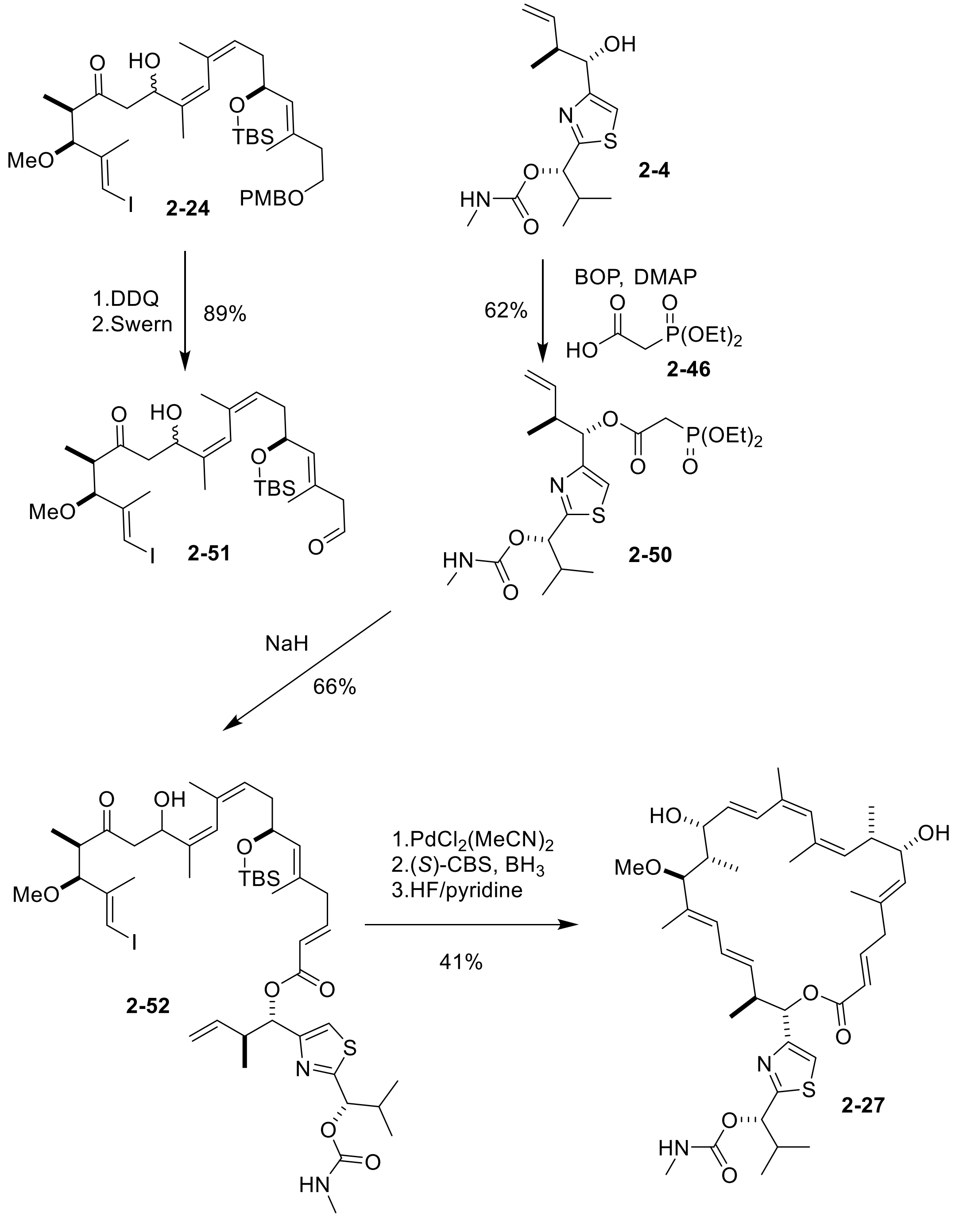
2-24
MeO
PMBO
TBS
2-4
1.DDQ
2.Swern
89%
BOP, DMAP
62%
P(OEt)2
2-46
2-51
2-50
NaH
66%
2-52
1.PdCl2(MeCN)2
2.(S)-CBS, BH3
3.HF/pyridine
41%
2-27

2.4 Highly Stereo- and regioselective approach to the C_9-C_{12} fragment of the archazolids

One of the important and most interesting structural features of the archazolid natural products is the C_9-C_{12} (*Z*,*Z*)-1,1,3,4-tetrasubstituted 1,3-diene which is part of a conjugated triene.[20] Menche's group ultimately utilized a 3-step aldol condensation after attempted Horner-Wadsworth-Emmons reactions failed, which then required a late-stage enantioselective CBS-reduction to install the C_{15} hydroxyl.[21] Trauner's Stille coupling at C10-C11 to complete the triene was successful but low-yielding (21%). In 2007, Negishi and Huang published an elegant approach to this synthetically challenging subunit (Scheme 2-17). This synthesis was accomplished by hydroboration of a 1-halo-1-alkyne. Following this was a migratory insertion of **2-54** after the addition of dimethyl zinc and a zinc promoted transmetalative iodinolysis to ultimately give compound **2-57**. Compounds **2-58** and **2-57** were then cross-coupled through palladium catalysis to give the conjugated triene 2-**59** in good yields (83% for **2-59a**; 81% for **2-59b**) as shown in Scheme 2-17. Interestingly, Negishi et al. use a similar disconnection approach as Trauner et al. (i.e. at C10-C11), but have a four-fold improvement of yields. Two protocols described, using either Zn-II or Zn-III, have provided potential intermediates for the synthesis of archazolids as isomerically ≥98% pure, however Negishi's group has not yet published any further synthetic studies on the archazolids.

Scheme 2-17. Negishi and Huang's synthesis of the C_9-C_{12} triene fragment of the archazolids.

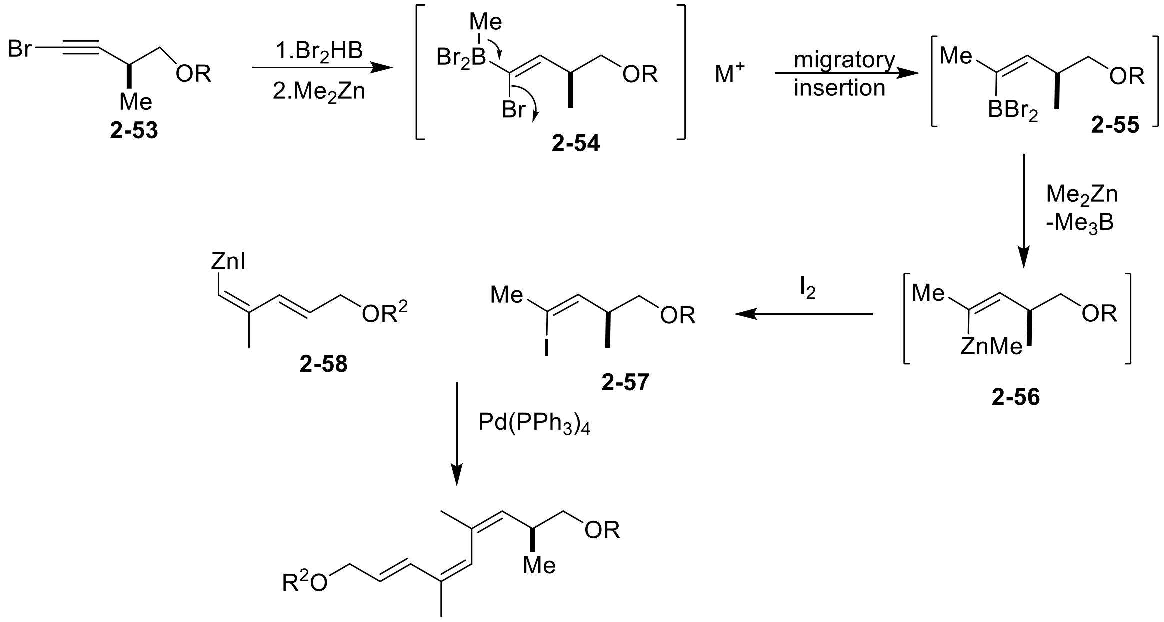

2-53
1.Br_2HB
2.Me_2Zn
2-54
M^+
migratory insertion
2-55
Me_2Zn
$-Me_3B$
2-56
I_2
2-57
2-58
$Pd(PPh_3)_4$

R = TBDPS
2-59a: R^2 = H (83%)
2-59b: R^2 = TBS (81%)

2.5 Previous Syntheses by the O'Neil Group

In 2011, archazolid F was discovered and isolated from the same bacterium, *Archangium gephyra*.[22] Archazolid F introduced a slightly new structure, but a similar activity to both archazolid A and archazolid B.[15] Instead of the alkene at C2 it was now shifted to C3. Due to the similar potency of archazolid F to archazolid B despite this structural change, it was hypothesized by our group that an analog of ArcB with the removal of the alkene at C2 would retain its biological activity.[23] This new compound, dihydroarchazolid B (DHArcB), thus became our synthetic target.

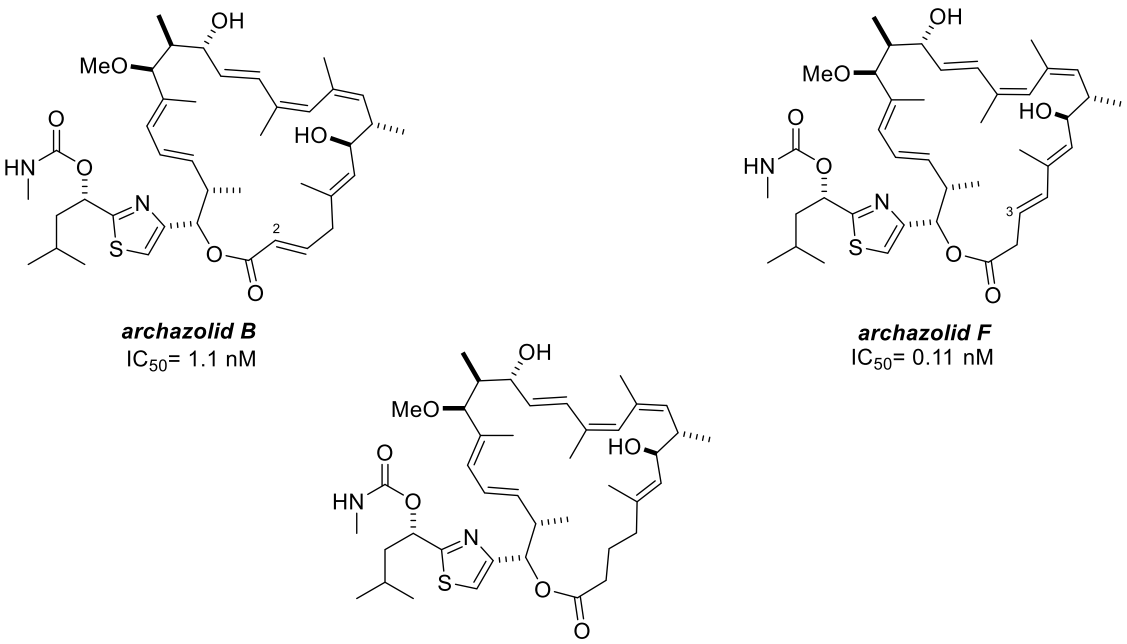

archazolid B
IC_{50}= 1.1 nM

archazolid F
IC_{50}= 0.11 nM

dihydroarchazolid B

Figure 2-2. Comparison between archazolid B and archazolid F as a basis for the simplified archazolid, dihydroarchazolid B.

From the decision to synthesize dihydroarchazolid B, a retrosynthesis was proposed by the O'Neil group (Scheme 2-18). DHArcB was split into three fragments that we refer to as the western fragment (**2-61**), the eastern fragment (**2-60**), and the side-chain **2-62**.

Scheme 2-18. O'Neil group's planned retrosynthesis of dihydroarchazolid B.

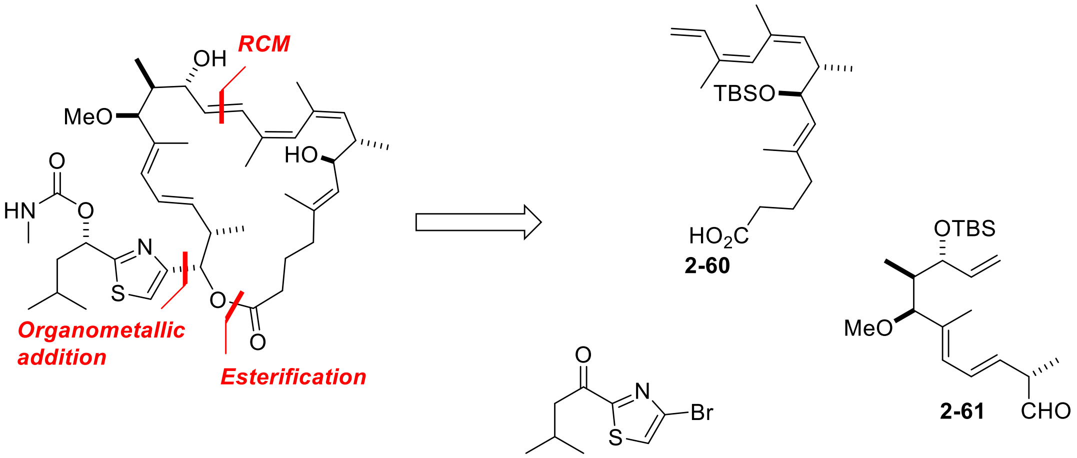

2-60

2-61

2-62

The synthesis of **2-60**, the eastern fragment, began with the TBS protection of 5-hexyn-1-ol (**2-63**) to **2-64** (Scheme 2-19). Compound **2-64** was then added to aldehyde **2-65** using trimethylaluminium and zirconocene dichloride, delivering **2-66** in 85% yield and with a 6:1 diastereomeric ratio.[24] The free hydroxyl was protected as its TBS-ether and the PMB protecting group was removed affording a primary alcohol that was oxidized using Swern conditions to form **2-67**. Aldehyde **2-67** was then reacted using a Still-Gennari modified Horner-Wadsworth-Emmons reaction[5] in order to generate the z-ester **2-69**. The primary TBS protected hydroxyl was oxidized directly to the carboxylic acid by treatment with the Jones reagent and the ester was reduced to the alcohol and oxidized to the aldehyde to form **2-71**. This aldehyde was then taken through the tandem allylzirconation/Peterson elimination sequence of Huang and Pi to generate the *Z*,*Z*-terminal triene **2-60** with 8:1 diastereoselectivity.[25]

Scheme 2-19. Completion of the eastern fragment, EZZE-triene **2-60**.

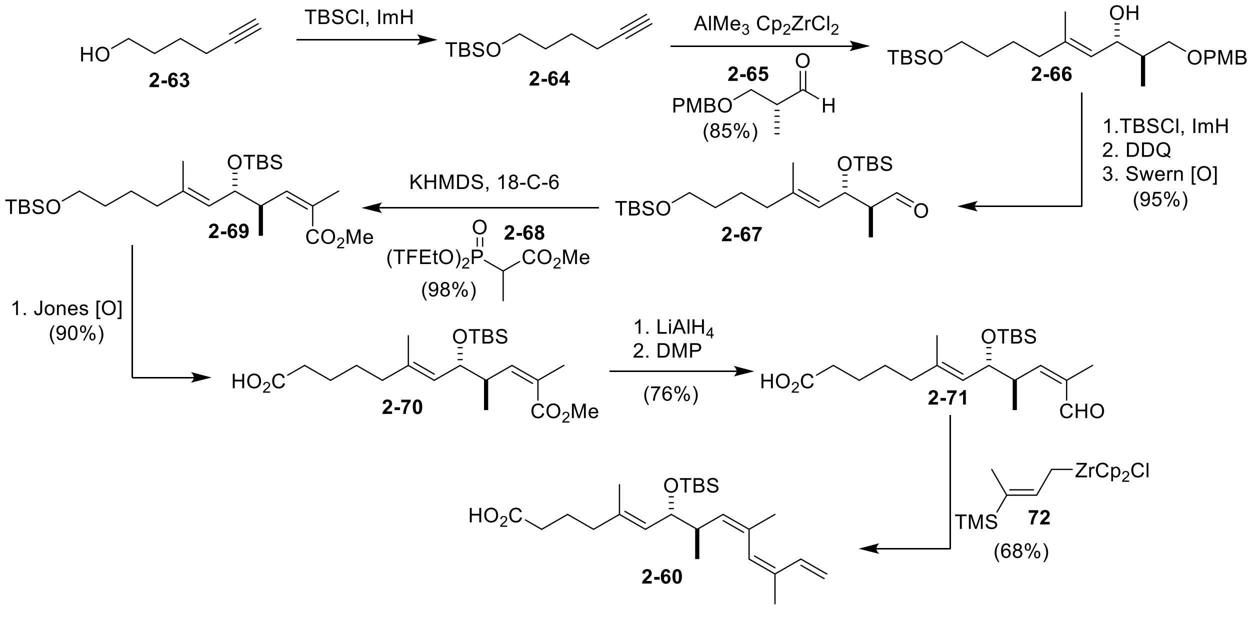
HO
2-63
TBSCl, ImH
TBSO
2-64
AlMe$_3$ Cp$_2$ZrCl$_2$
2-65
PMBO
H
O
(85%)
TBSO
2-66
OH
OPMB
1.TBSCl, ImH
2. DDQ
3. Swern [O]
(95%)
TBSO
2-67
OTBS
O
KHMDS, 18-C-6
2-68
(TFEtO)$_2$P
CO$_2$Me
(98%)
TBSO
2-69
OTBS
CO$_2$Me
1. Jones [O]
(90%)
HO$_2$C
2-70
OTBS
CO$_2$Me
1. LiAlH$_4$
2. DMP
(76%)
HO$_2$C
2-71
OTBS
CHO
ZrCp$_2$Cl
TMS
72
(68%)
HO$_2$C
OTBS
2-60

For **2-61**, the western fragment, the synthesis begins with the well-established synthesis of the Weinreb amide **2-75** (Scheme 2-20).[26] This was then converted to the ketophosphonate **2-**

77, which allowed for a Horner-Emmons coupling[27] with the (*R*)-Roche ester derived aldehyde **2-78** using $Ba(OH)_2$•$8H_2O$ for the highest *trans*-selectivity (>10:1).[28] The ketone was then converted to the methylether present in **2-80** by first a diastereoselective reduction with $NaBH_4$ followed by methylation of the resulting hydroxyl with LiHMDS and methyl triflate (MeOTf). The primary TBS group in compound **2-80** was then removed using HF/pyridine and the resulting primary alcohol was oxidized to the aldehyde using DMP to give **2-61**.[29]

Scheme 2-20. Completion of the western fragment **2-61**.

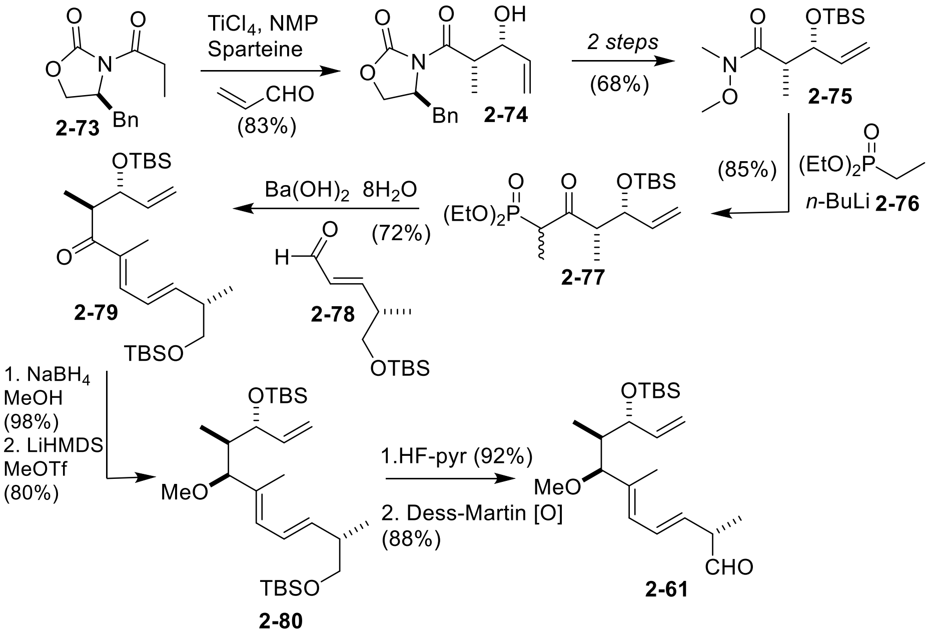
2-73
Bn
TiCl4, NMP
Sparteine
CHO
(83%)
OH
Bn
2-74
2 steps
(68%)
OTBS
2-75
(85%)
(EtO)2P
n-BuLi
2-76
(EtO)2P
OTBS
2-77
Ba(OH)2 8H2O
(72%)
H
2-78
OTBS
OTBS
2-79
TBSO
1. NaBH4
MeOH
(98%)
2. LiHMDS
MeOTf
(80%)
OTBS
MeO
TBSO
2-80
1.HF-pyr (92%)
2. Dess-Martin [O]
(88%)
OTBS
MeO
CHO
2-61

The side chain was synthesized from known ketothiazole **2-62** (Scheme 2-21).[30] The ketone in **2-62** was enantioselectively reduced using the CBS reagent and the resulting free hydroxyl[31] was protected as its TES-ether to give **2-81** in 74% for the two steps. Compound **2-81** was then treated with *tert*-butylithium for a lithium-halogen exchange with the bromide and the resulting organolithium was added to the western aldehyde fragment **2-61** to produce **2-82** as a mixture of diastereomers.[32] The free hydroxyl was then oxidized to the ketone using DMP and the TES group was deprotected using a mixture of HF/pyridine at 4 °C. Then in order to complete the western half of the archazolid, methyl amine and CDI were employed to install the carbamate found in compound **2-83**.

Scheme 2-21. Thiazole fragment coupling to the western fragment **2-61**.

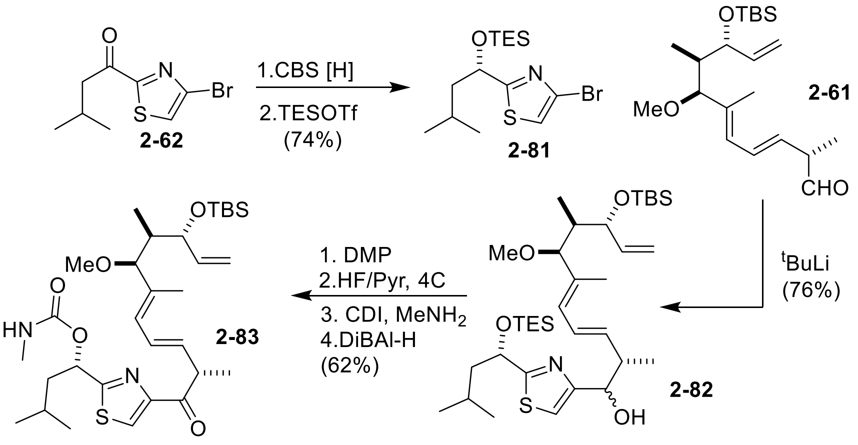
2-62
1.CBS [H]
2.TESOTf
(74%)
2-81
2-61
ᵗBuLi
(76%)
2-82
1. DMP
2.HF/Pyr, 4C
3. CDI, MeNH₂
4.DiBAl-H
(62%)
2-83

Once **2-83** had been produced, the ketone was stereoselectively reduced using L-Selectride and esterified with **2-60** using Yamaguchi's conditions (2,4,5-TCBC, TEA, and DMAP) to generate **2-84** as shown in Scheme 2-22. This set up an attempted macrocyclization by ring-closing metathesis.

Scheme 2-22. Esterification of the eastern and western fragments **2-60** and **2-83**.

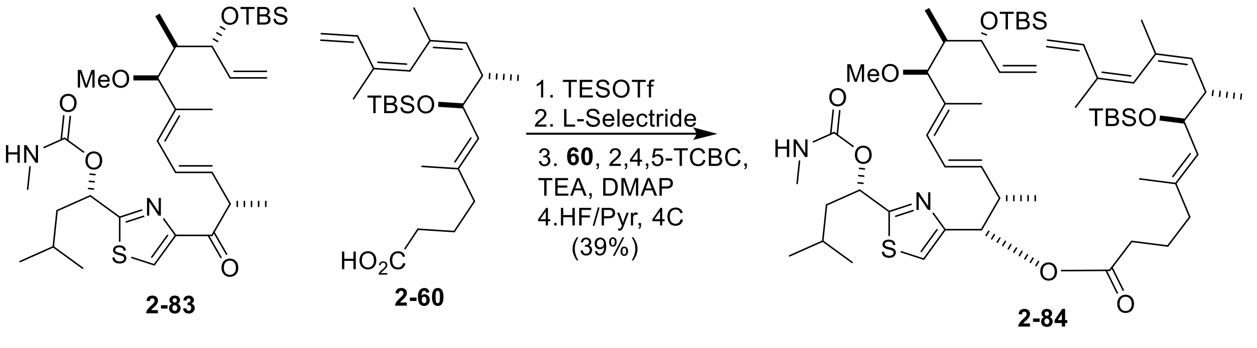
2-83
2-60
1. TESOTf
2. L-Selectride
3. 60, 2,4,5-TCBC, TEA, DMAP
4.HF/Pyr, 4C
(39%)
2-84

Using a ruthenium based catalyst, attempts were made to complete the synthesis of the protected DHArcB by RCM (Scheme 2-23). Unfortunately, it was discovered under a wide range of conditions that the catalyst was back biting instead of forming the macrocycle. Specifically, after engagement of the western alkene, it was cyclizing to create a cyclopentene with loss of ethylene.[33]

Scheme 2-23. Attempted coupling of the triene through RCM.

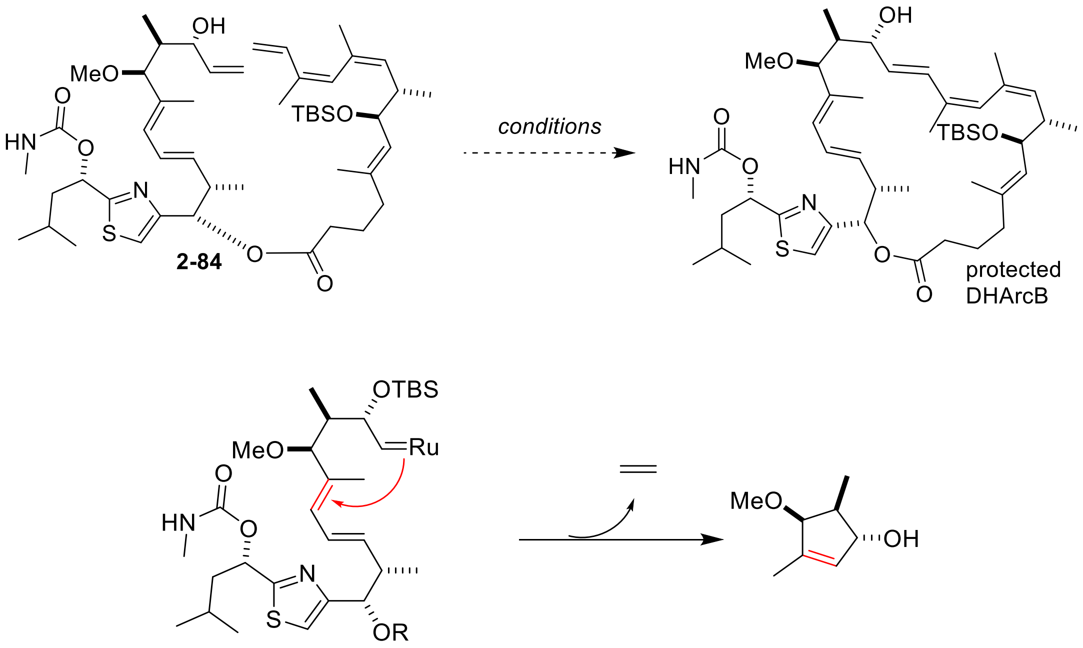
OH
MeO
O
HN
O
N
S
TBSO
2-84
O
O
conditions
OH
MeO
O
HN
O
N
S
TBSO
O
O
protected
DHArcB
OTBS
MeO
Ru
O
HN
O
N
S
OR
MeO
OH

Due to this competing back-biting during the attempted ring closing metathesis macrocyclization, a new cross metathesis was investigated. This was attractive because of the higher likely *trans*-selectivity that would be expected from the cross metathesis. However, knowing that the back-biting could occur, the fragments involved in the cross metathesis could not involve and the completed western fragment. Instead, a simpler cis-homodimer was investigated as a coupling partner with the eastern fragment **2-60**.

Scheme 2-24. Synthesis of the cis-homodimer **2-85**.

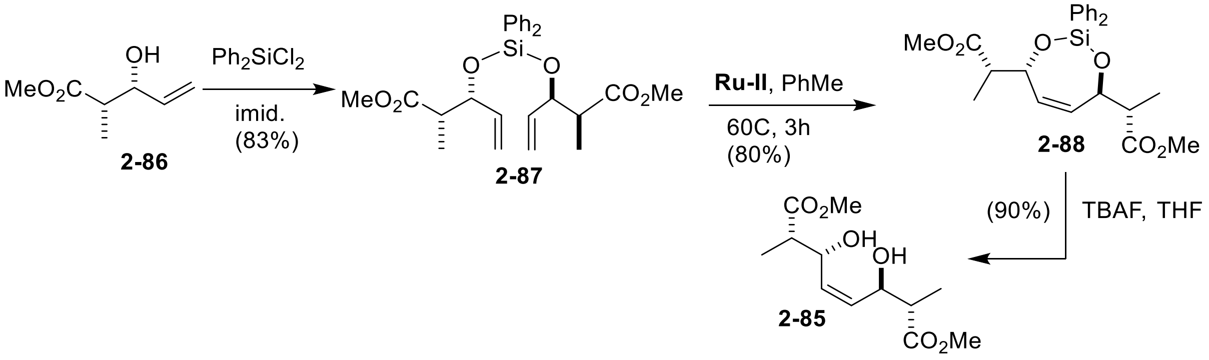

The *cis*-homodimer **2-85** was synthesized by starting with two equivalents of **2-86** and tethering them with diphenyldichlorosilane giving **2-87** (Scheme 2-24). Silyl-tethered RCM of **2-87** lead to a *cis*-siloxane **2-88**, which was desilylated with TBAF to give the *cis*-homodimer **2-85**. Overall, the cross metathesis with the *cis*-homodimer was successful in creating the desired product (Scheme 2-25). It was discovered that the optimal conditions were three equivalents of **2-85** using the Hoveyda-Grubbs ruthenium catalyst over 36 hours. However, this reaction could only produce a maximum of 40% yield, which lead to investigations into other coupling options.[34]

Scheme 2-25. Coupling of the cis-homodimer **2-85** with the eastern fragment **2-60**.

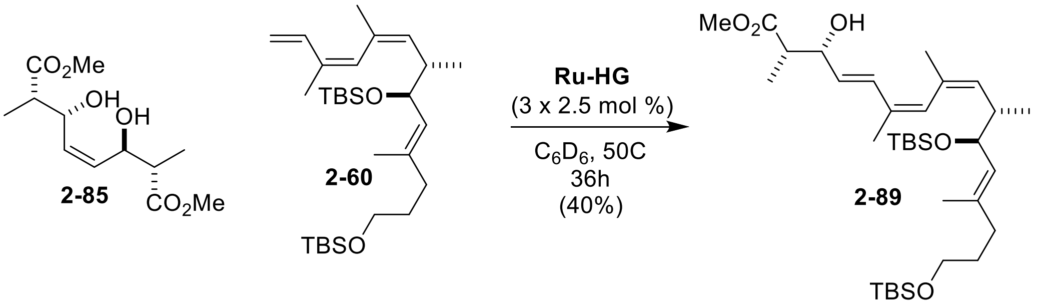

When considering an alternative non-metathesis based archazolid synthesis, we still wished to make use of the previously developed chemistry for the separate fragments. Ultimately, this led to the employment of a Stille coupling. Both the western and eastern fragment syntheses were adjusted to create a halide eastern fragment and an organostannane western fragment.

Scheme 2-26. Synthesis of the revised organostannane western fragment **2-96**.

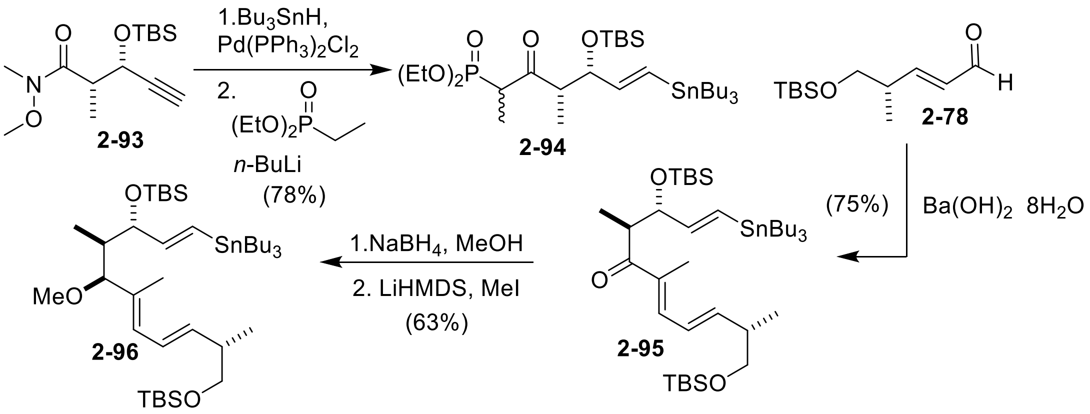

For the western fragment, the synthesis started with the known Weinreb amide **2-93** (Scheme 2-26).[35] This was converted to phosphonate **2-94**. Through a Horner-Wadsworth-Emmons olefination with aldehyde **2-78**, ketone **2-95** was obtained. The ketone was stereoselectively reduced and methylated as previously described giving **2-96** in 63% yield for the two steps. Synthesis of the eastern fragment halide began again from **2-69** (*ref.* Scheme 2-18), however the primary TBS protected hydroxyl was not oxidized to the carboxylic acid at this time. Instead, the Still-Gennari installed ester was reduced and oxidized to the aldehyde **2-90** and an iodo-Wittig with *in situ*-prepared phosphorane **2-91** was employed to create the vinyl iodide **2-92** (Scheme 2-27).

Scheme 2-27. Synthesis of the revised eastern fragment **2-92**.

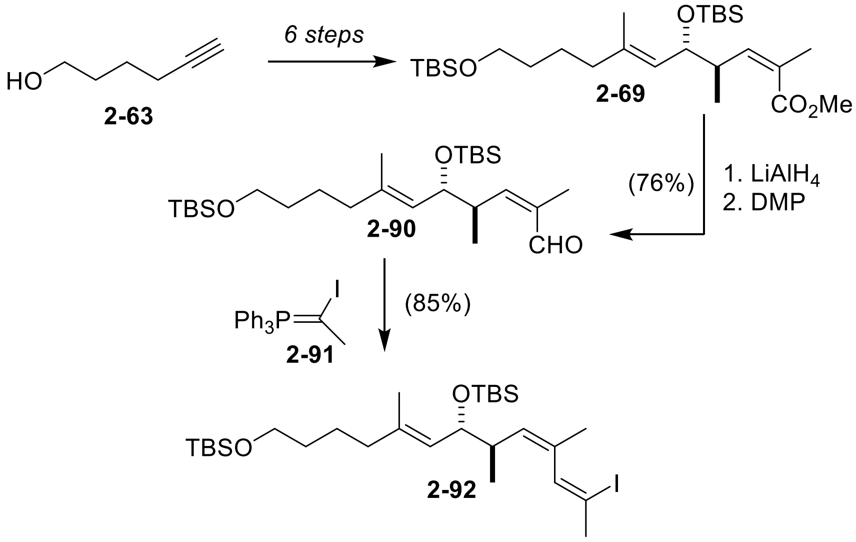

HO
2-63
6 steps
TBSO
OTBS
2-69
CO2Me
(76%)
1. LiAlH4
2. DMP
TBSO
OTBS
2-90
CHO
Ph3P
I
2-91
(85%)
TBSO
OTBS
2-92
I

With both the western and eastern fragments in hand, a Stille coupling was attempted. However, this reaction gave mostly unreacted vinyl iodide **2-92**, suggesting difficulties in the oxidative addition step of the catalytic cycle. It was hypothesized that switching the iodide and stannane positions could provide less sterically hindered conditions for the oxidative addition step. To that end, stannane **2-95** was iododestannylated to give iodide **2-96**, and iodide **2-92** was converted into stannane **2-97** by lithium-halogen exchange and trapping with Bu_3SnCl.[36] Compounds **2-97** and **2-96** underwent an efficient Stille coupling using Fürstner's conditions, providing **2-98** in 82% yield[37] (Scheme 2-28).

Scheme 2-28. Synthesis of revised coupling partners **2-96** and **2-97** as well as Stille coupling to synthesize **2-98**.

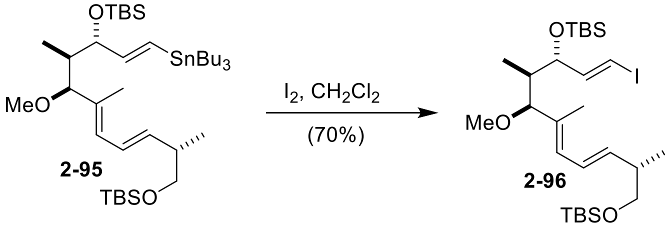

OTBS
SnBu3
MeO
2-95
TBSO
I2, CH2Cl2
(70%)
OTBS
I
MeO
2-96
TBSO

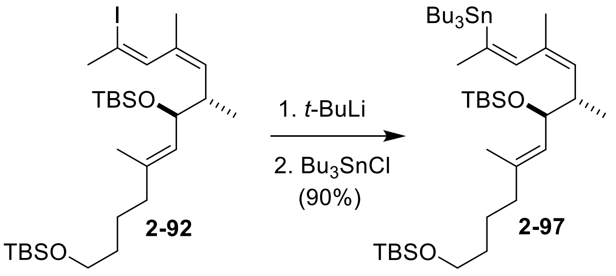

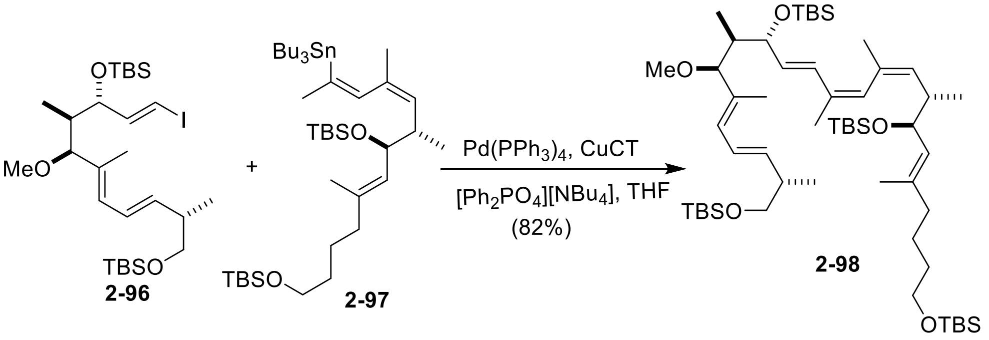

One main goal of this project was to understand the structure activity relationship, SAR, of the archazolids for V-ATPase inhibition. The O'Neil group had previously tested three archazolid fragments in an *Arabidopsis*-based V-ATPase assay using the compounds that they had synthesized (**2-99**, **2-100**, and **2-101**[38]), which are in Figure 2-3.

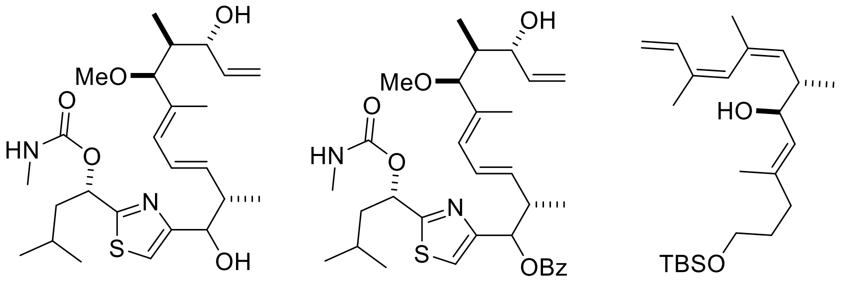

2-99 **2-100** **2-101**

Figure 2-3. The compounds that were used in an *Arabidopsis*-based V-ATPase assay.

None of these compound inhibited *Arabidopsis* growth which is an indicator for V-ATPase inhibition, leading the group to believe that macrocyclization is important for inhibition. Additionally, the C7 and C15 hydroxyls linked by the *Z*,*Z*,*E*-triene appeared to be important for

V-ATPase inhibition, as evidenced by the lower V-ATPase inhibitory activity of archazolids C and E where these hydroxyls are glycosylated (Figure 2-4). While compounds **2-99** through **2-101** did not contain an intact C7-C15 subunit, our Stille coupling product **2-102** (after deprotection) contained this important region of the archazolid structure. We hypothesized, therefore, that compound **2-102** might display V-ATPase inhibitory activity.

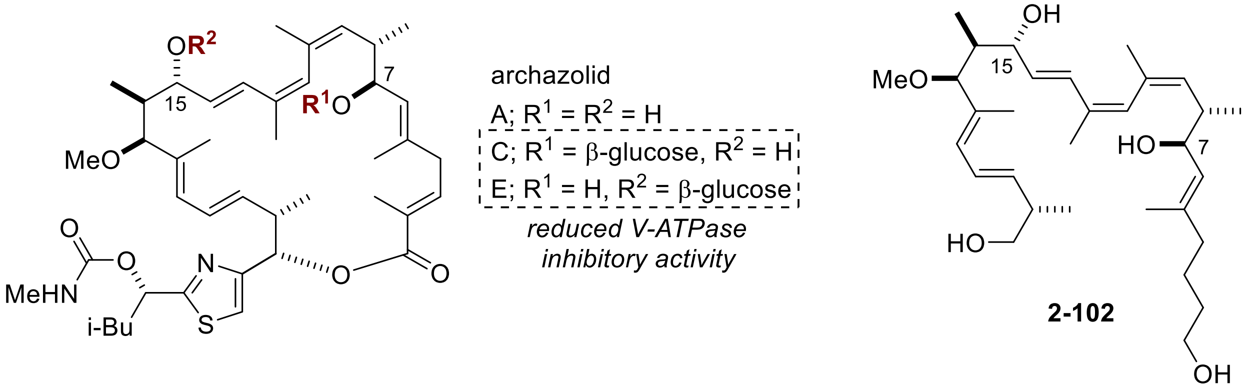
OR2
15
7
R1O
MeO
O
O
MeHN
i-Bu
N
S
O
O
archazolid
A; R1 = R2 = H
C; R1 = β-glucose, R2 = H
E; R1 = H, R2 = β-glucose
reduced V-ATPase
inhibitory activity
OH
MeO
15
HO
7
HO
2-102
OH

Figure 2-4. Demonstration of pharmacophore effects in **2-102**.

To test this, compound **2-102** was subjected to our *Arabidopsis*-based V-ATPase assay and shown to have an IC_{50} = 25 µM (Figure 2-4). This important result provides further evidence that the C7 and C15 hydroxyls connected by the triene are a pharmacophore for V-ATPase inhibition. The IC_{50} of **2-102** was roughly 100 x higher than the well-established V-ATPase inhibitor cocanamycin A (IC_{50} = 0.25 µM), however. Nonetheless, the modest activity archazolid of **2-102** is still significant and this compound can serve as a starting point to further understand archazolid V-ATPase inhibition.

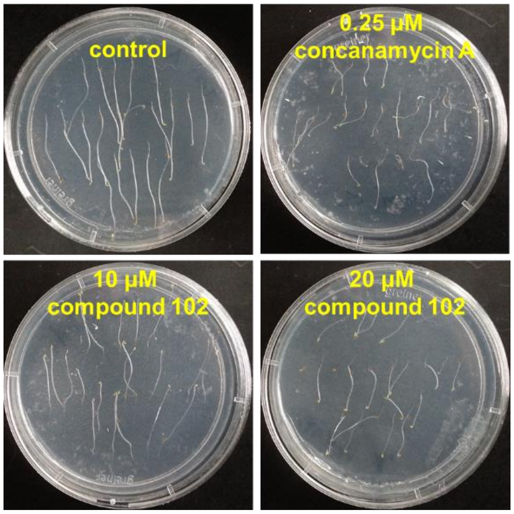

Figure 2-5. *Arabidopsis*-based V-ATPase inhibition of compound **2-102** and cocanamycin A.

In 2014, Reker et al. published a theoretical investigation into the biological activity of natural product derived fragments (NDPFs).[39] This query led to the development of an algorithm that allowed them to computationally evaluate fragments of natural products that could be potentially potent drugs on well known drug targets. They used archazolid A as a model for this algorithm and published an archazolid A based fragment (**2-103**) that they believe would possess a low IC_{50} against the cyclooxygenase-2 (COX-2) enzyme (Figure 2-6).

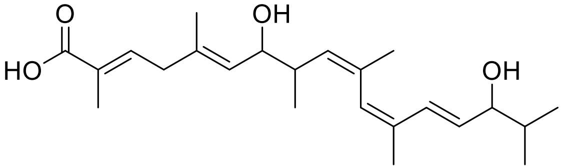

Fragment 1
2-103

Figure 2-6. Reker et Al. predicted potent COX-2 inhibitor fragment 1.

The authors went on to argue that archazolid A has a similar structure to the native substrate for COX-2, arachidonic acid (Figure 2-7). However, when assayed, archazolid A only had a 24 ± 6% inhibition of COX-2 at 10 µM.[39] Reker et al. justified this result with the fact that the inhibition site of COX-2 has a very narrow entry point, which could be blocking the large macrocyclic structure of archazolid A, whereas arachidonic acid (and fragment **2-103**) can get through due to its flexible and linear nature.[39] Due to the similarity of the predicted COX inhibitor **2-103** and our synthesized compound **2-102**, a COX-2 inhibition assay was performed. Somewhat surprisingly, compound **2-102** did not show any COX-2 inhibition (<5% at 200 μM), which could potentially be for two reasons: (1) either it is still too large to get to the buried site of inhibition, or (2) the carboxylic acid is a pharmacophore for COX inhibition.

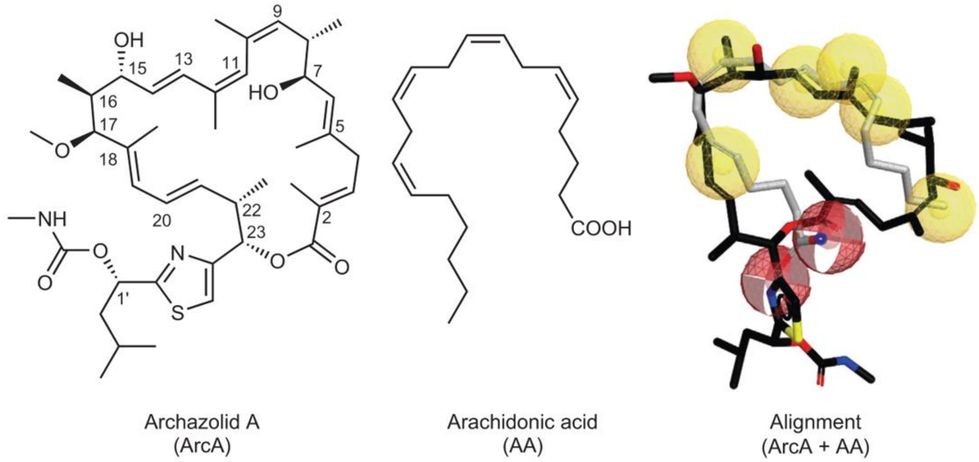

Archazolid A
(ArcA)

Arachidonic acid
(AA)

Alignment
(ArcA + AA)

Figure 2-7. Structural overlay of arachidonic acid and archazolid A.[39]

COX-2 inhibition is important in anti-cancer activity because it is highly upregulated in cancer cells.[40] It is also responsible for the inflammation response as well as proliferation of those cancer cells. Due to its importance in anti-cancer activity, and in order to better understand the lack of COX-inhibition for compound **2-102**, we set out to synthesize the hypothetical COX-2 inhibitor **2-103** proposed by Reker et al.

Chapter 3: Synthetic Plan and Work towards Proposed COX-2 Inhibitor Fragment 1 (2-103).

3.1 Suzuki Coupling

Even though the yields of the Stille coupling of **2-96** and **2-97** were high (82%, Scheme 2-26), this type of cross-coupling is not ideal due to the toxicity associated with organotin compounds. As an alternative, Suzuki couplings are preferred. Both Stille and Suzuki couplings use a palladium catalyst, however the organostannane of the Stille is replaced with an organoborane for the Suzuki. Overall, the Suzuki coupling is a four-step process: oxidative addition, base removal of the halide, transmetalation, and reductive elimination as shown in Figure 3-1.

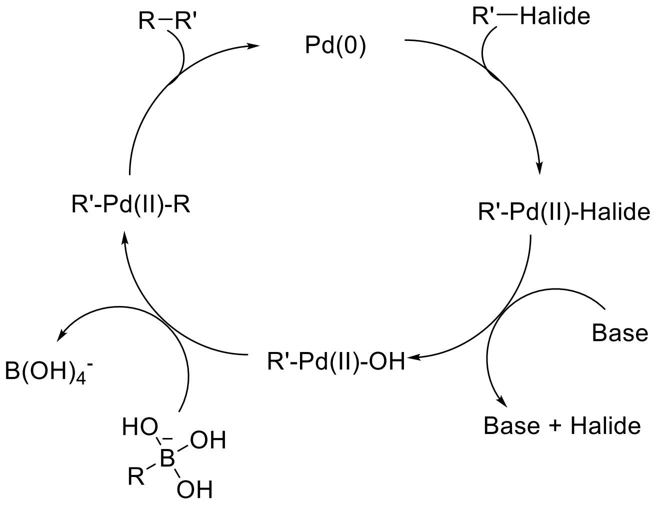

Figure 3-1. General Suzuki coupling mechanism.

Suzuki couplings were first discovered in 1979 and since then have become among the most widely applied palladium-catalyzed cross-coupling reactions.[1,2] These C-C bond forming reactions have variable conditions (e.g. choice of palladium catalyst, base, solvent, temperature) that can be optimized for specific substrates. Attributes such as these allow for them to be scaled for industrial applications as well as tailored to complex and unstable reactants. The number and type of applications has expanded exponentially since its discovery, culminating in a Nobel Prize in 2010. As shown in Figure **3-2**, since 1995 reports of Suzuki couplings have been increasing almost exponentially. Directly comparing the Stille coupling to the Suzuki coupling, both have had an increase in the number of publications since the 1990s, however the Suzuki coupling has been increasing at a much higher rate, potentially due to its commercial availability of precursors, high stabilities or organoborane reagents towards air and moisture, and potentially the most important, its use of nontoxic boronic acids.

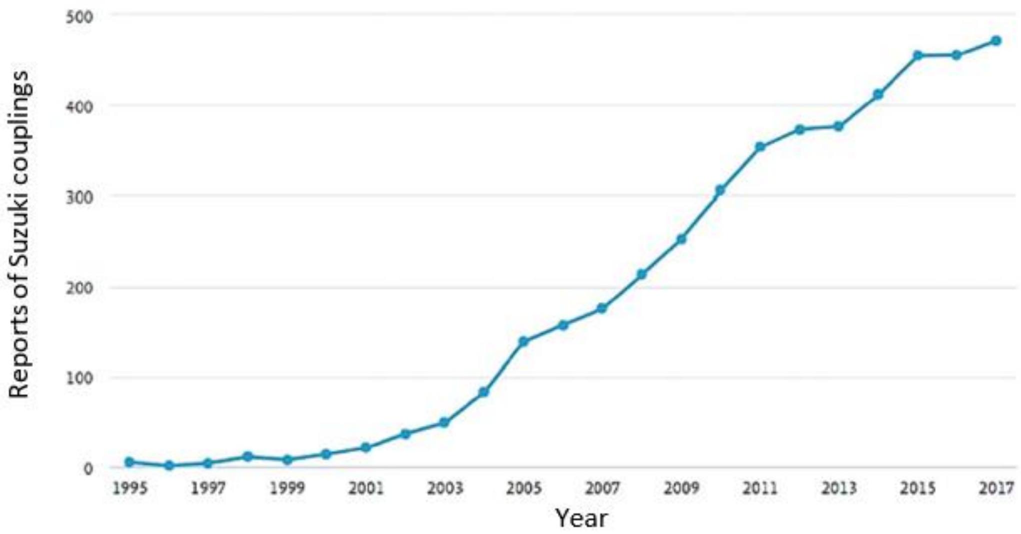

Figure 3-2. Documents containing reports of Suzuki couplings versus the year.[3]

Another comparison is presented in Figure 3-3, which describes the number of medicinal chemistry applications of different palladium-catalyzed reactions published over the last few decades. As can be seen, Suzuki couplings have emerged as the most widely used palladium-catalyzed process and among the most widely used of any reactions in this industry.[4]

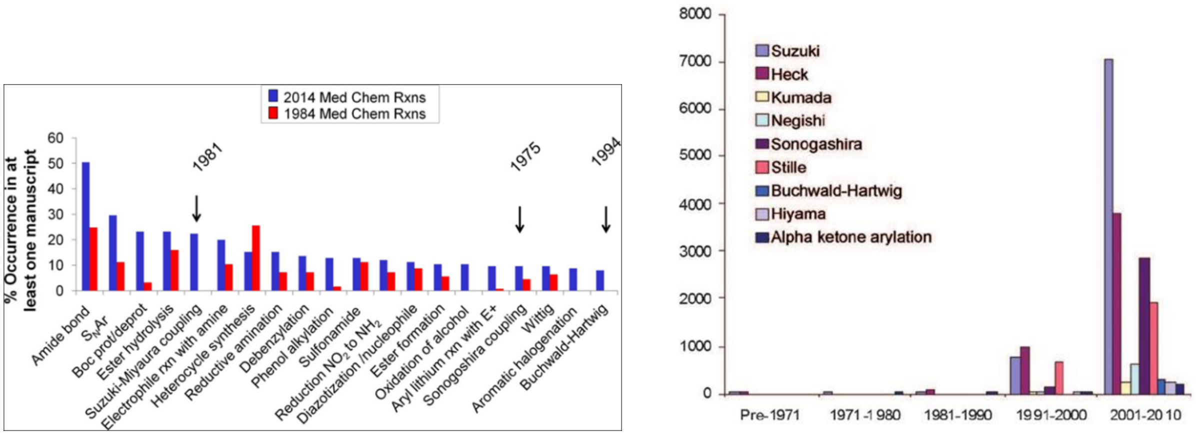

Figure 3-3. Two figures showing the asymptotic increase of Suzuki coupling reactions published as the reaction was discovered and utilized.[5,6]

Our investigations into a potential Suzuki coupling-based synthesis of the archazolid triene began with attempting to establish proof of principle that this type of coupling would work. The reaction could then be optimized in order to generate sufficient material for further studies. As outlined in the table below, when optimizing Suzuki couplings there typically are six parameters that can be varied; 1) nature of the boronate, 2) halide, 3) palladium source, 4) base, 5) solvent, 6) temperature of the reaction.

Table 3-1. The variable conditions of natural product synthesis utilizing Suzuki couplings, as detailed in by Koshvandi et al.[7]

Catalyst	Boronate	Halide	Base	Solvents	Temperature Range (°C)
$Pd(dppf)Cl_2$	acid, pin, KBF_3	I, Br	Cs_2CO_3, K_2CO_3, KOAc, Na_2CO_3, CsF/TBAB, KOH, K_3PO_4	DMF, tolune, ethanol, water, THF, dioxane, DME, MeCN,	rt-150
$Pd(OAc)_2$	pin, acid, isopropoxy	I, Br	Cs_2CO_3, K_2CO_3, Na_2CO_3	dioxane, water, DMF	80-100
$Pd(PhCN)_2Cl_2$	acid	Cl	CsF/TBAB	toluene, water	60
$Pd(PPh3)_2Cl_2$	acid, pin	Cl, I, Br	K_3PO_4, Na_2CO_3, NaOtBu, TEA	toluene, water, DME, methanol	70-80
$Pd(PPh_3)_4$	acid, pin, isopropoxy	I, Br, Cl, OTf, Phos	Ag_2O, Cs_2CO_3, CsF, K_2CO_3, K_3PO_4, Na_2CO_3, NaOH, TBAF,TIOEt, TEA	dioxane, water, DMF, THF, methanol, DME, toluene, ethanol, *i*-PrOH,	rt-110
$Pd(t\text{-}Bu_3P)_2$	ethylene glycol, boroxine, pin	I, Br	Na_2CO_3, Cs_2CO_3	DME, ethanol, THF, water	rt-100
Pd/C	acid	Br	Na_2CO_3	methanol	reflux
$Pd_2(dba)_3$	pin, acid	I, Br, OTf	K_3PO_4, Cs_2CO_3, KF, Na_2CO_3	DMF, ethanol, water, toluene, THF, methanol	rt-110
$Pd_2(PCy_3)_2$	acid	I	Na_2CO_3	toluene, methanol	65

The first condition that is often adjusted is the boronic ester. A recent review from Koshvandi, covering just natural product syntheses featuring Suzuki couplings that have been published from 2012 until 2017 (and therefore not comprehensive), described a total of seven different boron groups that had been utilized. Examples of Suzuki couplings utilizing a pinacol borane and a boroxine are shown below in order to illustrate the wide variety of boron groups that can be used in a Suzuki coupling.[7] A more complete list is given in Table 3-1.

Scheme 3-1. Two examples illustrating different boron groups used for Suzuki coupling.

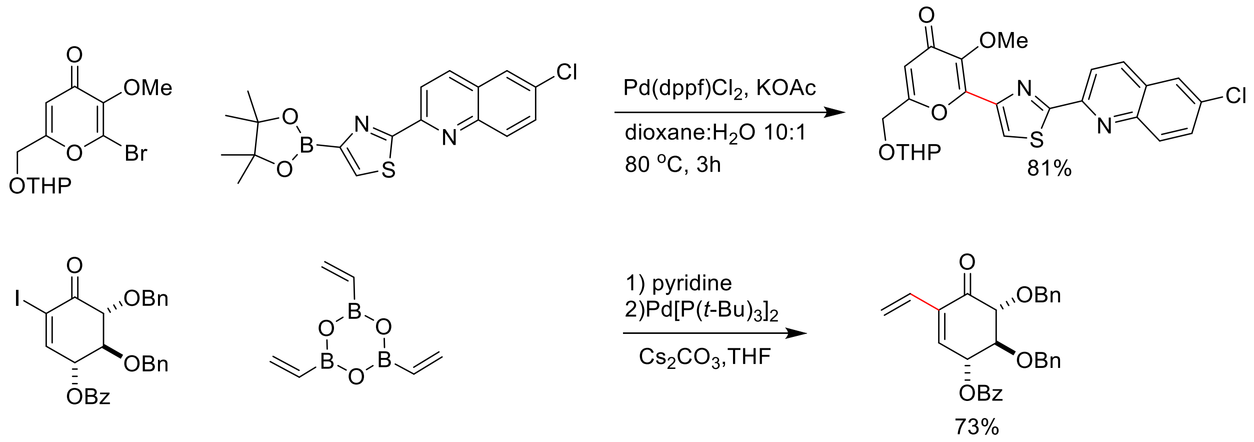
O
OMe
O
Br
OTHP
O
B
O
N
S
N
Cl
Pd(dppf)Cl2, KOAc
dioxane:H2O 10:1
80 °C, 3h
81%
I
OBn
OBn
OBz
B
O
O
B
O
B
1) pyridine
2)Pd[P(t-Bu)3]2
Cs2CO3,THF
73%

While these are two interesting examples, there are many other boron substituents that can be used. From a review published on the study of selecting boron reagents for Suzuki couplings, Lloyd-Jones et al. investigated the most common boron reagents. Within this review, they mapped out the uses, reactivity, and many other important attributes about specific boron species (Table 3-2)[8].

Table 3-2. An example of the wide variety of boron groups as well as benefits and attributes[8].

Class	Structure	Prep	Pros	Cons	Reactivity
Organoboranes	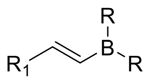	Hydroboration	Easily prepared	prone to oxidation, less reactive in transmetallation	boronate or oxo-palladium pathway, depending on boron lewis acidity
Boronic esters	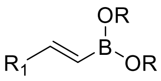	Miyaura borylation, Hydroboration	Easily prepared and purified, monermeric, stable to silica gel	less reactive in transmetalation	mecahnism of transmetalation uncertain
Boronic acids	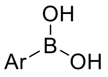	Organometallic	Easily prepared, atom-efficient, highly reactive in transmetalation	susceptible to protodeboronation, oxidation, and homocoupling	oxo-palladium pathway is kinetically the most likely pathway for transmetalation
Trifluoroborates	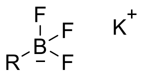	KHF_2, KF/tartaric acid	stable solids, monomeric, free-flowing, powder	can cause etching of glassware, hydrolysis rate and thus transmetalation rate is variable	prior hydrolysis to boronic acid necessary, electron poor = slow hydrolysis, electron rich = fast hydrolysis
N-Coordinated borates	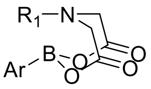	Condensation, Organometallic	stable solids, monermic, ICC	low atom efficiency	prior hydrolysis to boronic acid necessary for transmetalation
Boronates	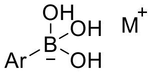	Condensation, Organometallic	Stable, monomeric, base-free SM coupling	not yet commercially availible	boronate pathway possible, but *in situ* liberation of base also likely
Boronamides	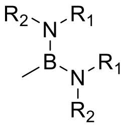	Condensation	monomeric, stable to aqueous SM coupling, silica-gel and work-up, ICC	low atom efficiency	prior hydrolysis to boronic acid necessary for transmetalation

Many different palladium sources can also be used ranging from $Pd(dppf)Cl_2$ to Pd/C, with $Pd(PPh_3)_4$ seeming to be the most common. The different palladium sources change not only the reactivity of the palladium, for instance starting with palladium (0) or palladium (II), but the differing ligands on palladium can also have effects on the reaction as a whole. Shown below are representative examples demonstrating the different types of palladium catalysts that can be chosen for Suzuki couplings (Scheme 3-2).

Scheme 3-2. Three examples of different palladium sources used in Suzuki couplings.

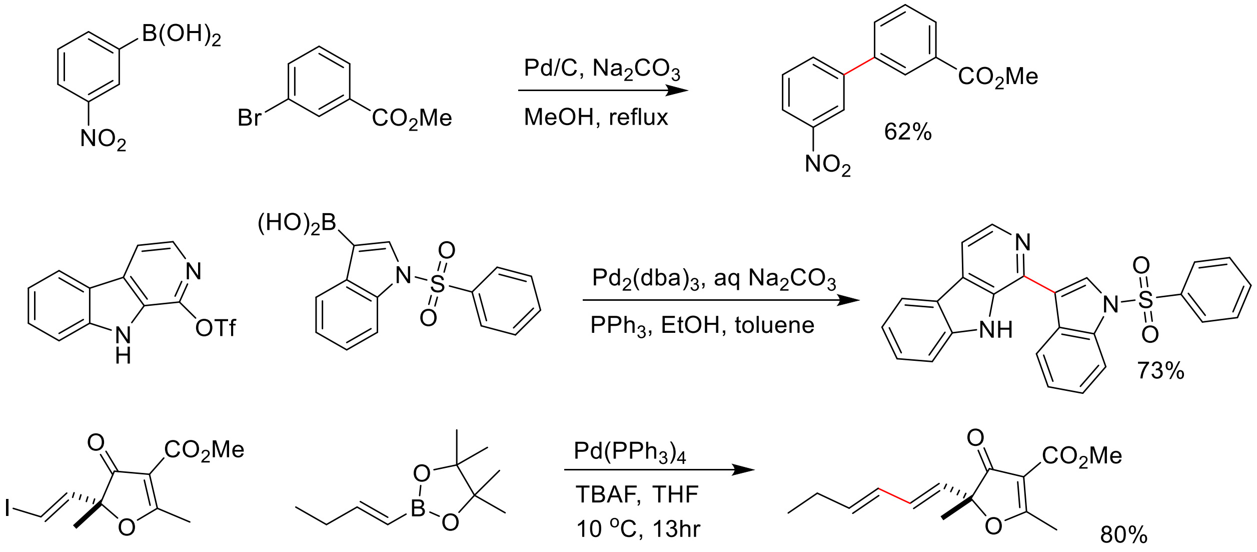
B(OH)2
NO2
Br
CO2Me
Pd/C, Na2CO3
MeOH, reflux
CO2Me
62%
NO2
(HO)2B
N
OTf
N
H
N
S
O
O
Pd2(dba)3, aq Na2CO3
PPh3, EtOH, toluene
N
NH
N
S
O
O
73%
O
CO2Me
I
O
O
B
O
Pd(PPh3)4
TBAF, THF
10 °C, 13hr
O
CO2Me
O
80%

One of the most important parameters to consider, which is often dependent on the stability of the reactants, is the choice of base for the reaction. The role of the base in Suzuki couplings is to not only activate the palladium source (e.g. to palladium (0) if starting with Pd(II)), but also to activate the boronate for the transmetalation step. The review from Koshvandi presented 15 different bases used in successful Suzuki couplings, but again this was limited to five years and therefore represents only a portion of bases that have been used in Suzuki couplings. The bases not only vary in pK_a, but also their size and counter ions, where again the choice of base is often influenced by substrate stability. Examples given in Scheme 3-3 show different bases ranging from NaOH to Ag_2O and K_3PO_4. From the other examples of Suzuki couplings, it can be noted that carbonates (e.g. Na_2CO_3), hydroxides (e.g. NaOH), and other bases can be used (Scheme 3-3).

Scheme 3-3. Three examples of different bases used in Suzuki couplings.

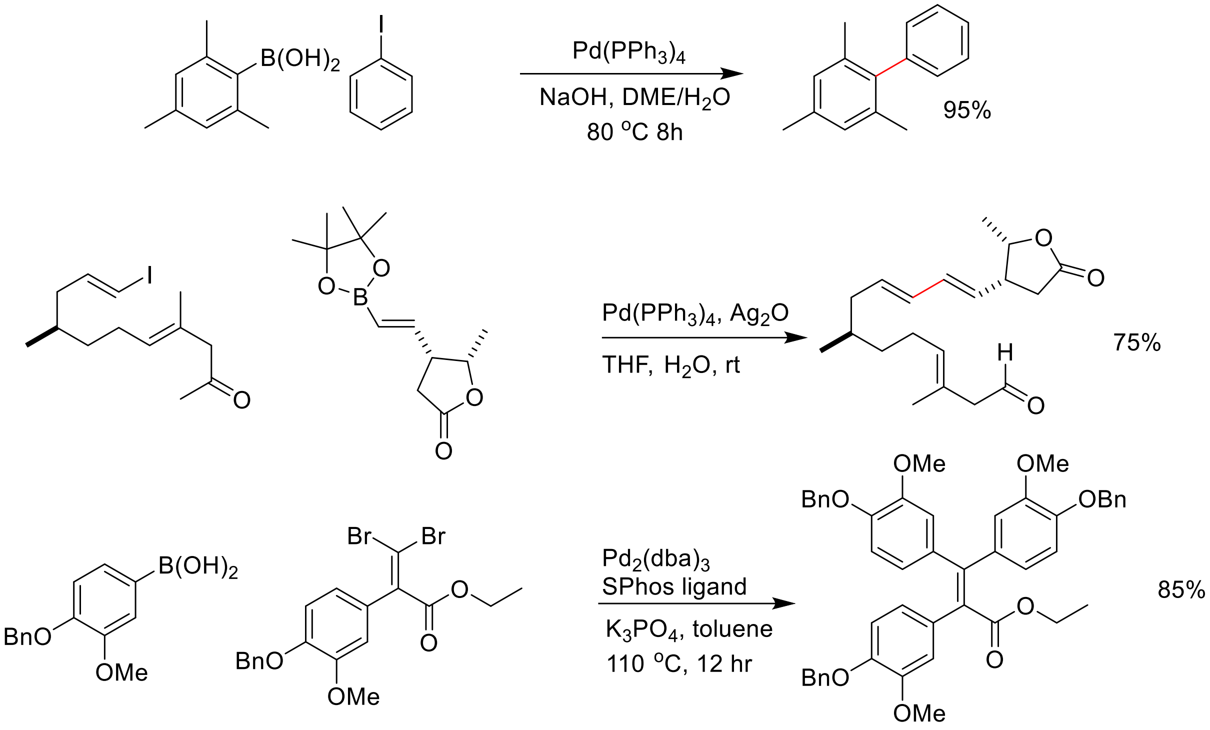

B(OH)2
I
Pd(PPh3)4
NaOH, DME/H2O
80 °C 8h
95%
I
O
B
O
O
O
O
Pd(PPh3)4, Ag2O
THF, H2O, rt
O
O
O
H
O
75%
B(OH)2
BnO
OMe
Br
Br
O
O
BnO
OMe
Pd2(dba)3
SPhos ligand
K3PO4, toluene
110 °C, 12 hr
OMe
OMe
BnO
OBn
O
O
BnO
OMe
85%

Other conditions that are often adjusted are the temperature of the reaction, the solvent, as well as any additives ($AsPh_3$, P(*t*-Butyl)$_3$, S-Phos) that might improve the reaction. Temperature can be increased to drive reaction progress. One method for accelerating Suzuki coupling by heat is to use microwave conditions. Microwave conditions can allow shorter reaction times due to more even heating within the reaction. For example, McCluskey et al. reported that the Suzuki coupling shown in Scheme 3-4 to create a biaryl framework gave only 13% yield after 5 days when performed under standard heating (refluxing THF) [9]. However, when this reaction was subjected to microwave conditions (100 W/150 °C) the yields were quantitative after 30 minutes.

Scheme 3-4. An example of microwave assisted Suzuki coupling improving yields as well as shortening the time of reaction.

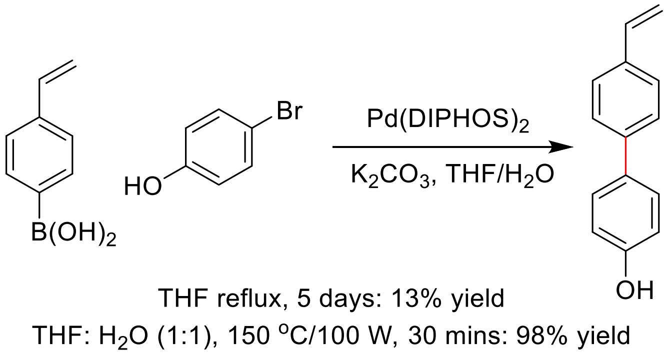
Br
HO
B(OH)$_2$
Pd(DIPHOS)$_2$
K$_2$CO$_3$, THF/H$_2$O
OH
THF reflux, 5 days: 13% yield
THF: H$_2$O (1:1), 150 ^{o}C/100 W, 30 mins: 98% yield

The choice of solvent allows for the most freedom in the Suzuki couplings with the qualifiers being that the reactants are soluble in the solvent as well as they will not interact with the catalyst or the base as a whole. However, as the push towards greener chemistry has gained more traction in research, there have been many recent publications with water being a part of the reaction mixture. This can be challenging, especially for natural product synthesis as many of these are small organic molecules that are not soluble in water. However, by adjusting the reaction conditions, Suzuki coupling of hydrophobic small molecules in water can still occur. One example is by Karimi et al. who used SiO_2 to anchor hydrophilic triethylene glycol imidazolium to encapsulate the palladium catalyst and the substrates within the ionic liquid functionalized magnetic nanoparticles which allowed for the Suzuki coupling to occur in water (Scheme 3-5)[10].

Scheme 3-5. An example of greener Suzuki couplings occurring within water.

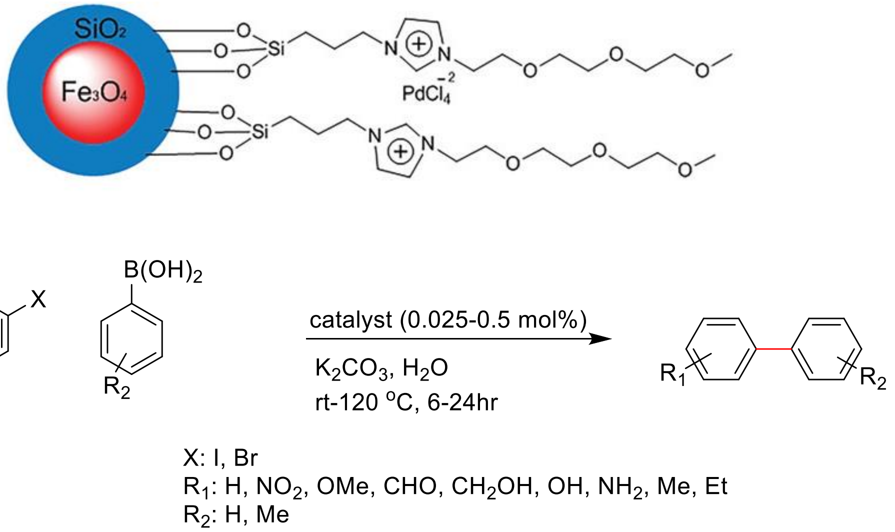
SiO2
Fe3O4
PdCl4 -2
B(OH)2
X
R1
R2
catalyst (0.025-0.5 mol%)
K2CO3, H2O
rt-120 °C, 6-24hr
X: I, Br
R1: H, NO2, OMe, CHO, CH2OH, OH, NH2, Me, Et
R2: H, Me

Substrate structure can also have a profound influence on the success of Suzuki couplings. The majority of the Suzuki reactions that have been reported occur between two sp^2 hybridized carbons, as Suzuki et al. first showed when they published their research in 1979.[11] However, recent publications have shown that Suzuki couplings can also be used between sp^3 and sp^2 hybridized carbons (Scheme 3-6).[12] This expanded scope makes this reaction seemingly limitless, and this reaction will no doubt continue to be a powerful tool in the organic chemist's toolbox.

Scheme 3-6. Examples of sp^3-sp^2 hybridized carbon Suzuki reactions.

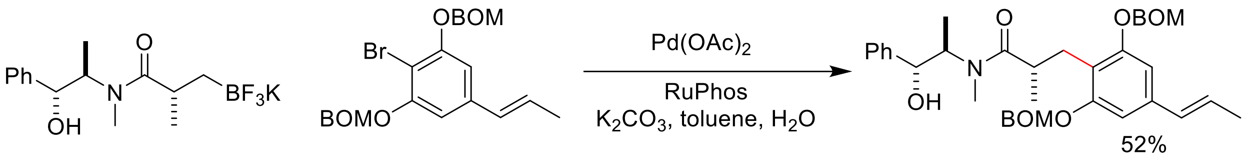
Ph
OH
O
N
BF3K
Br
OBOM
BOMO
Pd(OAc)2
RuPhos
K2CO3, toluene, H2O
52%

In order to narrow the possible Suzuki coupling conditions to be tested for our application, we opted to first investigate conditions that were used to couple fragments most similar to our own. In this way, a Suzuki reaction reported by Menche et al. that was used to synthesize the complex polyene polyketide etnangien was identified.[13] Due to the sensitive nature of the target polyene product, this group opted for the use of $Ba(OH)_2$ as base. In this way, compounds **3-1** and **3-2** were coupled to give the product **3-3** in 83% yield. We anticipated that the archazolid conjugated triene Suzuki target would be similarly sensitive, and decided that these conditions would be the starting point for our own investigations.

Scheme 3-7. Suzuki coupling within the synthesis of the complex polyene polyketide etnangien by Menche et al.[13]

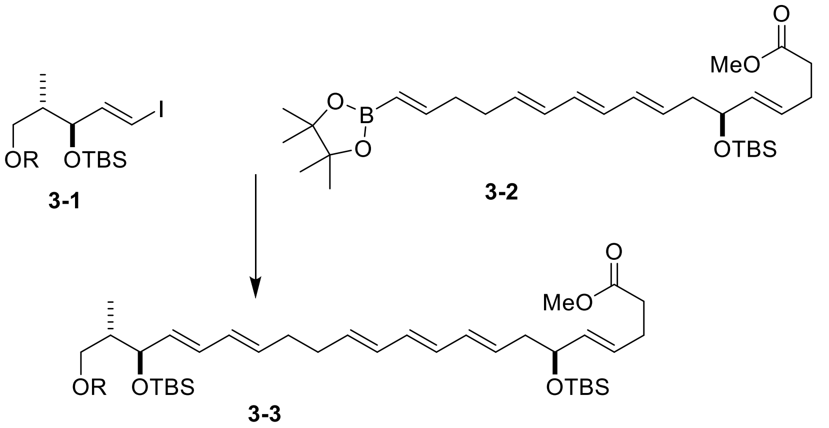

3.2 Synthetic Route Changes

My work began on the eastern fragment synthesis of dihydroachazolid B, adjusting the synthesis slightly to install a vinyl boronate rather than a vinyl stannane so that a Suzuki coupling could be employed rather than a Stille coupling. Overall, the general scheme stayed the same except for the last step, where instead of doing a transmetallation to a vinyl stannane from a vinyl iodide, we would employ a lithium halogen exchange and trapping with isopropoxy boronate and pinacol, in order to make the pinacol boronic ester as shown in Scheme 3-8.

Scheme 3-8. The updated eastern fragment **3-4** for Suzuki Coupling.

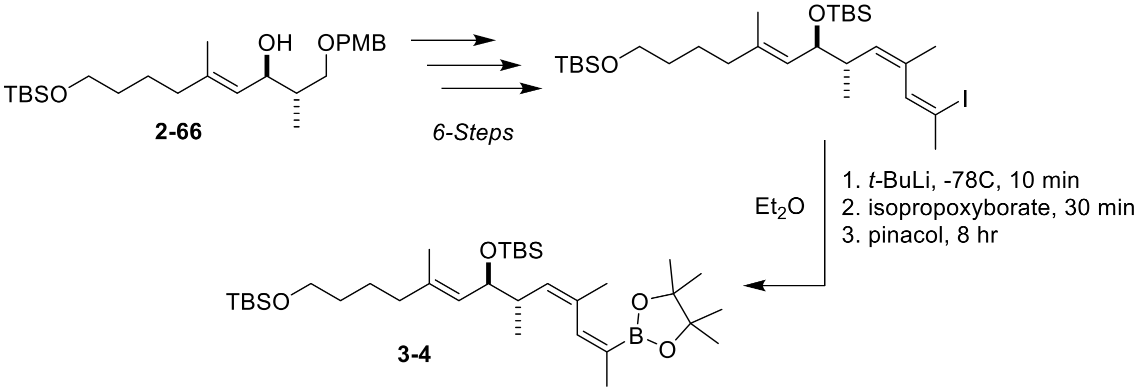
TBSO
OH
OPMB
2-66
6-Steps
TBSO
OTBS
I
Et$_2$O
1. *t*-BuLi, -78C, 10 min
2. isopropoxyborate, 30 min
3. pinacol, 8 hr
TBSO
OTBS
O
B
O
3-4

Working our way through the eastern fragment synthesis, it was realized that the overall progression was slowed down by the synthesis of the Still-Gennari phosphonate reagent **2-68**.[14] This compound was obtained by methylation of the commercial trifluoroethyl phosphonate **3-5** with KO^{t}Bu and methyl iodide. However, this reaction often proceeded with incomplete conversion giving a mixture of phosphonates **3-5** and **2-68** that were difficult to separate. Moreover, any amount of non-methylated **3-5** in the subsequent Still-Gennari produced the disubstituted alkene **3-6** that could not be separated from the desired trisubstituted alkene **2-69** by chromatography on silica.

Scheme 3-9. The difficult to purify phosphonates and their corresponding olefination products.

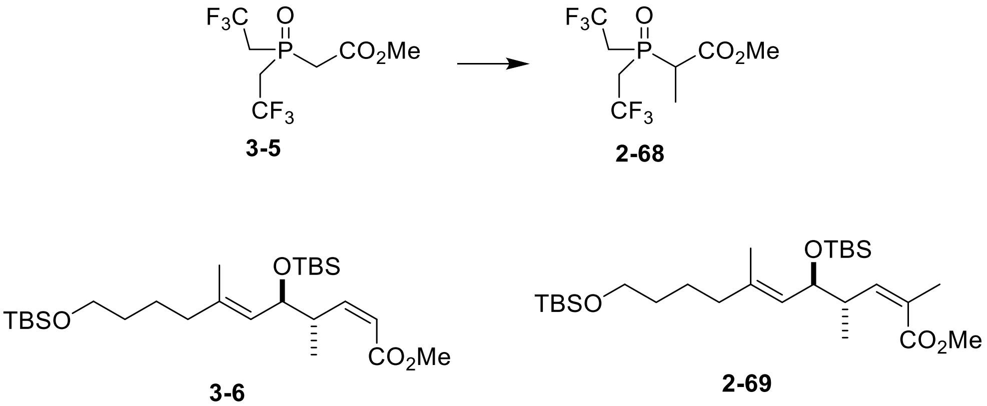
F$_3$C
O
P
CO$_2$Me
CF$_3$
3-5
F$_3$C
O
P
CO$_2$Me
CF$_3$
2-68
TBSO
OTBS
CO$_2$Me
3-6
TBSO
OTBS
CO$_2$Me
2-69

Because of the difficulty of this process, a new eastern fragment synthesis was devised where instead of producing a cis-alkene using an intermolecular Still-Gennari, it would be installed by using an intramolecular Horner-Wadsworth-Emmons reaction. This new synthesis differed from the original synthesis after the zirconocene step at the free secondary hydroxyl **2-66** (Scheme 3-10)**.** The free hydroxyl was esterified with DCC and phosphonate **3-13** (synthesized in three steps from dibromo **3-9** as shown in Scheme 3-10) to create ester **3-7**. This ester was then taken through a PMB deprotection as well as oxidation to give aldehyde **3-8**.

Scheme 3-10. Shortened eastern fragment synthesis through the use of phosphonate **3-13**.

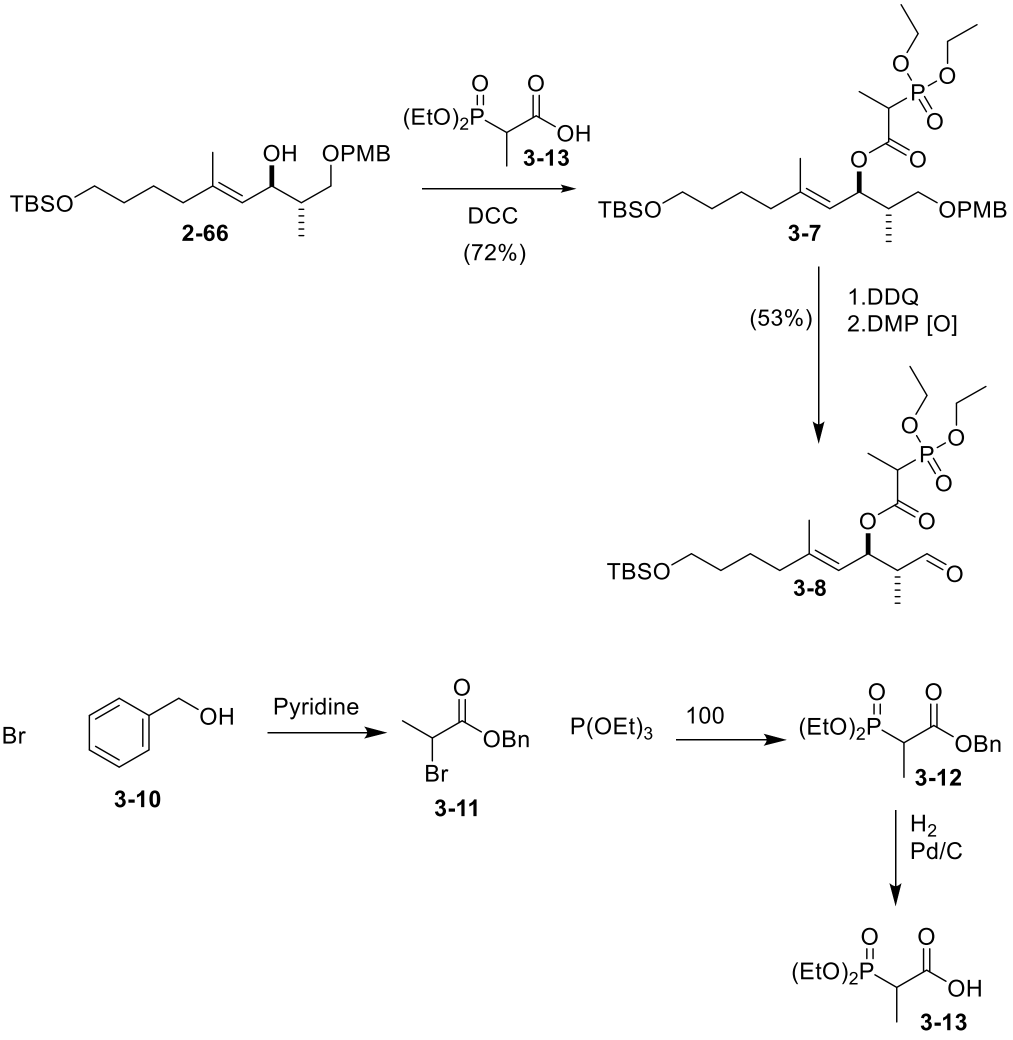
TBSO
OH
OPMB
2-66
(EtO)2P
O
OH
3-13
DCC
(72%)
3-7
(53%)
1.DDQ
2.DMP [O]
3-8
Br
3-9
3-10
Pyridine
OBn
3-11
P(OEt)3
100
3-12
H2
Pd/C
3-13

It was at this point that we could now employ the intramolecular Horner-Wadsworth-Emmons to create the cis-alkene in the form of lactone **3-14**.[15] A number of bases were screened as outlined in Table 3-3. A mixture of products was observed when the HWE olefination was attempted. Through careful analysis of the two distinct products, it was determined that while our desired lactone was being created, the reaction was also producing the elimination product **3-15**, presumably through the E2 mechanism (Scheme 3-11).

Scheme 3-11. Formation of diene **3-15** through the E2 mechanism.

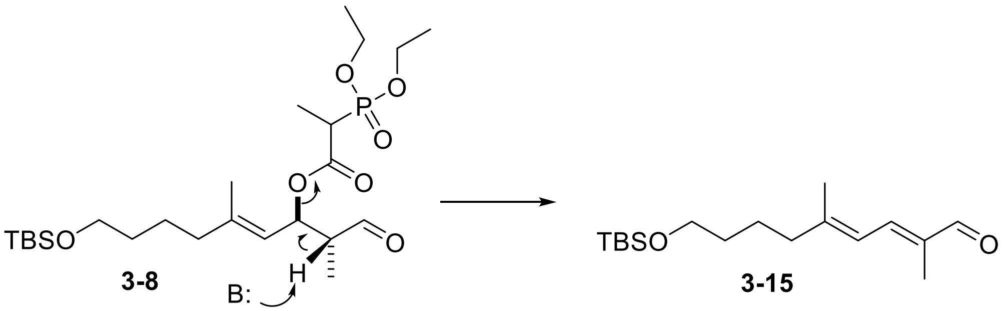

Multiple conditions were tested in order to receive the highest selectivity towards the desired lactone and it was found that through activation with barium hydroxide, a maximum of 5:1 selectivity for the lactone versus the E2 product could be obtained.

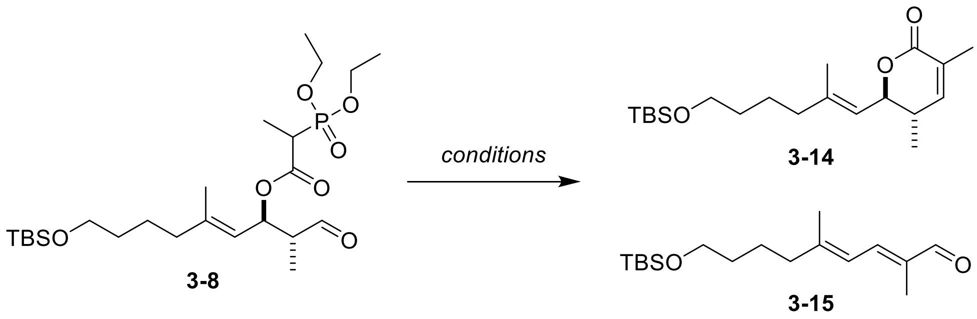

Table 3-3. Optimization of intramolecular HWE reaction of **3-8** to produce lactone **3-14**.

Base	**pKa**	**Metal Chelator**	**3-14 : 3-15**[a]
TEA	9	Lithium[b]	2:1
K_2CO_3	10.25	Potassium	1:1
DIPEA	10.75	Lithium[b]	5:1
DBU	12	Lithium[b]	1:20<
$Ba(OH)_2$	15.7	Barium	5:1
KHMDS	26	Potassium	1:20<
NaH	35	Sodium	5:1

[a]Determined by NMR. [b]Lithium sources was LiCl.

Once the lactone was obtained, it was reduced to the lactol **3-16** with DIBAl-H, which is in equilibrium with the aldehyde **3-17**. An iodo-Wittig was attempted using ethyltriphenylphosphonium iodide under the same conditions that were used for our previous Stille-based synthesis, but unfortunately only the starting lactol was ever recovered. It was hypothesized that the lactol was much more stable than the aldehyde **3-15** that was needed for the iodo-Wittig (Scheme 3-12). Thus, we attempted to warm the reaction slowly to room temperature in order to promote equilibration and create more of the aldehyde. However, this resulted in decomposition of the phosphonium-ylide, evidenced by loss of its characteristic bright red color upon warming.

Scheme 3-12. Proposed pathway to synthesize vinyl iodide **3-18** from lactone **3-14**.

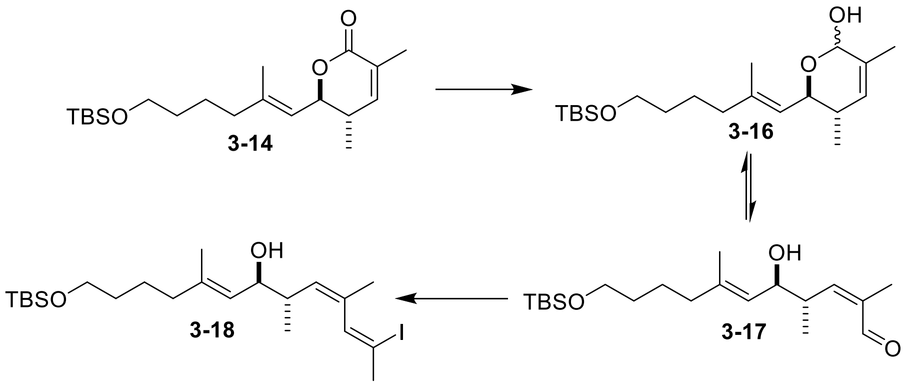

3.3 Boron-Wittig Chemistry

Due to our inability to convert lactol **3-16** to vinyl iodide **3-18**, a new method of installing a vinyl boronate was investigated. We envisioned an alternative Wittig approach but instead of using a phosphonium iodide, it would use an alkyl diboronate to directly convert lactol **3-16** to vinyl boronate **3-19** as shown in Scheme 3-13.

Scheme 3-13. Proposed pathway from lactol **3-16** to vinyl boronate **3-19** through a boron-wittig reaction.

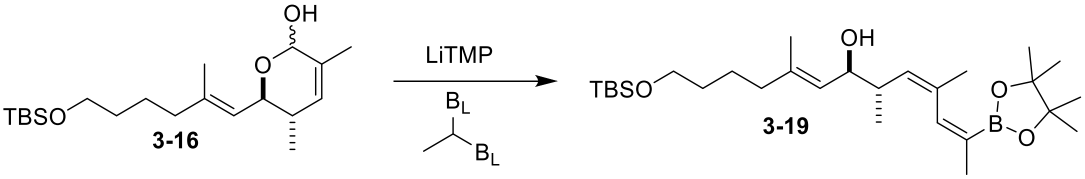

B_L = Bpin or Bdmpd

In 2010 Endo et al. published a new synthesis of tetrasubstituted alkenylboronates.[16] They found that after deprotonation of a 1,1-organodiboronate, it could undergo a nucleophilic addition to a carbonyl compound, specifically a ketone, followed by elimination to give the corresponding vinyl boronate ester (3-14).[16]

Scheme 3-14. General reaction boron-Wittig reaction scheme proposed by Endo et al.[16]

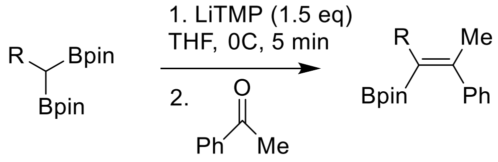
R
Bpin
Bpin
1. LiTMP (1.5 eq)
THF, 0C, 5 min
2.
O
Ph
Me
R
Me
Bpin
Ph

In their paper, Endo et al. showed that with a variety of 1,1-organodipinacolboronates they generally received both high yields (34-98%) and high stereoselectivity (>99:1) in favor of the *E* isomer (Table 3-4).

Table 3-4. Variety of 1,1-diboronates and their yields, and selectivity.[16]

Entry	1,1-diboronate	product	%yield (*E/Z*)
1	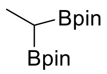	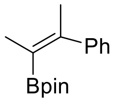	94 (>99:1)
2	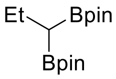	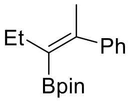	94 (>99:1)
3	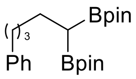	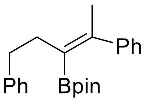	83 (>99:1)
4	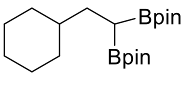	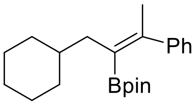	74 (>99:1)
5	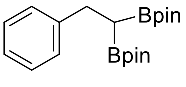	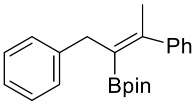	98 (>99:1)
6	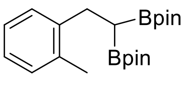	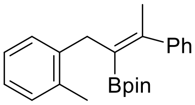	75 (>99:1)
7	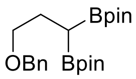	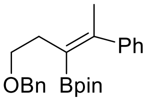	34 (>99:1)

The reaction was also tested on a variety of a ketones with differing substituents and steric bulkiness. Once again, they received high yields with high *E*-stereoselectivity. They were able to show that aryl ketones bearing an electron-withdrawing or electron-donating substituent did not change the overall stereoselectivity while only slightly changing the yield of the reactions. For example, entry 11 containing an electron-donating methoxy group was obtained in 74% and 99:1 *E*:*Z* whereas entry 10 possesses no electron-withdrawing group on its benzene and was obtained in 98% and 99:1 *E*:*Z* (Table 3-5).[16]

Table 3-5. Variety of ketones and their corresponding yields and selectivity.[16]

Entry	ketone	product	%yield (*E/Z*)
1	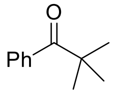	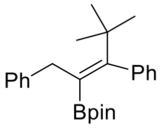	93 (>99:1)
2	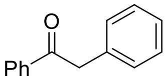	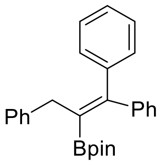	98 (>99:1)
3	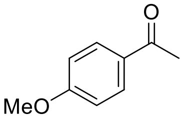	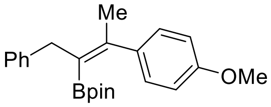	72 (>99:1)
4	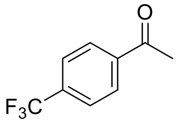	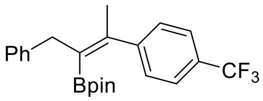	70 (>99:1)

Dr. James Morken took this reaction one step further to control the stereoselectivity of synthesized trisubstituted alkenes. For this, they first synthesized the stable alkylborates from diboranes. Then, these reactants were used in a boron-Wittig reaction with aldehydes using

LiTMP as base. The first experiment reported was a reaction of hexanal with several bis-boronate esters **3-20** through **3-22** (Scheme 3-15).[17]

Scheme 3-15. Stereospecific synthesis of trisubstituted vinyl boronates proposed by Morken et al.[17]

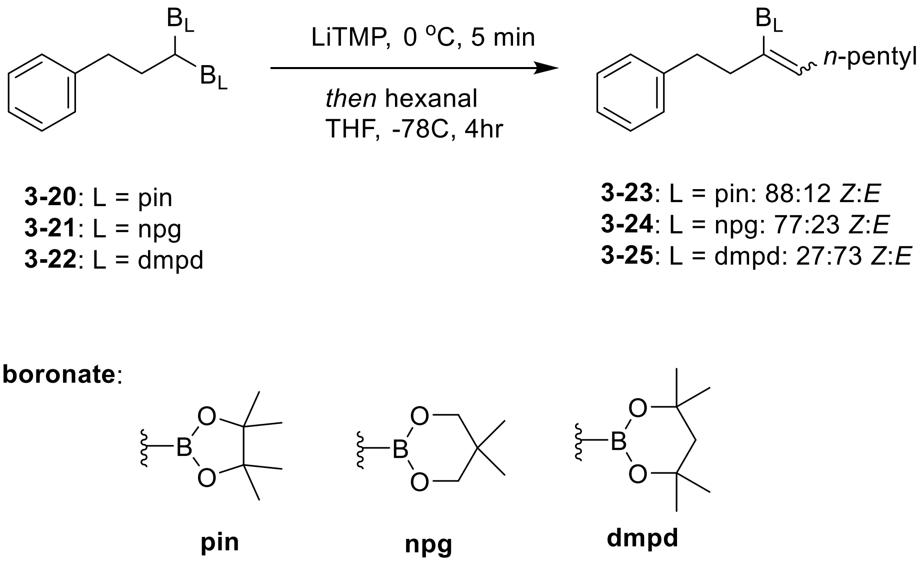

3-20: L = pin
3-21: L = npg
3-22: L = dmpd

3-23: L = pin: 88:12 *Z*:*E*
3-24: L = npg: 77:23 *Z*:*E*
3-25: L = dmpd: 27:73 *Z*:*E*

What Morken et al. noticed was that the stereochemistry was dramatically affected by the nature of the boronic ester employed in the form of a geminal bis(boronate). They could completely reverse the stereoselectivity based on the specific boronic ester they chose.[17] Specifically, when using a pinacol boronic ester, they received an 88:12 *Z*:*E* ratio whereas the dimethylpentanediolato (dmpd) boronic ester produced a 27:73 *Z*:*E* ratio of products. In order to investigate this influence further, they constructed and employed a variety of alpha-branched aldehydes and examined their reaction with geminal pinacol-, npg, and dmpd bis(boronates). In all cases LiHMDS was used as base, the reactions were conducted by deprotonating the bis(boronate) with 1.2 equivalents of LiHMDS at 0 °C for 5 minutes, then cooling the reaction mixture to -78 °C, adding the aldehyde, and stirring for four hours (Scheme 3-16).[17]

Scheme 3-16. Variety of substrates shown by Morken at al. demonstrating substrate selectivity based on boronic ester.[17]

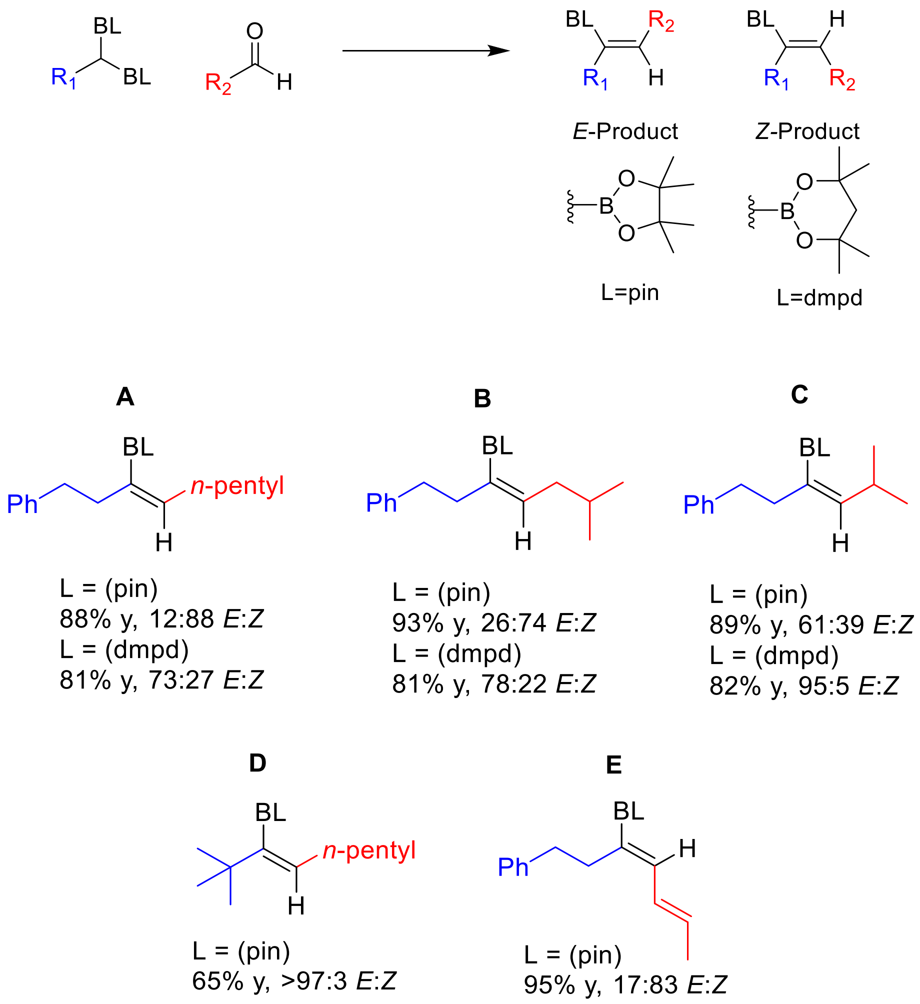
BL
R_1
BL
O
R_2
H
BL
R_2
R_1
H
BL
H
R_1
R_2
E-Product
Z-Product
O
B
O
L=pin
O
B
O
L=dmpd
A
BL
Ph
n-pentyl
H
L = (pin)
88% y, 12:88 *E*:*Z*
L = (dmpd)
81% y, 73:27 *E*:*Z*
B
BL
Ph
H
L = (pin)
93% y, 26:74 *E*:*Z*
L = (dmpd)
81% y, 78:22 *E*:*Z*
C
BL
Ph
H
L = (pin)
89% y, 61:39 *E*:*Z*
L = (dmpd)
82% y, 95:5 *E*:*Z*
D
BL
n-pentyl
H
L = (pin)
65% y, >97:3 *E*:*Z*
E
BL
H
Ph
L = (pin)
95% y, 17:83 *E*:*Z*

Through their data collection, they noticed that usually the *E* conformation is favored by the dimethylpentanediolato (dmpd) boronic ester whereas the *Z* conformation was favored by the pinacol (pin) boronic ester. However, Morken et also remarked that: "the *E* isomer is favored when either large boronate substitutuents (R^1) or large aldehyde substituents (R^2) are employed, and this selectivity can be enhanced with the dmpd ligand. In contrast, when both a small aldehyde (i.e., linear alkyl R^2) and a small boronate are employed, the *Z* product stereochemistry is favored."[17]

To apply this work to our own research, we first had to synthesize the bis(boronates) that we would be using. To make the ethyl bis(boronate), copper(I) iodide, lithium methoxide, and the diboronate of choice (i.e. either B_2dmpd_2 or B_2pin_2), were diluted in a flask with DMF. Then, 1,1-dibromoethane was added to the flask and it was allowed to stir overnight. In this way, after chromatography on silica, boronates **3-27** and **3-28** could be obtained in 43% yield (Scheme 3-17).

Scheme 3-17. Synthesis of ethyl bis(boronate)s **3-27** and **3-28**.

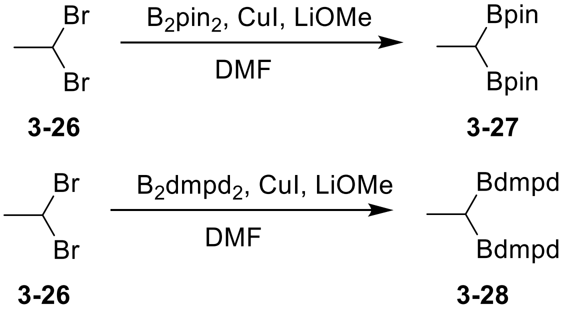

When Morken's conditions, -78 °C for four hours, were employed with the reaction of the bis(pinacol)boronate **3-27**, however, only starting material was recovered. Since we understood the enhanced stability of the lactol, we decided that the reaction mixture had to be warmed to room temperature in order for the reaction to occur.

It was clear from the crude NMR that both the *Z* and the *E* isomer were present in differing amounts. Post purification, the isomers were separated, isolated, and studied by using 1- and 2-D NMR techniques. Ultimately it was determined that the reaction gave a 2:5 ratio of geometric isomers in favor of the undesired *Z*-isomer as outlined below.

After separation of the isomers by chromatography on silica, we set out to determine which spectra belonged to which isomer. In this analysis we used three NMR techniques in order to spectroscopically differentiate the *cis* versus *trans* isomers and confirm their identities. The first step in this process was taking a clean ^{1}H NMR spectra, then utilizing this spectrum for two 2D NMR techniques, COSY and NOESY, or homonuclear correlation spectroscopy and nuclear Overhauser effect spectroscopy respectively. What these three spectra allowed us to do was to assign the important alkene and methyl protons and see their correlation to each other as well as their relationship within space. In the end, we were looking for a direct spatial relationship between a specific hydrogen and hydrogens on a particular methyl group, which was observed using the NOESY spectra as illustrated in Figure 3-4 below.

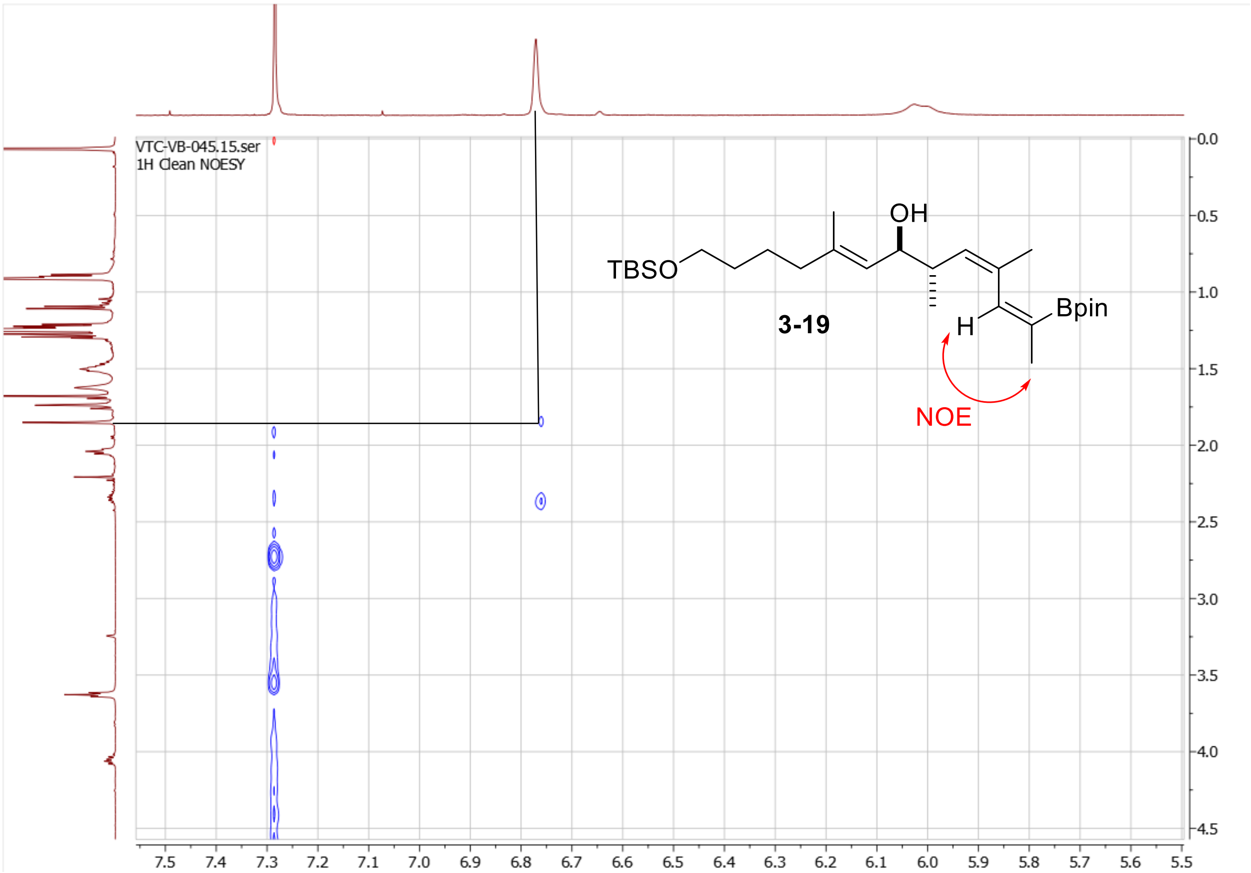

Figure 3-4. Demonstration of NOE spatial relationship between proton and methyl group on the (*E*)-alkene.

The proton assignments for compound **3-19** were designated from spectral work with the ^{1}H, and ^{1}H NOESY, which allowed us to then look at the spatial relationships, or the closeness in space, of these protons. Illustrated by Figure 3-4, there is a clear spatial relationship between the proton and methyl group shown. This interaction, shown in the NOE spectra, shows that these groups are close in proximity that can only be achieved with an *E* alkene formation.

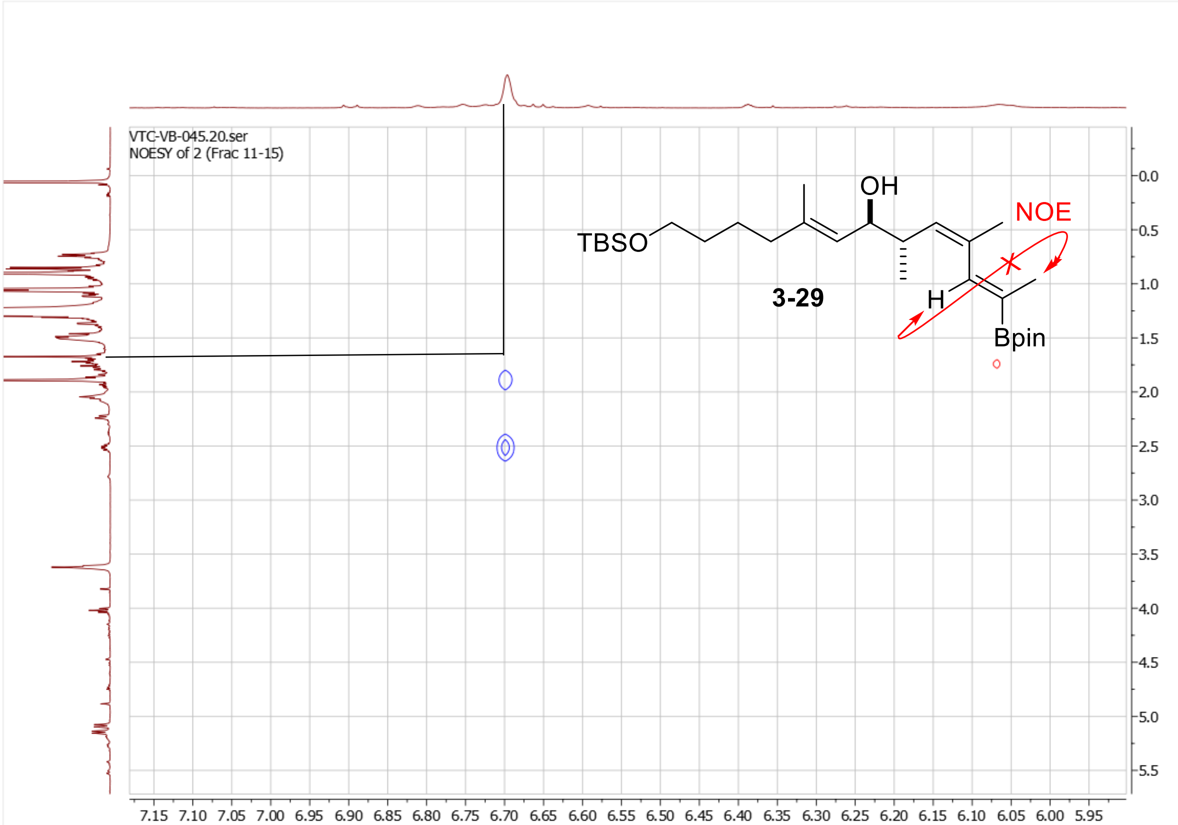

Figure 3-5. Demonstration of no NOE spatial relationship between proton and methyl group on the (*Z*)-alkene.

From Figure 3-5, it can be seen that there is no spatial relationship for compound **3-29** between the proton and the methyl group indicated. Instead, for this molecule the spatial interaction would be with the boronic ester and thus there is no NOESY peak between the methyl and the protons of interest. Thus, from this spectra it was determined that this, the major product obtained, represented the *Z* alkene isomer.

Although this first attempt gave primarily the undesired isomer, it still provided proof of concept that borylation of the lactol was successful. Based on Morken's work, we assumed that switching to the dmpd ester would give the desired *E* stereochemistry as the major isomer. Using the same method used to make the bispinacol(boronate), the bisdmpd(boronate) was synthesized and reacted with the lactol (Scheme 3-18). Gratifyingly, there was a single isomer observed from the crude and purified NMR spectra. Unfortunately however, through analysis with the same NMR techniques described above, it was determined that this reaction was stereoselectively producing the *Z* alkene, rather than the desired *E* alkene.

Scheme 3-18. Boron-Wittig reaction forming the undesired *E* isomer with the lactol.

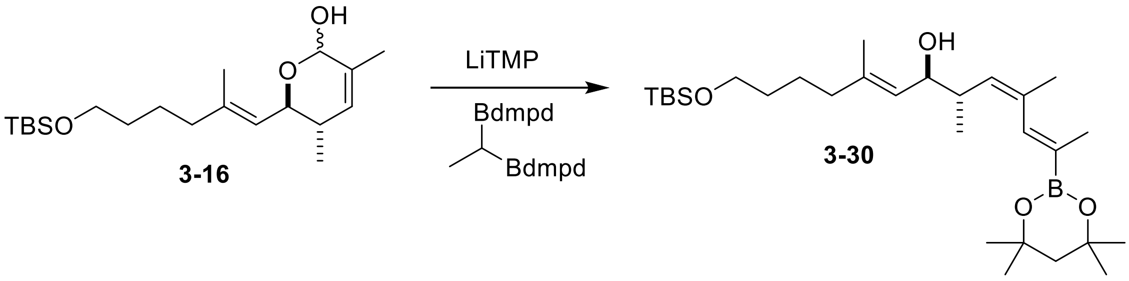

That we were obtaining the same major product from both the pinacol-diboronate and dmpd-diboronate was surprising given that Morken generally observed a reversal of selectivity between these two types of reagents.[17] We noted, however, that our reactions were performed at higher temperature (room temp.) compared to Morken (-78 °C) due to the lower reactivity of the lactol. This hypothesis was tested by performing the boron-wittig on the aldehyde that was obtained from the original synthesis, **2-90** (Scheme 3-19). However, the same results as the lactol were obtained, with the *Z*-isomer **3-30** being the major product obtained in 76% yield.

Scheme 3-19. Boron-Wittig reaction forming the undesired E isomer with the aldehyde.

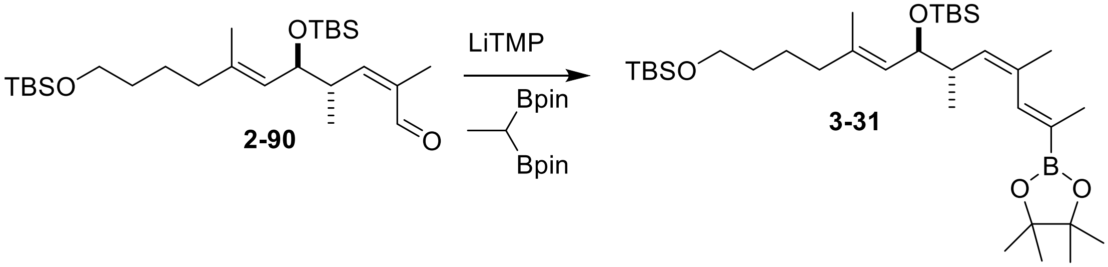

We hypothesized that the *E*-product is favored for our system due to steric considerations at the transition state for the elimination step. After addition of the lithiated diboron to the aldehyde, the resulting alkoxide must rotate to become *syn*-coplanar with one of the boron groups in order for elimination to occur. As shown in Scheme 3-20, rotation in one direction would place the R_1 group eclipsed with the boronic ester, whereas the other direction would have this group eclipsed with a methyl and a hydrogen eclipsed with the boronic ester. If the boronic ester is effectively larger than the methyl, that would explain a preference for the *Z*-isomer we observe.

Scheme 3-20. Fischer projections displaying the steric clash of the Boron-Wittig reaction for the formation of both the *Z* and *E* isomers.

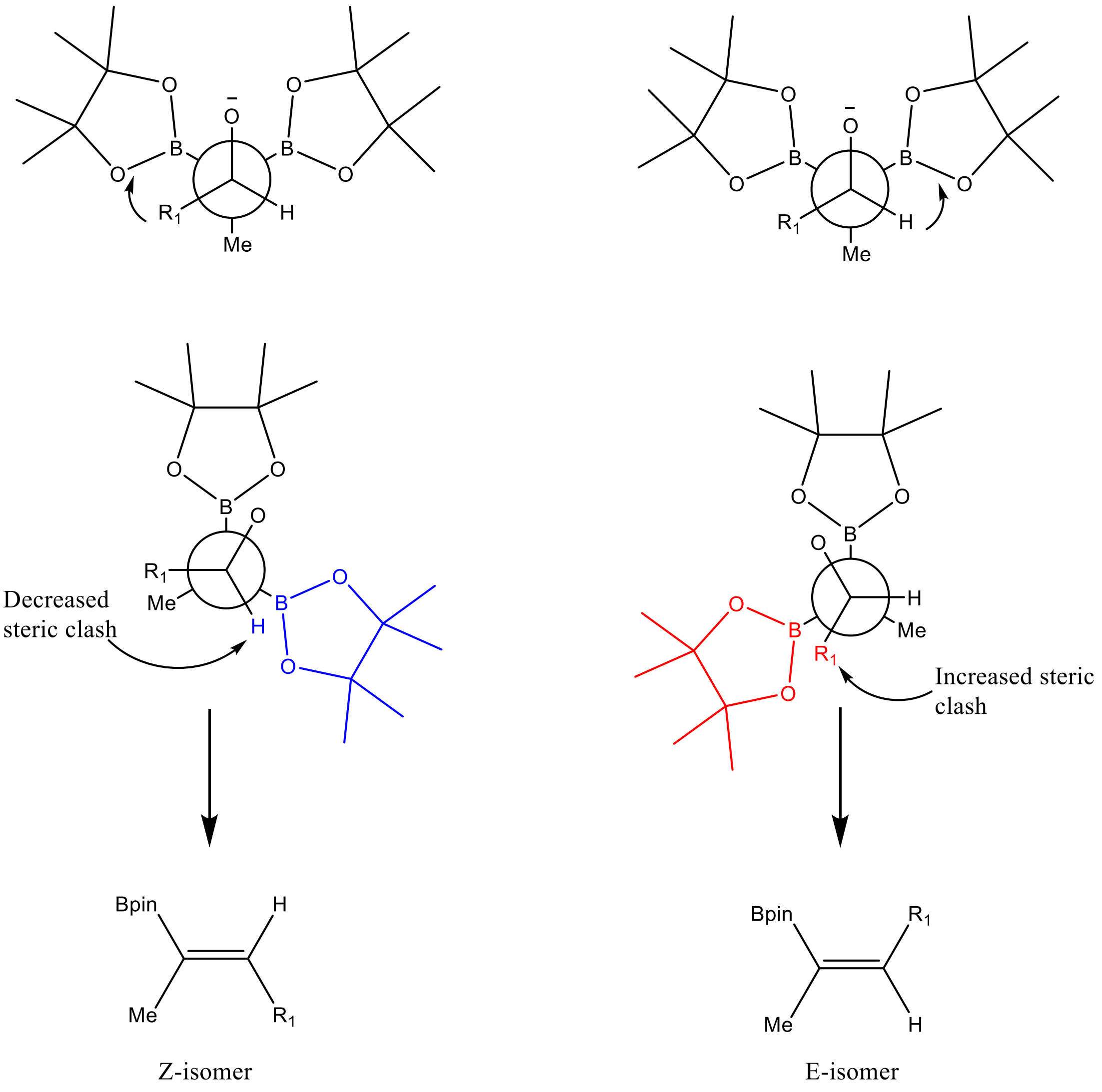
O
B
R1
H
Me
Decreased steric clash
Increased steric clash
Bpin
Z-isomer
E-isomer

Due to the incorrect stereoselectivity from the boron Wittig chemistry, it was decided that the overall yield of the desired product would be highest if the original synthesis path via the vinyl iodide was taken that could then be converted to a vinyl boronate (Scheme 3-21).

Scheme 3-21. Proposed retrosynthesis of Reker et al.'s fragment 1.

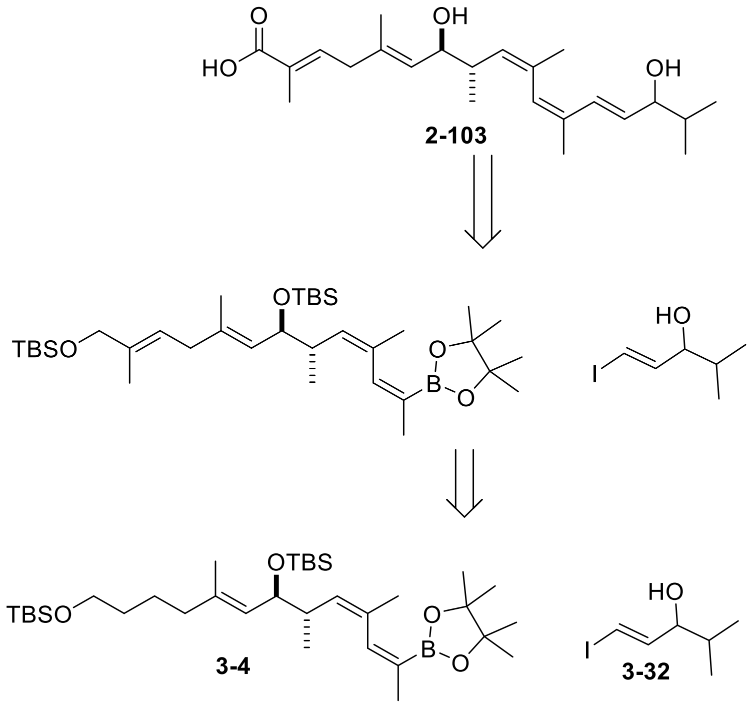

Aside from an "eastern" vinyl boronate, vinyl iodide **3-32** also needed to be synthesized in order to make the hypothetical COX inhibitor proposed by Reker. An important part of this was creating the stereocenter for the hydroxyl on **3-32**. For this, we devised two different syntheses that could select for either enantiomer (Scheme 3-22).

Scheme 3-22. Synthesis of vinyl iodide **3-31**.

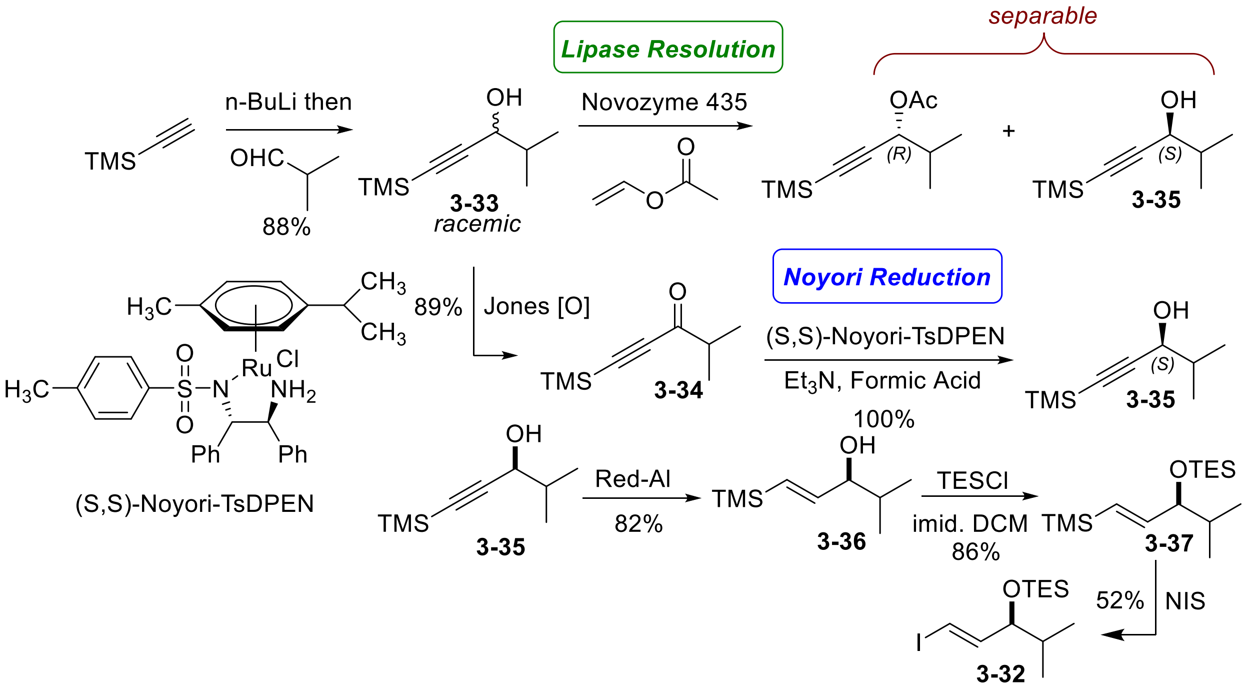

separable
Lipase Resolution
n-BuLi then
OHC
88%
TMS
OH
3-33
racemic
Novozyme 435
OAc
(R)
+
(S)
3-35
CH3
H3C
89%
Jones [O]
O
3-34
Noyori Reduction
(S,S)-Noyori-TsDPEN
Et3N, Formic Acid
100%
Ru
Cl
NH2
Ph
(S,S)-Noyori-TsDPEN
Red-Al
82%
3-36
TESCl
imid. DCM
86%
OTES
3-37
52%
NIS
I
3-32

The synthesis of **3-32** began with addition of lithiated TMS-acetylene to isobutyraldehyde that gave racemic alcohol **3-33** in an 86% yield. The racemic alcohol could then be oxidized to the ketone using Jones conditions (89% yield) and then enantioselectively reduced with the Noyori catalyst in order to create the *S*-hydroxyl **3-35** (100% yield, 98% e.e.) or stereoselectively acetylated using Novozyme 435 (Table 3-6). This (*S*)-alcohol was then stereoselectively reduced to form the trans alkene using Red-Al in diethyl ether and then protected using triethylsilane (TES) to afford **3-37** in 70% yield for the two steps. The TMS group was then exchanged with an iodide utilizing an iododesylation using *N*-iodosuccinimide, 2,6-lutidine, and 1,1,1,3,3,3,-hexafluoro-2-isopropanol, HFIP in a 52% yield to create the coupling fragment **3-32**.

We also investigated the resolution of racemic alcohol **3-33** as an alternative method for the preparation of enantioenriched vinyl iodide **3-32** which can be seen in Table 3-6. As expected, at low conversions the acylated product was obtained in high ee however the recovered alcohol was less enantioenriched. Ultimately good yields and enantiomeric excess (ee) could be obtained for both compounds by using 200% *w/w* Novozyme 435 for 65 hr or 100% *w/w* after extended reaction times (113 hr).

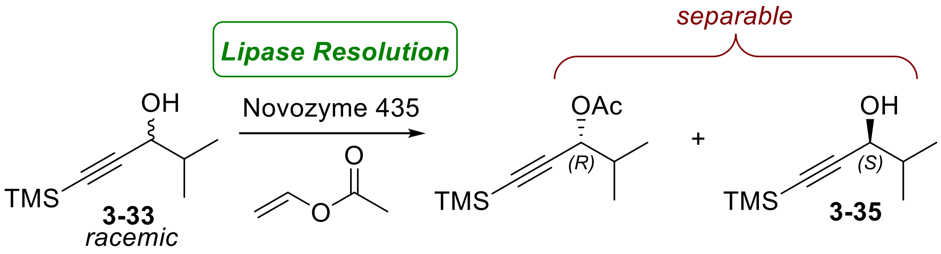
separable
Lipase Resolution
Novozyme 435
OH
TMS
racemic
OAc
(R)
+
OH
(S)
TMS
TMS
O
O

3-33

3-35

Table 3-6. Resolution data for alcohol **3-35**.

Reaction	**(S)-Enriched Product (Alcohol) e.e.**	**(R)-Enriched Product (Acetate) e.e.**	**Conversion[a]**
(S)-Noyori	98%	n/a	n/a
Novozyme 5 hr.	6%	97%	14.50%
Novozyme 23 hr.	26%	98%	22.50%
Novozyme 65 hr.	51%	96%	39.40%
Novozyme 65 hr., 200% *w/w* enzyme	87%	92%	49.50%
Novozyme 113 hr.	82%	97%	48.50%

[a]Conversion determined by NMR spectroscopy.

Once both fragments of the target molecule were in hand, Suzuki couplings were attempted. The first vinyl boronate taken through the coupling was **3-19** which did not have the secondary hydroxyl protected because it was produced through the revised synthetic pathway via a lactol boron-Wittig. The first conditions used were taken from Menche et al. as previously described consisting of $Ba(OH)_2$, $Pd(dppf)Cl_2$ in DMF at 55 °C for 6 hours.[13] While these initial couplings were able to produce some of the desired product, the yields were lower than the original Stille coupling, roughly around 40% (Scheme 3-23).

Scheme 3-23. Initial Suzuki coupling reaction.

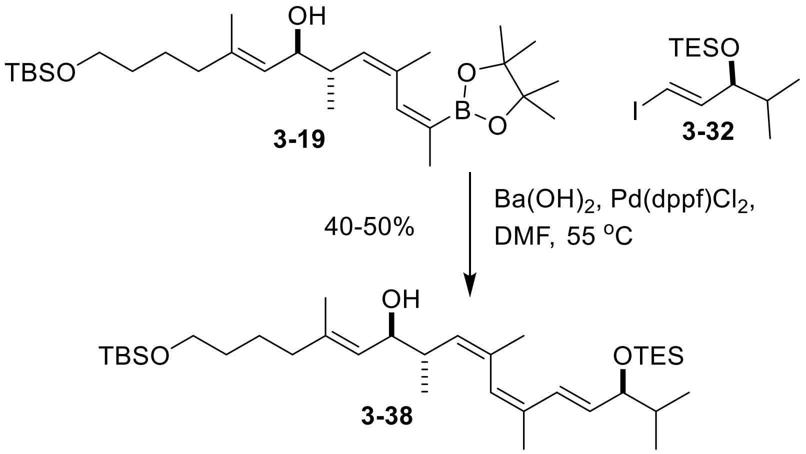

Strangely, the fully protected vinyl boronate (**3-4**), synthesized through the original pathway, failed to undergo successful coupling under the same conditions as the unprotected **3-19**. Instead, the crude NMR spectra showed a mixture of the starting vinyl iodide and vinyl boronate, along with another set of peaks that were unidentified. Believing that the Suzuki coupling should work, and after checking that both the starting materials were not contaminated with impurities, different parameters were investigated that might lead to more consistent results. First, the barium hydroxide was activated by heating the solid to 150 °C under vacuum for 1.5 hours, but this led to the formation of more of the unexpected side product. We thought that the harsher conditions of the more activated base were causing an increase in the side product, so we decided to change the base to cesium carbonate, Cs_2CO_3. Using the same conditions as the original Suzuki coupling procedure, some of the product as well as the side product was observed in the crude NMR. Thinking that this base could be activating enough for both the palladium as well as the pinacol boronate without the extra influence from heating, the reaction was allowed stir at room temperature overnight instead of at 55 °C for 6 hours. This method was successful in minimizing the side product, but starting materials were still present. In a subsequent experiment, after the initial overnight reaction, the solution was resubjected with another 10 mol % of the palladium catalyst. Under these conditions, yields have been consistently around 80% from a method consisting of reacting the starting materials with 10 mol% $Pd(dppf)Cl_2$ and Cs_2CO_3 in degassed DMF, letting the solution stir overnight and then adding an additional 10 mol% $Pd(dppf)Cl_2$. The solution is then quenched after 6 more hours and purified by chromatography on silica (Scheme 3-24).

Scheme 3-24. Updated and final Suzuki coupling reaction.

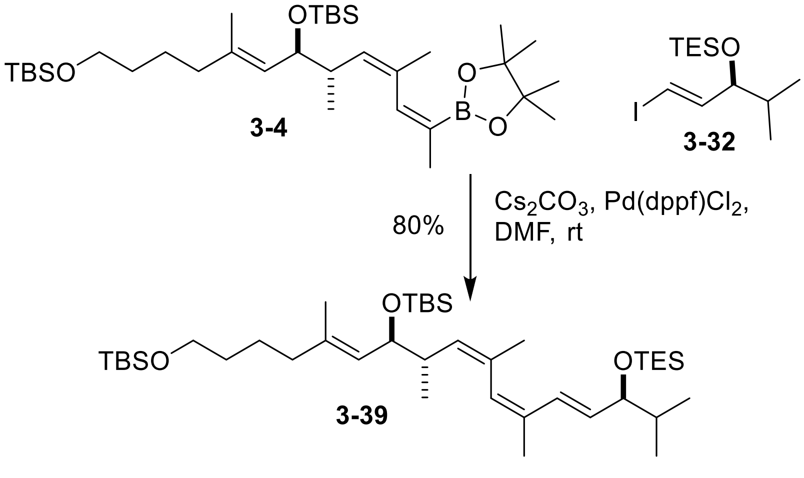

Once the Suzuki coupling had been achieved and optimized, **3-39** and the *ZEE* coupled product, **3-40**, were deprotected using 60% HF•pyr, pyridine in THF for 3 days to afford the corresponding deprotected products **3-41** and **3-42** in 65% yields (Scheme 3-25).

Scheme 3-25. The deprotection of **3-39** and **3-40** to **3-41** and **3-42** respectively.

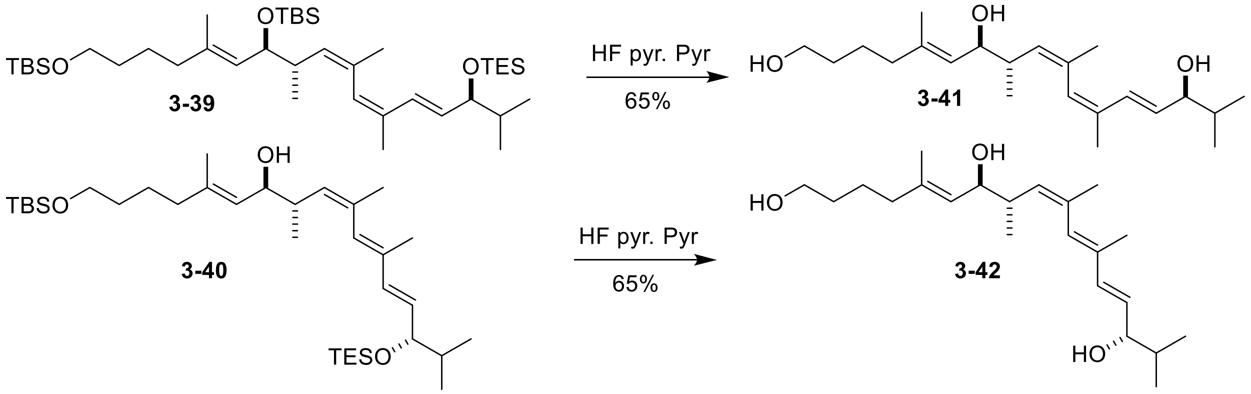

With the deprotected compounds in hand, they were subjected to both a COX inhibition assay as well as an *Arabidopsis*-based V-ATPase assay. Within the COX assay, neither compound was inhibitory up to 125 μM. This could be because neither possess a carboxylic acid, which is present on both Reker's proposed inhibitor as well as the native COX substrate, arachidonic acid (Figure 3-6). This carboxylic acid could be a crucial pharmacophore and explain why there is no inhibition for **3-40** and **3-41**.

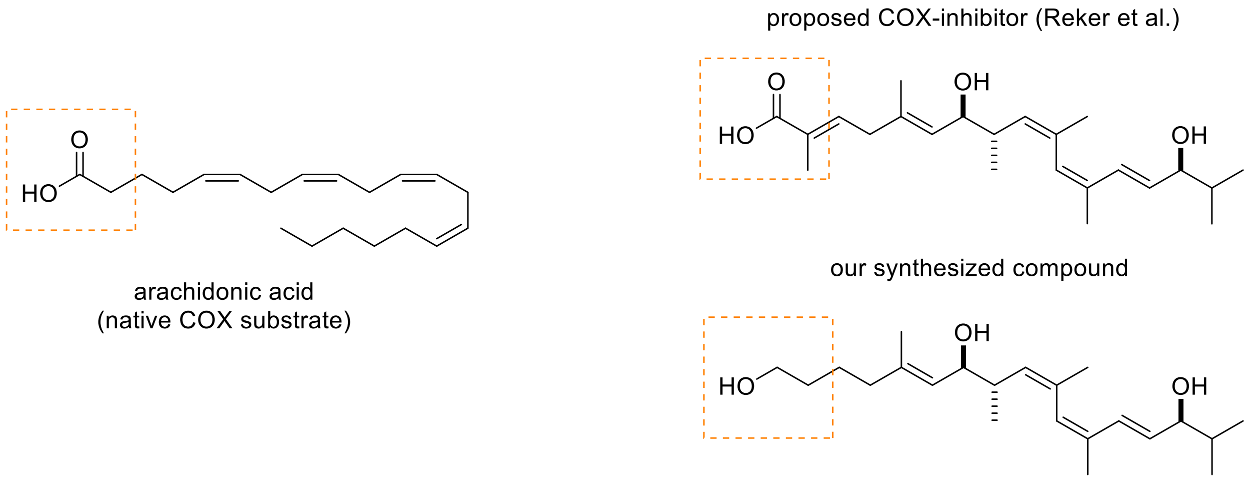

proposed COX-inhibitor (Reker et al.)

our synthesized compound

arachidonic acid
(native COX substrate)

Figure 3-6. Comparison of structures for the COX assay, our synthesized compound, Reker's proposed COX-inhibitor, and the native COX substrate, arachidonic acid.

The *Arabidopsis*-based V-ATPase assay gave interesting data. Triene **3-40** containing the *Z,Z,E*-triene found in the natural product showed inhibition as the concentrations were increased up to 200 μM. However, the non-natural *Z,E,E*-triene compound **3-41** did not show any inhibition even up to 200 μM. This provides support for the importance of not only the C7 and C15 hydroxyls but also the configuration of the conjugated triene connecting these two hydroxyls for V-ATPase inhibition (Figure 3-7).

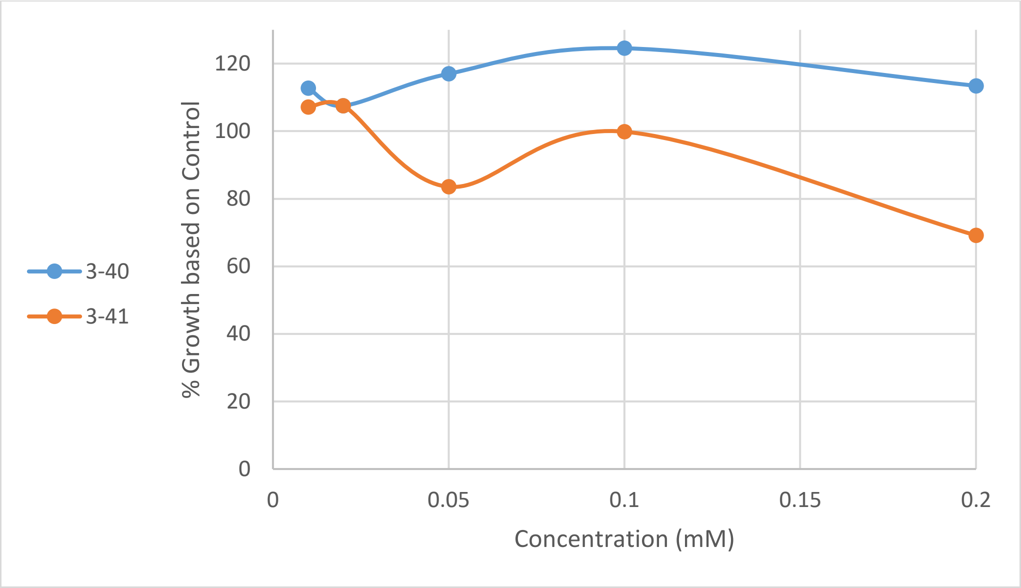

Figure 3-7. *Arabidopsis*-based V-ATPase assay data showing the inhibited growth of the *Arabidopsis* seeds due to V-ATPase inhibition.

Chapter 4: Future Work

In conclusion, within in this work we were able to test an alternative route to the eastern fragment of the archazolids and understand the overall reactivity of a boron-Wittig alternative. We were able to nearly synthesize a hypothetical COX and V-ATPase inhibitor. Through this synthesis we were able to employ a greener alternative to the Stille cross coupling by using an organoborane and a Suzuki coupling. We were also able to show V-ATPase inhibition with the truncated fragment of the dihydroarchazolid B as well as demonstrate the importance of the *ZZE* (natural product triene) isomer. Our compounddid not inhibit COX up to 125 μM in our assay, suggesting that the carboxylic acid terminus in Reker's proposed COX inhibitor may be crucial for COX inhibitory activity (Figure 3-6).

In the future, the V-ATPase inhibition will be tested at higher concentrations for **3-40** as well with the (R)-hydroxyl from the western fragment rather than the natural product (*S*)-hydroxyl. Compound **3-40** may also be oxidized up to the carboxylic acid for the COX inhibition assay using the proposed synthesis shown in Scheme 4-1.

Scheme 4-1. The proposed synthesis of the carboxylic acid derivative from our starting compound **3-40**.

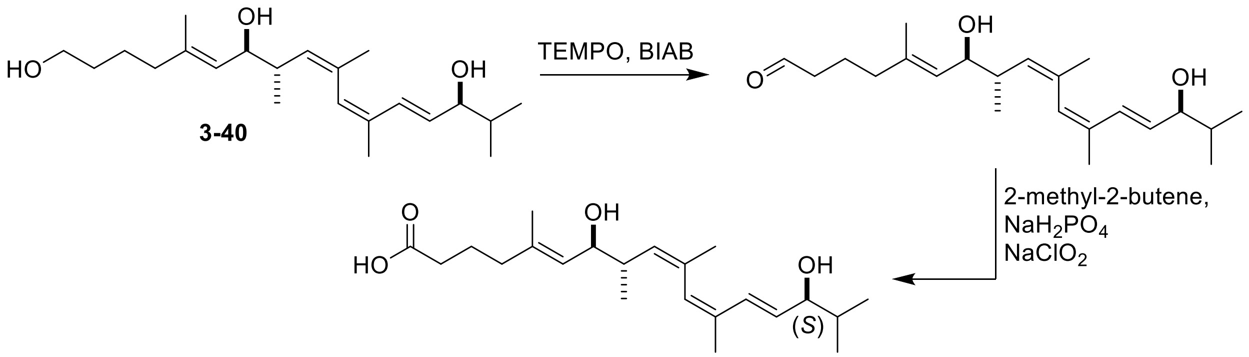

Experimental

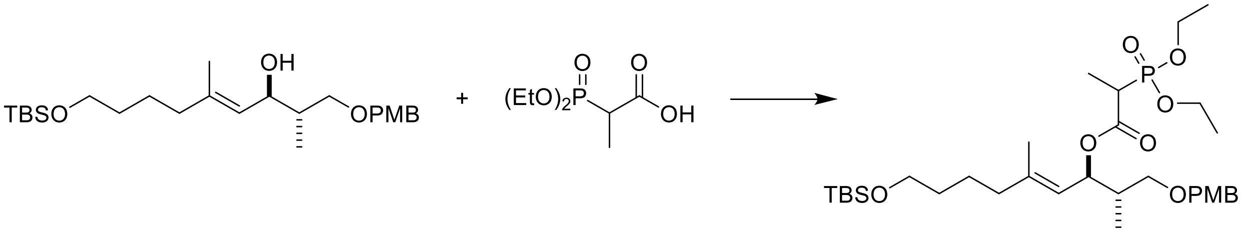

To a solution of alcohol **2-66** (500 mg, 1.2 mmol) in DCM (1.6 mL), phosphate **3-13** (249 mg, 1.2 mmol) was added and the solution was cooled to 0°C. DCC (293 mg, 1.42 mmol) was added and the solution was allowed to warm to room temperature and stir for 24 hrs. The resulting solution was filtered, quenched with H_2O (10 mL), extracted with DCM (2 x 10 mL). The combined organic extracts were dried over $MgSO_4$, filtered and concentrated *in vacuo*. Purification by flash column chromatography on silica (4:1 to 1:1 to 1:2 hexanes:ethyl acetate) afforded the ester **3-7** (604 mg, 82%) as an oil.

IR (ATR) 2931, 2856, 1730, 1612, 1586, 1513, 1460, 1386, 1301, 1246, 1172, 1093, 1023, 962, 904, 834, 818, 774, 734, 661. ^{1}H NMR (500 MHz, $CDCl_3$): δ 7.24 (d, *J* = 8.7 Hz, 2H), 6.86 (d, *J* = 8.7 Hz, 2H), 5.59 (ddd, *J* = 18.6, 9.7, 6.7 Hz, 1H) 5.09 (d, *J* = 9.7 Hz, 1H), 4.43 (d, *J* = 10.22 Hz, 1H) 4.40 (d, *J* = 10.22 Hz, 1H) 4.11 (m, 4H), 3.80 (s, 3H), 3.59 (t, *J* = 5.9 Hz, 2H) 3.42 (dd, *J* = 9.25, 5.79 Hz, 1H) 3.35 (dd, *J* = 9.33, 6.13 Hz, 1H) 3.30 (dd, *J* = 9.25, 6.31 Hz, 1H) 3.31 (dd, *J* = 9.33, 6.13 Hz, 1H) 2.95 (dq, *J* = 23.3, 7.4 Hz, 1H), 2.17 (s, 9H), 2.11 (m, 1H), 2.02 (m, 2H), 1.72 (s, 3H), 1.45 (m, 3H), 1.40 (ddd, *J* = 18.05, 7.26, 3.40 Hz, 3H), 1.30 (m, 6H), 0.93 (dd, 6.96, 4.39 Hz, 2H), 0.88 (s, 9H), 0.03 (s, 6H). ^{13}C NMR (125 MHz, $CDCl_3$): δ 159.10, 142.25, 130.62, 129.16, 120.37, 113.72, 113.70, 73.74, 72.73, 71.73, 62.96, 62.50, 55.28, 40.03, 39.50, 37.81, 32.41, 32.35, 25.97, 24.02, 18.36, 16.77, 12.70, 11.76, -5.27.

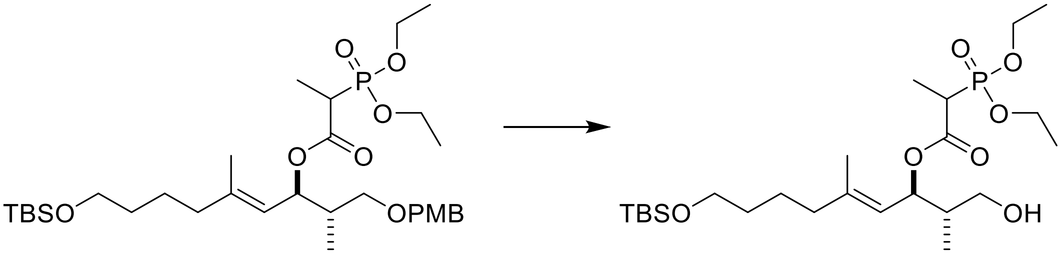

To a solution of **3-7** (250 mg, 0.398 mmol) in a DCM:H_2O mixture (20 mL:0.2 mL), DDQ (180 mg, 0.795 mmol) was added portion wise and stirred at room temperature for 1 hr. The resulting solution was quenched with aqueous sodium bicarbonate (50 mL) and extracted with DCM (2 x 50 mL). The combined organic extracts were dried over $MgSO_4$, filtered and concentrated *in vacuo*. Purification by flash column chromatography on silica (1:2 to 0:1 hexanes:ethyl acetate) afforded the free alcohol (168 mg, 83%) as an oil.

IR (ATR) 3406, 2928, 2856, 1471, 1455, 1384, 1360, 1253, 1100, 1081, 1030, 1002, 977, 935, 834, 773, 737, 661. ^{1}H NMR (500 MHz, $CDCl_3$): δ 5.41 (dt, *J* = 19.99, 9.22 Hz, 1H) 5.09 (dd, 23.05, 9.70 Hz, 1H), 4.13 (m, 4H), 3.75 (dd, *J* = 11.58, 3.48 Hz, 0.5H), 3.63 (dd, *J* = 11.42, 3.81 Hz, 0.5H), 3.58 (t, *J* = 6.08 Hz, 2H), 3.49 (ddd, *J* = 11.46, 6.35, 4.53, 1H), 3.00 (dq, *J* = 23.93, 7.01 Hz, 1H), 2.01 (t, *J* = 7.40, 2H), 1.84 (tt, *J* = 17.31, 7.10, 5.32, 1H), 1.72 (dd, *J* = 7.054, 1.36, 3H), 1.70, (dt, *J* = 21.94, 1.39, 1.39 Hz, 1H), 1.44 (m, 5H), 1.39 (d, *J* = 7.27, 1H), 1.36 (d, *J* = 7.25, 1H), 1.31 (t, *J* = 7.06, 7.04, 3.23, 6H), 0.87 (s, 9H), 0.02 (s, 6H) ^{13}C NMR (125 MHz, $CDCl_3$): δ 169.28, 141.90, 122.26, 75.58, 75.11, 64.24, 62.94, 40.26, 39.35, 32.28, 25.95, 23.85, 18.34, 16.83, 16.38, 13.75, 11.69, -5.29.

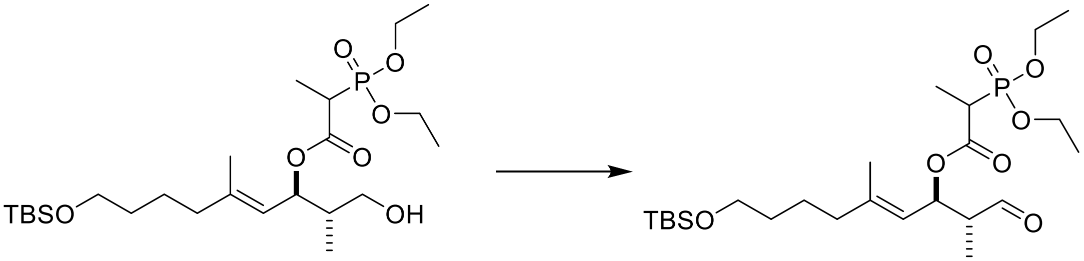

To a solution of the free alcohol (624 mg, 1.23 mmol) in DCM (6.13 mL), $NaHCO_3$ (515 mg, 6.13 mmol) was added and stirred 0°C. DMP (520 mg, 1.23 mmol) was added portionwise and allowed to stir for 1 hr. The resulting solution was diluted with DCM (20 mL) and stirred vigorously with sodium thiosulfate pentahydrate (50 mL) for 30 min. The layers were allowed to separate and the organics extracted with DCM (2 x 50 mL). The combined organic extracts were dried over $MgSO_4$, filtered and concentrated *in vacuo*. Purification by flash column chromatography on silica (4:1 to 1:1 to 1:2 to 0:1 hexanes:ethyl acetate) afforded the aldehyde **3-8** (371 mg, 60%) as an oil.

IR (ATR) 2930, 2857, 1730, 1460, 1387, 1302, 1249, 1171, 1095, 1020, 958, 906, 834, 774, 731, 660. ^{1}H NMR (500 MHz, $CDCl_3$): δ 9.69 (dd, *J* = 18.55, 2.35 Hz, 1H), 5.75 (ddd, *J* = 11.63, 9.50, 7.75 Hz, 1H), 5.11 (d, *J* = 9.52, 1H), 4.11 (m, 4H), 3.58 (t, *J* = 6.01 Hz, 2H), 2.97 (dq, *J* = 23.56, 7.31 Hz, 1H), 2.65 (m, 1H), 2.02 (t, *J* = 6.37 Hz, 2H), 1.76 (d, *J* = 1.4 Hz, 3H), 1.45 (m, 5H), 1.40 (dd, *J* = 7.20, 1.87 Hz, 2H) 1.31 (tt, *J* = 6.94, 5.41 Hz, 6H), 1.06 (dd, *J* = 7.16, 2.48 Hz, 3H) 0.87 (s, 9H), 0.03 (s, 6H).

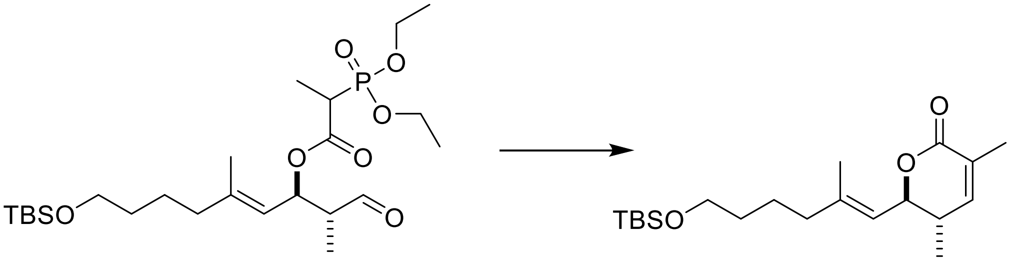

$Ba(OH)_2•8H_2O$ (340 mg, 1.1 mmol) was heated at 120°C for 1.5 hours under vacuum, then allowed to cool to room temperature. THF (7 mL) was added to the flask and allowed to stir fir 10 minutes. Aldehyde **3-8** (181 mg, 0.36 mmol) was added to the solution and allowed to stir overnight. The solution was quenched with aqueous $NaHCO_3$ (20 mL) and extracted with MTBE (2 x 20mL). The combined organic extracts were dried over $MgSO_4$, filtered and concentrated *in vacuo*. Purification by flash column chromatography on silica (20:1 to 10:1 to 4:1 hexanes:ethyl acetate) afforded the lactone **3-14** (72.2 mg, 57%) as an oil.

IR (ATR) 2952, 2928, 2856, 1716, 1460, 1359, 1253, 1226, 1199, 1154, 1134, 1099, 1005, 981, 834, 810, 773, 731, 661. ^{1}H NMR (500 MHz, $CDCl_3$): δ 6.34 (s, 1H), 5.22 (d, *J* = 9.02 Hz, 1H), 4.68 (dd, *J* = 10.50, 9.02 Hz, 1H), 3.57 (m, 2H), 2.45 (ddtt, *J* = 14.56, 7.17, 4.76, 2.39 Hz, 1H), 2.03 (t, *J* = 5.41 Hz, 2H), 1.87 (dd, *J* = 2.40, 1.54 Hz, 3H), 1.67 (d, *J* = 1.49 Hz, 3H), 1.46 (m, 3H), 0.98 (d, *J* = 7.27 Hz, 3H), 0.85 (d, *J* = 5.95 Hz, 1H), 0.85 (s, 9H), 0.00 (s, 6H). ^{13}C NMR (125 MHz, $CDCl_3$): δ 165.96, 145.52, 143.82, 127.37, 121.50, 80.36, 62.86, 39.24, 34.59, 32.30, 25.95, 23.78, 18.31, 16.88, 15.94, -5.30.

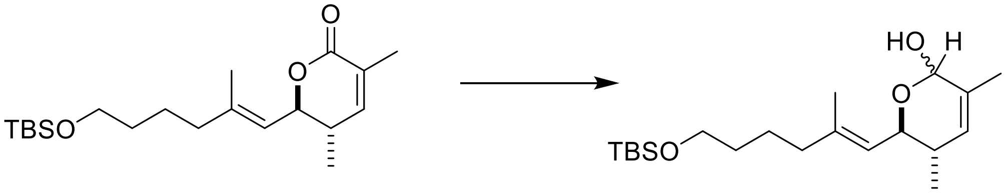

To a solution of DCM (5 mL) at -78°C, DiBAl-H (0.106 mL, 0.597 mmol) was added and stirred for 10 min. Lactone **3-14** (175 mg, 0.498 mmol) was added slowly and allowed to stir for 1 hour. The reaction was quenched by stirring vigorously with Rochelle's salt (20 mL) for 1 hr. The organic layers were extracted with DCM (2 x 20 mL), collected, dried over $MgSO_4$, filtered and concentrated *in vacuo*. Purification by flash column chromatography on silica (4:1 hexanes:ethyl acetate) afforded the lactol **3-16** (141.4 mg, 80%) as an oil.

IR (ATR) 3397, 2928, 2856, 1460, 1384, 1253, 110, 1080, 1030, 1002, 976, 935, 833, 773, 737, 661. ^{1}H NMR (500 MHz, $CDCl_3$): δ 5.48 (s, 1H), 5.16 (m, 2H), 4.24 (t, J = 9.33 Hz, 1H), 3.61 (t, J = 5.99 Hz, 3H), 2.89 (s, 1H), 2.09 (m, 1H), 2.06 (m, 2H), 1.73 (m, 3H), 1.71 (d, J = 1.47 Hz, 3H), 1.50 (m, 3H), 0.89 (s, 9H), 0.86 (d, J = 7.13, 3H), 0.04 (s, 6H). ^{13}C NMR (125 MHz, $CDCl_3$): δ 141.98, 132.03, 129.75, 12.65, 91.94, 69.63, 63.01, 39.38, 35.14, 32.41, 25.97, 23.96, 18.93, 18.35, 16.95, 16.38, -5.27.

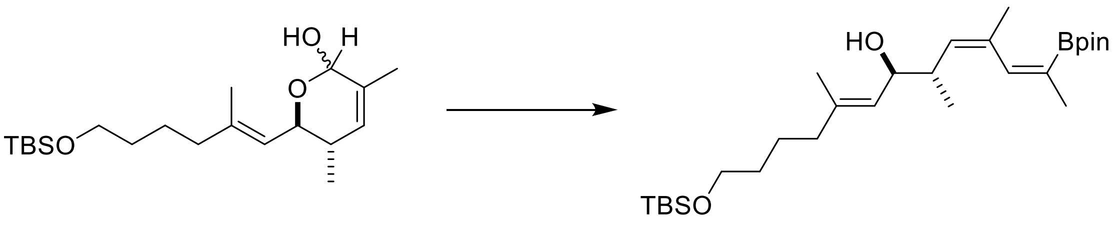

To a solution of Tetramethylpiperidine (137 mg, 0.97 mmol) in THF (0.5 mL) at -78°C, *n*-BuLi (0.388 mL, 2.5 M) was slowly added. The solution was allowed to warm to 0°C and 1,1-dipinacolboroethane (187 mg, 0.65 mmol) was added and stirred. After 10 minutes, lactol **3-16** (114.6 mg, 0.32 mmol) was added and the solution was allowed to slowly warm to room temperature overnight. The solution was diluted with diethyl ether (10 mL) and filtered through a silica plug. The solution was concentrated *in vacuo*. Purification by flash column chromatography on silica (20:1 to 10:1 to 4:1 hexanes:ethyl acetate) afforded the vinyl boronate **3-19** (22.5 mg, 14%) as an oil.

IR (ATR) 2977, 2933, 2879, 1460, 1305, 1268, 1215, 1142, 1105, 1016, 967, 846, 775, 736, 669. ^{1}H NMR (500 MHz, $CDCl_3$): δ 6.68 (s, 1H), 5.13 (d, 9.24 Hz, 1H) 5.07 (d, *J* = 9.24 Hz, 1H), 4.01 (t, *J* = 8.46 Hz, 1H), 3.60 (m, 2H), 2.50 (m, 1H), 2.04 (d, *J* = 5.90 Hz, 2H), 1.88 (dd, *J* = 5.34, 1.34 Hz, 4H) 1.66 (s, 3H), 1.48 (m, 1H) 1.24 (d, *J* = 3.31 Hz, 3H), 1.21 (d, 4.15 Hz, 12H), 1.04 (d, *J* = 7.31 Hz, 2H), 0.89 (s, 9H), 0.84 (d, *J* = 6.73 Hz, 2H), 0.72 (q, *J* = 7.29 Hz, 1H) 0.04 (s, 6H). ^{13}C NMR (125 MHz, $CDCl_3$): δ 140.12, 139.32, 136.49, 130.68, 126.10, 82.85, 72.41, 63.01, 40.19, 39.50, 32.45, 25.94, 24.81, 24.51, 24.08, 23.94, 23.23, 18.31, 16.80, 9.03, -5.30.

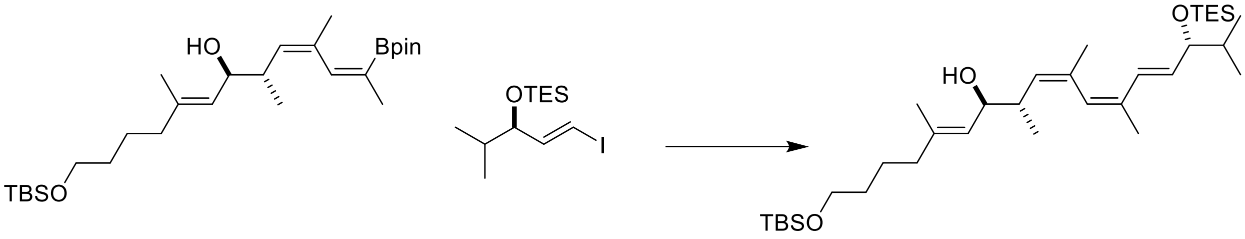

To a solution of DMF (0.6 mL), vinyl boronate **3-19** (100 mg, 0.2 mmol) and vinyl iodide **3-32** (69 mg, 0.20 mmol) were added. The solution was allowed bubbled with N_2 for 10 minutes, then $Pd(dppf)Cl_2$ and $Ba(OH_2)\bullet 8H_2O$ were added simultaneously. The solution heated to 55°C and stirred for 6hrs. The reaction was diluted with MTBE (10mL) and quenched with H_2O (25 mL). The organic layer was dried with $MgSO_4$ and concentrated *in vacuo*. Purification by flash column chromatography on silica (10:1 to 4:1 hexanes:ethyl acetate) afforded the protected cis/cis/trans triene **3-38** (30.7 mg, 26%) as an oil.

IR (ATR) 2955, 2930, 2875, 1460, 1352, 1344, 1254, 1143, 1103, 1004, 969, 835, 774, 741, 724, 666. ^{1}H NMR (500 MHz, $CDCl_3$): δ 6.37 (d, *J* = 15.73 Hz, 1H), 5.84 (s, 1H), 5.64 (dd, *J* = 15.72, 7.94 Hz, 1H), 5.16 (d, 9.76 Hz, 1H), 5.10 (d, *J* = 8.77 Hz, 1H), 4.02 (t, *J* = 8.77 Hz, 1H), 3.82 (t, *J* = 6.95 Hz, 1H), 3.60 (t, *J* = 5.89 Hz, 2H), 2.34 (m, 1H), 2.02 (m, 2H), 1.86 (s, 3H), 1.84 (s, 3H) 1.66 (s, 3H), 1.55 (s, 1H), 1.47 (m, 4H), 1.24 (d, *J* = 3.80 Hz, 6H), 0.93 (t, *J* = 7.94 Hz, 9H), 0.89 (s, 9H), 0.84 (t, *J* = 6.45 Hz, 3H), 0.56 (q, *J* = 7.94 Hz, 6H) 0.04 (s, 6H). ^{13}C NMR (125 MHz, $CDCl_3$): δ 139.78, 135.13, 132.43, 130.94, 129.00, 128.70, 125.73, 82.91, 72.26, 63.03, 40.50, 39.49, 35.07, 32.45, 25.97, 24.84, 24.55, 20.35, 18.40, 16.73, 16.36, 9.07, 6.88, 5.04, -5.27.

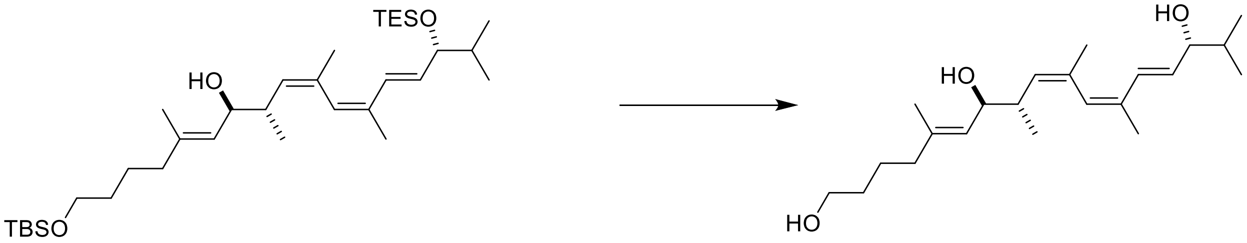

Cis/cis/trans triene **3-38** (77.2 mg, 0.053 mmol) was added to a solution of THF (1.2 mL) and pyridine (0.3 mL). The solution was cooled to 4°C for 30 min, then a solution of 60% HF•pyr (0.2 mL) was added. The reaction mixture was placed in the fridge (4°C) overnight, then it was quenched with aqueous $NaHCO_3$ (20 mL) and extracted with ethyl acetate (2 x 10 mL). The organic layer was dried with $MgSO_4$ and concentrated *in vacuo*. Purification by flash column chromatography on silica (1:1 to 1:2 hexanes:ethyl acetate) afforded the deprotected cis/cis/trans triene **3-41** (30.1 mg, 65%) as an oil.

IR (ATR) 3338, 2957, 2929, 2870, 1667, 1638, 1585, 1447, 1378, 1366, 1328, 1257, 1203, 1175, 1136, 1106, 1065, 1003, 973, 935, 858, 817, 769, 736, 697, 667. ^{1}H NMR (500 MHz, C_6D_6): δ 6.84 (d, *J* = 15.85, 1H), 5.78 (dd, *J* = 15.85, 6.64 Hz, 1H), 5.73 (s, 1H), 5.25 (m, 2H), 4.12 (t, *J* = 8.00 Hz, 1H), 3.90 (t, *J* = 6.22 Hz, 1H), 3.40 (m, 2H), 2.60 (m, 1H), 1.89 (m, 2H), 1.81 (s, 3H), 1.78 (s, 3H), 1.57 (s, 3H), 1.36 (m, 5H), 1.03 (d, *J* = 6.22 Hz, 3H) 0.95 (dd, *J* = 11.55, 7.11 Hz, 6H). ^{13}C NMR (125 MHz, C_6D_6): δ 138.50, 133.57, 132.78, 131.96, 130.53, 129.07, 77.71, 72.53, 62.10, 40.43, 39.07, 34.12, 32.07, 24.43, 23.70, 19.88, 18.49, 18.06, 16.76, 16.43

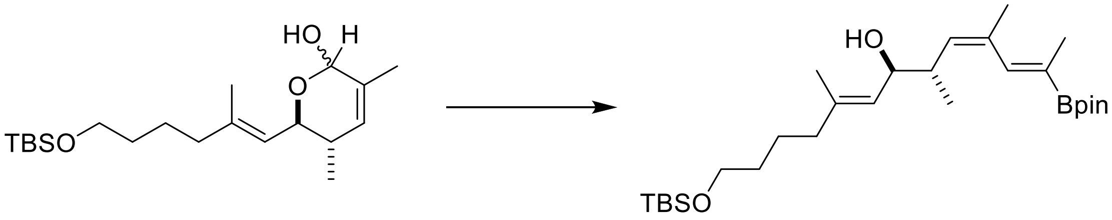

To a solution of Tetramethylpiperidine (89 mg, 0.63 mmol) in THF (0.4 mL) at -78°C, *n*-BuLi (0.25 mL, 2.5 M) was slowly added. The solution was allowed to warm to 0°C and 1,1-dipinacolboroethane (89 mg, 0.65 mmol) was added and stirred. After 10 minutes, lactol **3-16** (111.7 mg, 0.32 mmol) was added and the solution was allowed to slowly warm to room temperature overnight. The solution was diluted with diethyl ether (10 mL) and filtered through a silica plug. The solution was concentrated *in vacuo*. Purification by flash column chromatography on silica (20:1 to 10:1 to 4:1 hexanes:ethyl acetate) afforded the vinyl boronate **3-29** (67.5 mg, 43%) as an oil.

IR (ATR) 2977, 2933, 2879, 1460, 1305, 1268, 1215, 1142, 1105, 1016, 967, 846, 775, 736, 669. ^{1}H NMR (500 MHz, $CDCl_3$): δ 6.74 (s, 1H), 5.13 (m, 2H), 4.04 (dd, *J* = 8.91, 7.49 Hz, 1H), 3.61 (t, *J* = 5.92 Hz, 2H), 2.34 (m, 1H), 2.03 (m, 2H), 1.84 (s, 3H), 1.71 (s, 3H), 1.65 (s, 3H) 1.48 (m, 4H), 1.29 (s, 12H), 1.22 (d, *J* = 3.76 Hz, 3H), 0.89 (s, 9H), 0.04 (s, 6H). ^{13}C NMR (125 MHz, $CDCl_3$): δ 142.48, 139.72, 136.49, 130.34, 125.70, 83.08, 72.19, 63.06, 39.53, 32.50, 29.71, 25.98, 24.79, 23.99, 23.65, 18.37, 16.71, 16.16, 15.36, 10.41, -5.26.

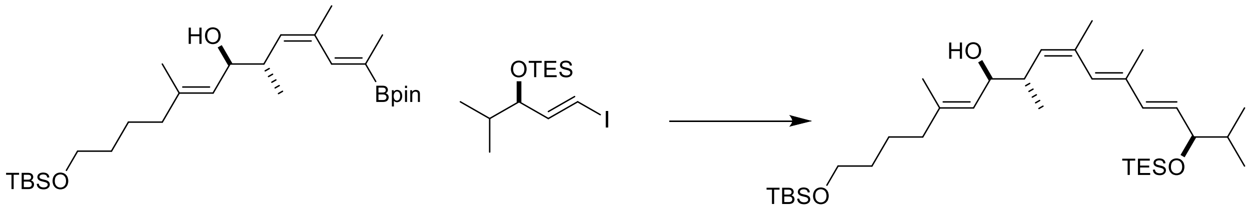

To a solution of DMF (1.67 mL), *Z*-vinyl boronate **3-29** (82.3 mg, 0.167 mmol) and vinyl iodide **3-32** (68.3 mg, 0.20 mmol) were added. The solution was allowed bubbled with N_2 for 10 minutes, then Pd(dppf)Cl_2 and Ba(OH_2)•8H_2O were added simultaneously. The solution heated to 55°C and stirred for 6hrs. The reaction was diluted with MTBE (10mL) and quenched with H_2O (25 mL). The organic layer was dried with $MgSO_4$ and concentrated *in vacuo*. Purification by flash column chromatography on silica (10:1 to 4:1 hexanes:ethyl acetate) afforded the protected cis/cis/trans triene **3-40** (30.7 mg, 26%) as an oil.

IR (ATR) 2955, 2930, 2875, 1460, 1352, 1344, 1254, 1143, 1103, 1004, 969, 835, 774, 741, 724, 666. ^{1}H NMR (500 MHz, C_6D_6): δ 6.33 (d, *J* = 15.75 Hz, 1H), 6.13 (s, 1H), 5.75 (dd, *J* = 15.57, 7.20 Hz, 1H), 5.25 (m, 2H), 4.10 (t, *J* = 7.79 Hz, 1H), 3.95 (t, *J* = 6.52 Hz, 1H), 3.54 (t, *J* = 6.18 Hz, 2H), 2.53 (dtt, *J* = 10.06, 6.83, 6.78 Hz, 1H), 1.95 (m, 2H), 1.82 (s, 3H), 1.79 (s, 3H) 1.57 (s, 3H), 1.48 (m, 5H), 1.04 (t, *J* = 7.90 Hz, 9H), 0.99 (s, 9H), 0.95 (dd, *J* = 6.89, 1.60 Hz, 3H) 0.88 (t, *J* = 6.89 Hz, 6H), 0.66 (dq, *J* = 8.19, 2.15 Hz, 6H), 0.07 (s, 6H). ^{13}C NMR (125 MHz, C_6D_6): δ 138.01, 135.32, 134.38, 134.20, 131.90, 130.51, 130.32, 127.03, 78.98, 71.91, 62.74, 40.57, 39.39, 35.28, 32.43, 31.60, 25.82, 24.04, 22.69, 18.29, 16.35, 13.98, 6.88, 5.22, -5.48.

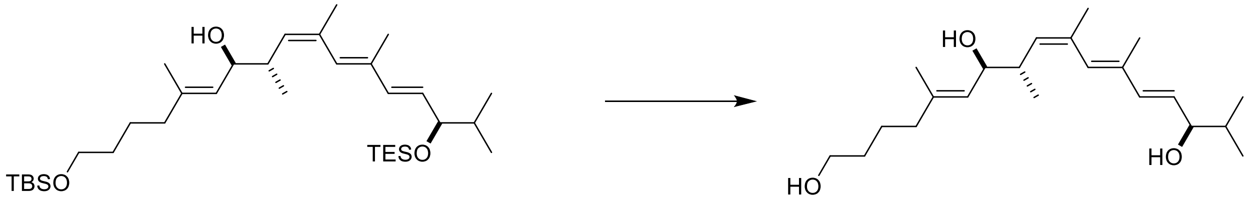

Cis/trans/trans triene **3-40** (56 mg, 0.097 mmol) was added to a solution of THF (1.2 mL) and pyridine (0.3 mL). The solution was cooled to 4°C for 30 min, then a solution of 60% HF•pyr (0.2 mL) was added. The reaction mixture was placed in the fridge (4°C) overnight, then it was quenched with aqueous $NaHCO_3$ (20 mL) and extracted with ethyl acetate (2 x 10 mL). The organic layer was dried with $MgSO_4$ and concentrated *in vacuo*. Purification by flash column chromatography on silica (1:1 to 1:2 hexanes:ethyl acetate) afforded the deprotected cis/trans/trans triene **3-42** (32.6 mg, 96%) as an oil.

IR (ATR) IR (ATR) 3338, 2957, 2929, 2870, 1667, 1638, 1585, 1447, 1378, 1366, 1328, 1257, 1203, 1175, 1136, 1106, 1065, 1003, 973, 935, 858, 817, 769, 736, 697, 667. ^{1}H NMR (500 MHz, C_6D_6): δ 6.32 (d, *J* = 15.70 Hz, 1H), 6.09 (s, 1H), 5.66 (dd, *J* = 15.65, 6.81 Hz, 1H), 5.26 (dq, *J* = 10.08, 1.52 Hz, 2H), 4.13 (dd, *J* = 8.84, 6.14 Hz, 1H), 3.78 (t, *J* = 6.98 Hz, 1H), 3.37 (t, *J* = 6.67 Hz, 2H), 2.53 (dq, *J* = 9.92, 6.74 Hz, 1H), 1.91 (m, 2H), 1.80 (d, *J* = 12.05, 6H), 1.69 (sept., *J* = 6.67 Hz, 1H), 1.56 (s, 3H), 1.36 (m, 4H), 1.03 (d, *J* = 6.84 Hz, 3H), 0.97 (d, *J* = 6.67 Hz, 3H), 0.90 (d, *J* = 6.84 Hz, 3H). ^{13}C NMR (125 MHz, C_6D_6): δ 138.02, 135.53, 134.30, 131.64, 130.85, 130.10, 126.98, 77.60, 72.00, 62.18, 40.54, 39.36, 34.22, 32.24, 24.05, 23.89, 18.39, 17.88, 16.39, 14.03.

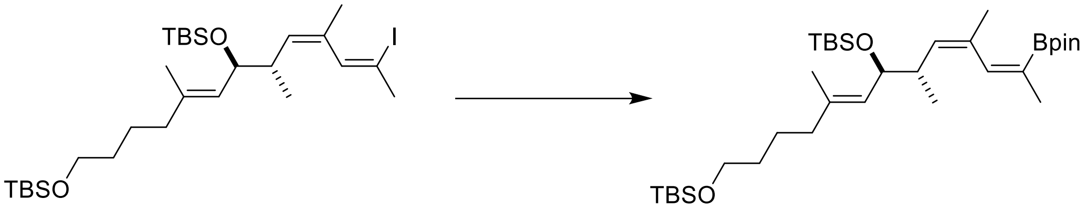

t-BuLi (0.11 mL, 1.7M) was added to dry diethyl ether (1 mL) at -78°C. Vinyl iodide (50 mg, 0.082 mmol) was added to the solution and stirred for 10 minutes. Then, isoproproxy borate (0.03 mL, 0.123 mmol) was added and the solution was stirred for 30 minutes before pinacol (20 mg, 0.164 mmol) was added and the solution warmed to room temperature. It was allowed to stir overnight before being diluted with MTBE (10 mL), washed with NH_4Cl (10 mL), water (10 mL), and finally brine (10 mL). The organic extracts were dried with $MgSO_4$ and concentrated *in vacuo*. The oil was then resubjected into dry THF (1 mL) and pinacol (20 mg, 0.164 mmol) for 2 hours. The solution was concentrated *in vacuo.* Purification by flash column chromatography on silica (20:1 to 10:1 hexanes:ethyl acetate) afforded the fully protected vinyl boronate **3-4** (27.3 mg, 53%) as an oil.

IR (ATR): 2954, 2928, 2856, 1471, 1461, 1388, 1378, 1370, 1333, 1299, 1253, 1214, 1165, 1143, 1101, 1057, 1031, 1005, 963, 938, 812, 772, 695, 668. ^{1}H NMR (500 MHz, $CDCl_3$): δ 6.69 (s, 1H), 5.10 (d, *J* = 8.83 Hz, 1H), 5.05 (d, *J* = 8.83 Hz, 1 H) 4.15 (dd, *J* = 9.16, 5.72 Hz, 1H), 3.60 (t, *J* = 6.09 Hz, 2H), 2.64 (m, 1H), 1.98 (t, *J* = 7.38 Hz, 3H), 1.87 (s, 3H), 1.85 (s, 3H), 1.57 (d, *J* = 1.57 Hz, 3H) 1.45 (m, 3H), 1.28 (s, 12H), 0.89 (s, 12H) 0.85 (s, 9H), 0.04 (s, 6H), -0.02 (d, *J* = 14.42 Hz, 6H). ^{13}C NMR (125 MHz, $CDCl_3$): δ 138.15, 135.33, 133.45, 132.69, 127.21, 83.34, 72.95, 63.04, 39.45, 32.45, 25.98, 25.88, 24.79, 24.04, 23.90, 23.00, 18.36, 18.18, 16.67, 16.06, -5.26.

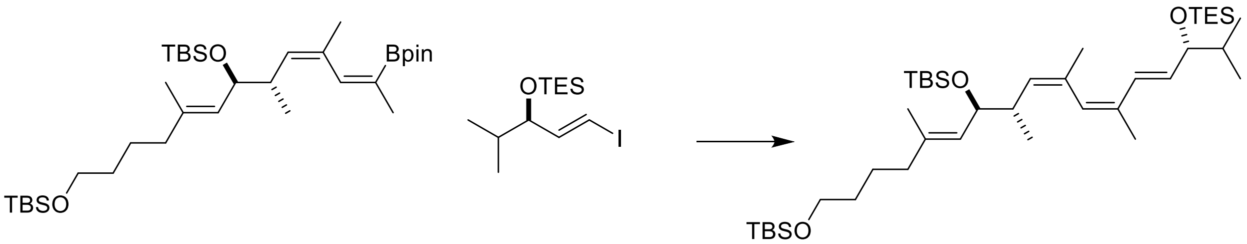

Vinyl boronate **3-4** (58.8 mg, 0.093 mmol) and vinyl iodide **3-32** (25 mg, 0.076 mmol) was dissolved in DMF (1 mL). The solution was degassed by the freeze, pump, and thaw method two times. Then, Pd(dppf)Cl_2 (4 mg, 0.004 mmol) and Cs_2CO_3 (40 mg, 0.12 mmol) was added and the solution was freeze, pump, thawed once again. The resulting solution was allowed to stir overnight and then an additional equivalent of Pd(dppf)Cl_2 (4 mg, 0.004 mmol) was added. The solution was allowed to stir for an additional 6 hours, then it was diluted with MTBE (5 mL) and quenched with water (20 mL). The solution was extracted with MTBE (2x20 mL). The combined organic extracts were dried with $MgSO_4$ and concentrated *in vacuo*. Purification by flash column chromatography on silica (20:1 hexanes:ethyl acetate) afforded the fully protected cis/cis/trans triene **3-39** (41.9 mg, 80%) as an oil. The product was unable to be purified away from a side product and this mixture was taken direction into the next reaction.

^{1}H NMR (500 MHz, C_6D_6): δ 6.69 (d, *J* = 15.70 Hz, 1H) 6.01 (s, 1H), 5.77 (dd, *J* = 15.70, 7.70 Hz, 1H) 5.33 (m, 2H), 4.28 (dd, *J* = 8.86, 5.49 Hz, 1H), 3.98 (t, *J* = 6.72 Hz, 1H), 3.55 (s, 2H), 1.96 (m, 2H), 1.94 (s, 3H), 1.87 (s, 3H) 1.79 (m, 1H), 1.59 (s, 3H) 1.50 (m, 4H), 1.13 (d, *J* = 6.96, 1H), 1.08-1.00 (m, 18H), 1.03 (s, 9H)0.99 (s, 9H), 0.66 (m 6H), 0.13 (s, 6H), 0.07 (s, 6H).

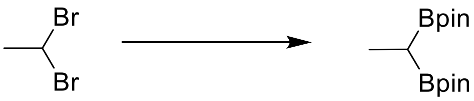

Copper (I) iodide (197 mg, 1.04 mmol), lithium methoxide (980 mg, 25.9 mmol), and B_2Pin_2 (5 g, 19.7 mmol) were added to a dried flask. The solids were dissolved in DMF (21 mL) and allowed to stir for 10 minutes. 1,1-dibromoethane (1.95 g, 10.4 mmol) was added to the flask and the solution was allowed to stir overnight. The resulting solution was quenched with water (50 mL) and extracted with hexanes (2 x 30 mL). The organic extracts were dried with $MgSO_4$ and concentrated *in vacuo*. Purification by flash column chromatography on silica (20:1 hexanes:ethyl acetate) afforded the bis(pinacol)boronate **3-27** (1.2464 g, 43%) as an oil. The spectroscopic data correlated the published data.

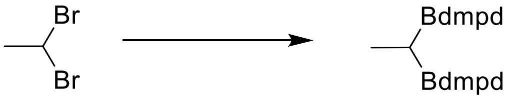

Copper (I) iodide (39.5 mg, 0.21 mmol), lithium methoxide (197 mg, 5.18 mmol), and B_2dmpd_2 (1 g, 3.94 mmol) were added to a dried flask. The solids were dissolved in DMF 4.5 mL) and allowed to stir for 10 minutes. 1,1-dibromoethane (389 mg, 2.1 mmol) was added to the flask and the solution was allowed to stir overnight. The resulting solution was quenched with water (50 mL) and extracted with hexanes (2 x 30 mL). The organic extracts were dried with $MgSO_4$ and concentrated *in vacuo*. Purification by flash column chromatography on silica (20:1 hexanes:ethyl acetate) afforded the bis(dmpd)boronate **3-28** (439.3 mg, 68%) as an oil. The spectroscopic data correlated the published data.

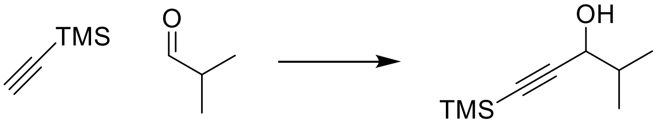

n-Butyllithium (7.2 mL, 2.5M) was added dropwise to trimethylsilylacetylene (3.0 mL, 21.6 mmol) in THF (90 mL) at -78ºC and stirred for 30 minutes. Isobutyraldehyde (1.65 mL, 18.0 mmol) was then added and the mixture was stirred for 90 minutes. The crude reaction mixture was quenched with aq. NH_4Cl (100 mL) and extracted with MTBE (2 x 100 mL). The combined organic extracts were dried over $MgSO_4$, filtered through cotton, and concentrated under vacuum. The crude product was purified by chromatography over silica gel (10:1 Hexanes:EtOAc) to give **3-33** (3.16 g, 18.5 mmol, 85.8%) as an oil.

R_f = 0.55 in 4:1. IR (ATR): 3333, 3130, 3057, 3026, 2960, 2927, 2171, 1601, 1493, 1452, 1384, 1250, 1030, 992, 839, 758, 696. ^{1}H NMR (500 MHz, $CDCl_3$): δ 4.17 (d, *J* = 5.8 Hz, 1H) 1.89 (o, *J* = 5.8 Hz, 1H), 1.03 (d, *J* = 6.8 Hz, 3H), 1.01 (d, *J* = 6.8 Hz, 3H), 0.20 (s, 9H). ^{13}C NMR (500 MHz, $CDCl_3$): δ 105.54, 90.19, 68.35, 34.45, 18.04, 17.44, -0.10.

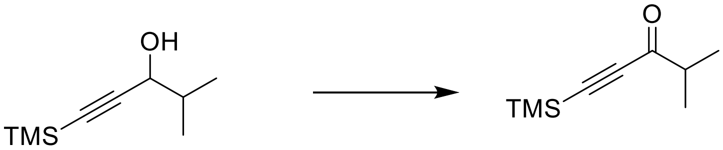

Jones' reagent (CrO_3 in aqueous H_2SO_4) (4.62 mL, 18.5 mmol) was added dropwise to a solution of compound **3-33** (3.16 g, 18.5 mmol) in acetone (90 mL) and the mixture was stirred for 20 minutes. Additonal Jones' reagent (0.2 mL) was then added dropwise until the reaction mixture began to turn yellow. Isopropanol (1 mL) was then added dropwise to the mixture until the reaction turned blue to quench the reaction. The crude reaction mixture was extracted with

MTBE (2 x 45 mL), dried over $MgSO_4$, filtered through cotton, and concentrated under vacuum to give **3-34** (2.78 g, 16.5 mmol, 89.4%) that could be used without further purification.

R_f = 0.75 in 4:1. IR (ATR): 2969, 2936, 2903, 2875, 2151, 1742, 1676, 1467, 1385, 1252, 1183, 1129, 1065, 1004, 962, 891, 842, 761. ^{1}H NMR (500 MHz, $CDCl_3$): δ 2.66 (sept., *J* = 7.0 Hz, 1H), 1.21 (d, *J* = 7.0 Hz, 6H), 0.27 (s, 9H). ^{13}C NMR (500 MHz, $CDCl_3$): δ 191.98, 101.06, 98.78, 42.84, 17.87, -0.72.

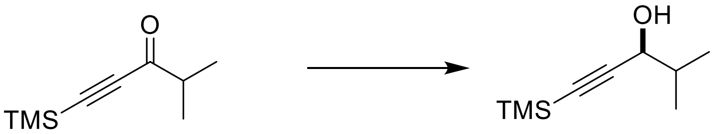

Triethylamine (6.72 mL, 50.5 mmol) was added to (S,S)-Noyori-TsDPEN (0.210 g, 0.33 mmol) in DCM (55 mL). This mixture was added to compound **3-34** and the solution was then cooled to 0 ºC. Formic acid (4.36 mL, 115.5 mmol) was added dropwise over 100 minutes and the reaction was then stirred to room temperature for 15 hours. The crude mixture was concentrated under vacuum. Pentane (62 mL), sodium carbonate (9.68 g, 70.0 mmol), and $MgSO_4$ (5.92 g) were added and the resulting mixture was stirred for 2 hours before filtering through cotton and concentrating under vacuum. The crude product was purified by chromatography over silica gel (gradient of 20:1 to 10:1 to 4:1 to 1:1) giving **3-35** (2.8083 g, 16.5 mmol, 100%) as an oil.

R_f = 0.62 in 4:1. IR (ATR): 3345, 2960, 2900, 2874, 2173, 1728, 1470, 1408, 1383, 1368, 1249, 1131, 1032, 992, 838, 759, 698. ^{1}H NMR (500 MHz, $CDCl_3$): δ 4.17(d, *J* = 5.9 Hz, 1H), 1.89(o, *J* = 5.9 Hz, 1H), 1.03(d, *J* = 6.8 Hz), 1.01(d, *J* = 6.8 Hz, 2H), 0.20 (s, 9H). ^{13}C NMR (500 MHz, $CDCl_3$): δ 105.55, 90.18, 68.34, 34.44, 18.04, 17.43, -0.10.

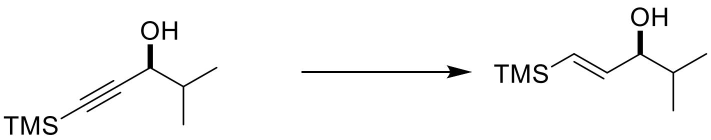

Sodium bis(2-methoxyethoxy)aluminum hydride (2.65 mL, 3.07M) was added dropwise to compound **3-35** (1.0313 g, 6.05 mmol) in diethyl ether (15 mL) at 0 ºC and stirred to room temperature for 15 hours. The crude reaction mixture was quenched by stirring with ethyl acetate (50 mL) and aq. Rochelle's salt (50 mL) for 1 hour. The quenched mixture was extracted with ethyl acetate (2 × 50 mL). The combined organic fractions were dried over $MgSO_4$, filtered through cotton, and concentrated under vacuum. The crude product was purified by chromatography over silica gel (gradient of 20:1 to 10:1) giving **3-36** (0.859 g, 4.98 mmol, 82.4%) as an oil.

R_f = 0.53 in 4:1. IR (ATR): 3355, 3057, 3025, 2956, 2923, 1721, 1621, 1601, 1582, 1493, 1452, 1247, 1025, 989, 866, 835, 762, 742, 694. ^{1}H NMR (500 MHz, $CDCl_3$): δ 6.06 (dd, *J* = 9.5, 5.6 Hz, 1H), 5.88 (dd, *J* = 9.4, 1.3 Hz, 1H), 3.88 (s, 1H), 1.76 (o, *J* = 6.9 Hz, 1H), 0.94 (d, *J* = 7.1 Hz, 3H), 0.92 (d, *J* = 7.2 Hz, 3H), 0.10 (s, 9H). ^{13}C NMR (500 MHz, $CDCl_3$): δ 146.98, 130.48, 79.61, 33.55, 18.35, 17.64, -1.26.

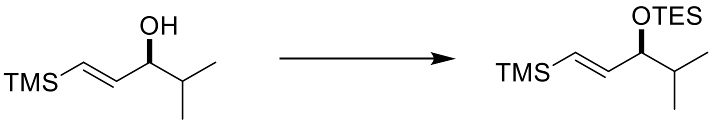

Chlorotriethylsilane (0.117 mL, 0.696 mmol) was added to a solution of compound **3-36** (0.100 g, 0.580 mmol) and imidazole (0.0790 g, 1.16 mmol) in DCM (1.66 mL) at 0ºC and then stirred at room temperature for 3 hours. The crude reaction mixture was quenched with water (10 mL) and extracted with DCM (2 × 10 mL). The combined organic fractions were dried over $MgSO_4$, filtered through cotton, and concentrated under vacuum. The crude product was purified by chromatography over silica gel (20:1) to give **3-37** (0.1453 g, 0.501 mmol, 86.3%) as an oil.

R_f = 0.85 in 20:1. IR (ATR): 2954, 2911, 2876, 1620, 1459, 1414, 1259, 1059, 1004, 992, 872, 834, 721, 691. ^{1}H NMR (500 MHz, $CDCl_3$): δ 5.97 (dd, *J* = 18.7, 6.5 Hz, 1H), 5.75 (dd, *J* = 18.8, 1.1 Hz, 1H), 3.77 (ddd, *J* = 6.4, 1.0 Hz, 1H), 1.66 (o, *J* = 6.5 Hz, 1H), 0.96 (t, *J* = 8.0 Hz, 9H), 0.90 (d, *J* = 6.8, 3H), 0.85 (d, *J* = 6.8 Hz, 3H), 0.59 (dq, *J* = 7.7, 2.5 Hz, 6H), 0.08 (s, 9H). ^{13}C NMR (500 MHz, $CDCl_3$): δ 147.91, 129.98, 81.17, 34.35, 18.39, 18.18, 6.88, 5.00, -1.32.

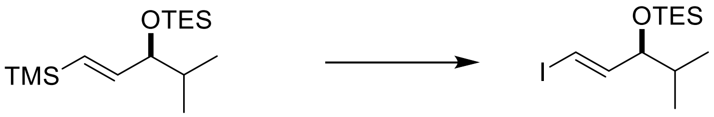

N-iodosuccinimide (0.169 g, 0.751 mmol) was added to compound **3-37** (0.144 g, 0.501 mmol) and 2,6-lutidine (0.081 mL, 0.701 mmol) in 1,1,1,3,3,3-hexafluoroisopropanol (2.00 mL) at 0ºC and stirred for 15 minutes. The crude reaction mixture was quenched with water (5 mL) and extracted with DCM (2 × 10 mL). The combined organic fractions were washed in sequence with sodium thiosulfate (25 mL), hydrochloric acid (25 mL, 1M), water (25 mL), sodium bicarbonate (25 mL), then dried over $MgSO_4$, filtered through cotton, and concentrated under vacuum. The crude product was purified by chromatography over silica gel (hexanes) to give **3-32** (0.0885 g, 0.260 mmol, 52.0%) as an oil.

R_f = 0.33 in hexanes. IR (ATR): 2955, 2910, 2875, 1607, 1459, 1414, 1384, 1364, 1238, 1182, 1162, 1118, 1103, 1071, 1004, 948, 828, 723. ^{1}H NMR (500 MHz, $CDCl_3$): δ 6.53 (dd, *J* = 14.4, 6.8 Hz, 1H), 6.20 (dd, *J* = 14.4, 1.1 Hz, 1H), 3.83 (ddd, *J* = 6.7, 5.7, 1.1 Hz), 1.69 (do, *J* = 6.8, 1.1 Hz, 1H), 0.97 (t, *J* = 8.0 Hz, 9H), 0.91 (d, *J* = 6.8, 3H), 0.87 (d, *J* = 6.8, 3H), 0.60 (q, *J* = 8.2 Hz, 6H). ^{13}C NMR (500 MHz, $CDCl_3$): 147.81, 80.18, 76.26, 34.34, 18.01, 17.82, 6.82, 4.90.

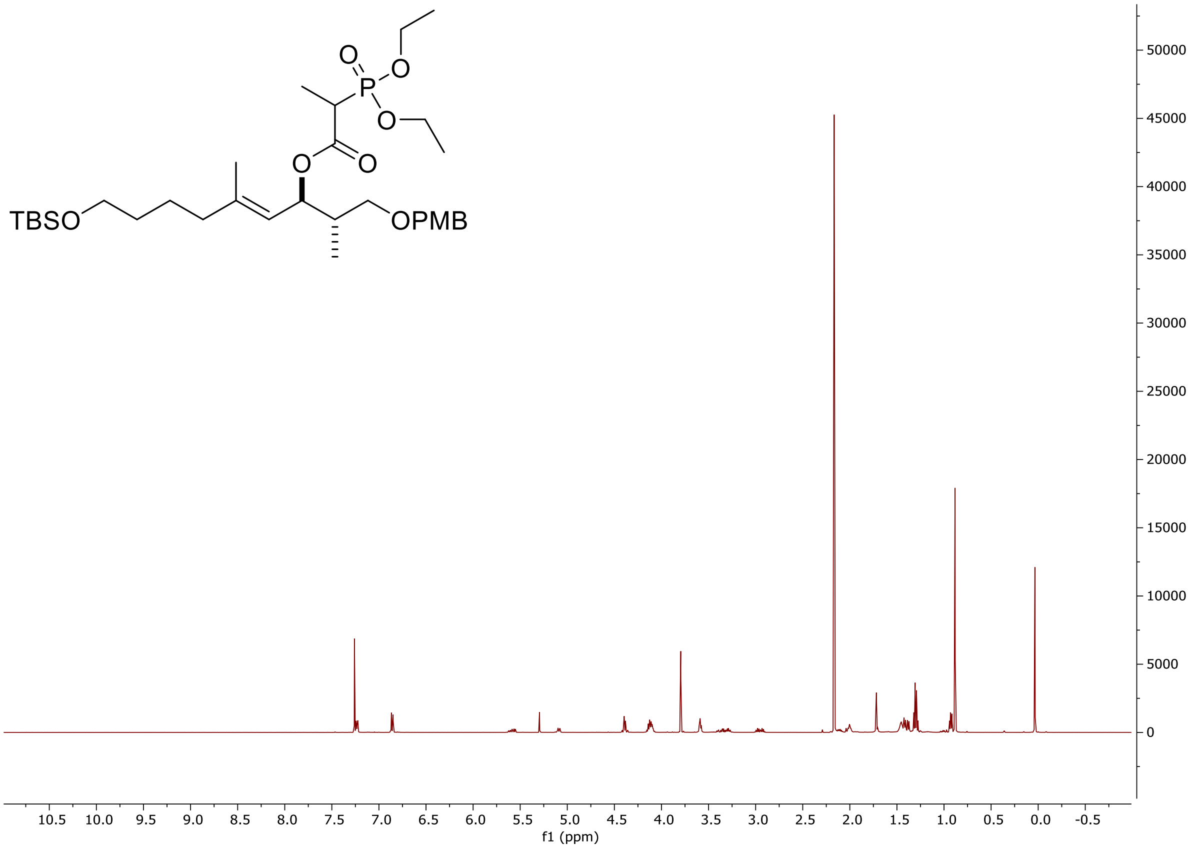
TBSO
OPMB
O
P
50000
45000
40000
35000
30000
25000
20000
15000
10000
5000
0
10.5 10.0 9.5 9.0 8.5 8.0 7.5 7.0 6.5 6.0 5.5 5.0 4.5 4.0 3.5 3.0 2.5 2.0 1.5 1.0 0.5 0.0 -0.5
f1 (ppm)

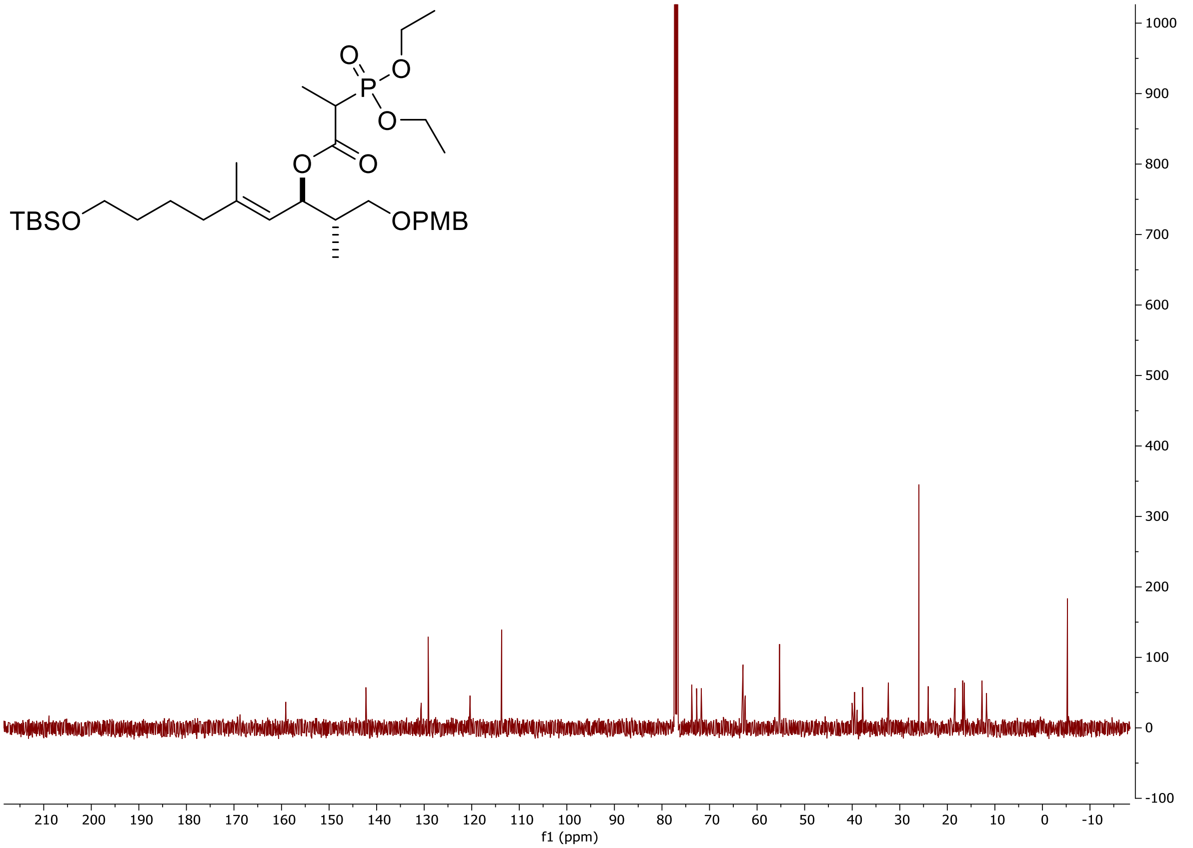
TBSO
OPMB
O
P
1000
900
800
700
600
500
400
300
200
100
0
-100
210 200 190 180 170 160 150 140 130 120 110 100 90 80 70 60 50 40 30 20 10 0 -10
f1 (ppm)

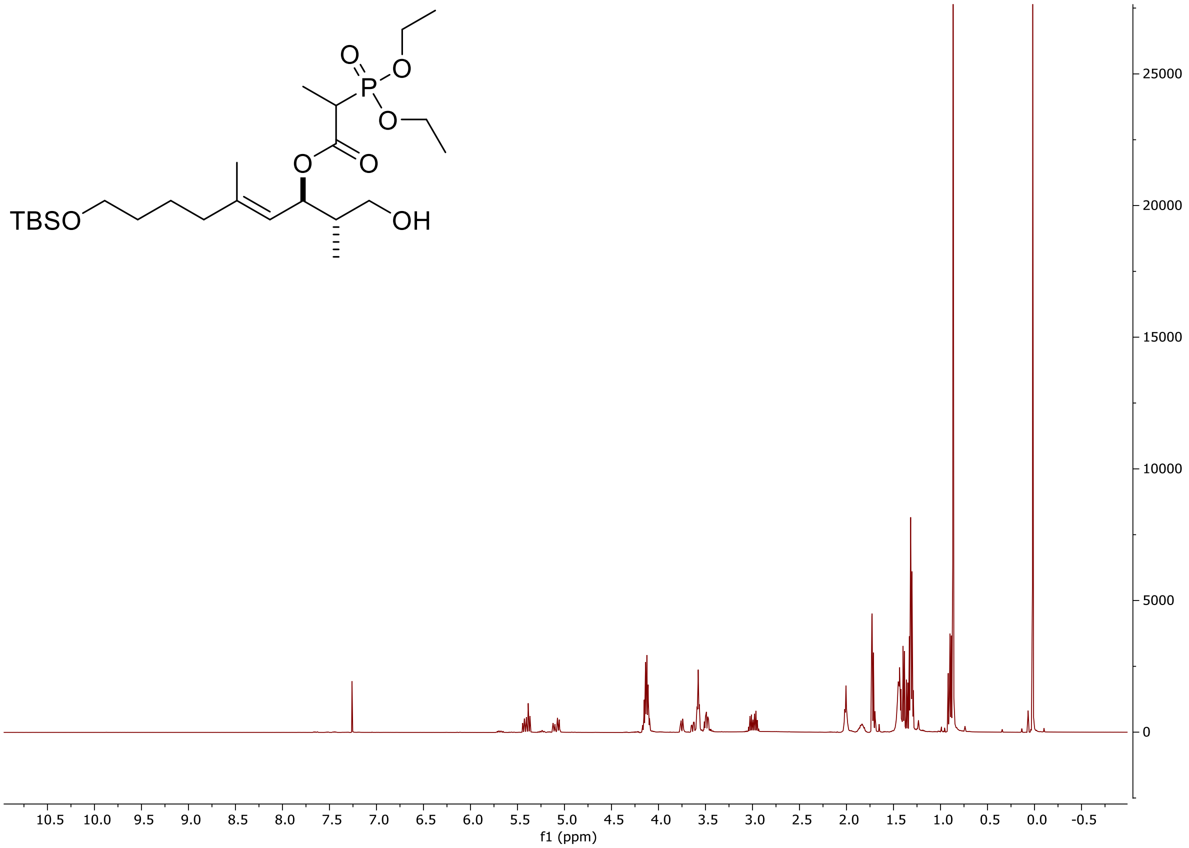
TBSO
OH
O
P
10.5 10.0 9.5 9.0 8.5 8.0 7.5 7.0 6.5 6.0 5.5 5.0 4.5 4.0 3.5 3.0 2.5 2.0 1.5 1.0 0.5 0.0 -0.5
f1 (ppm)
25000
20000
15000
10000
5000
0

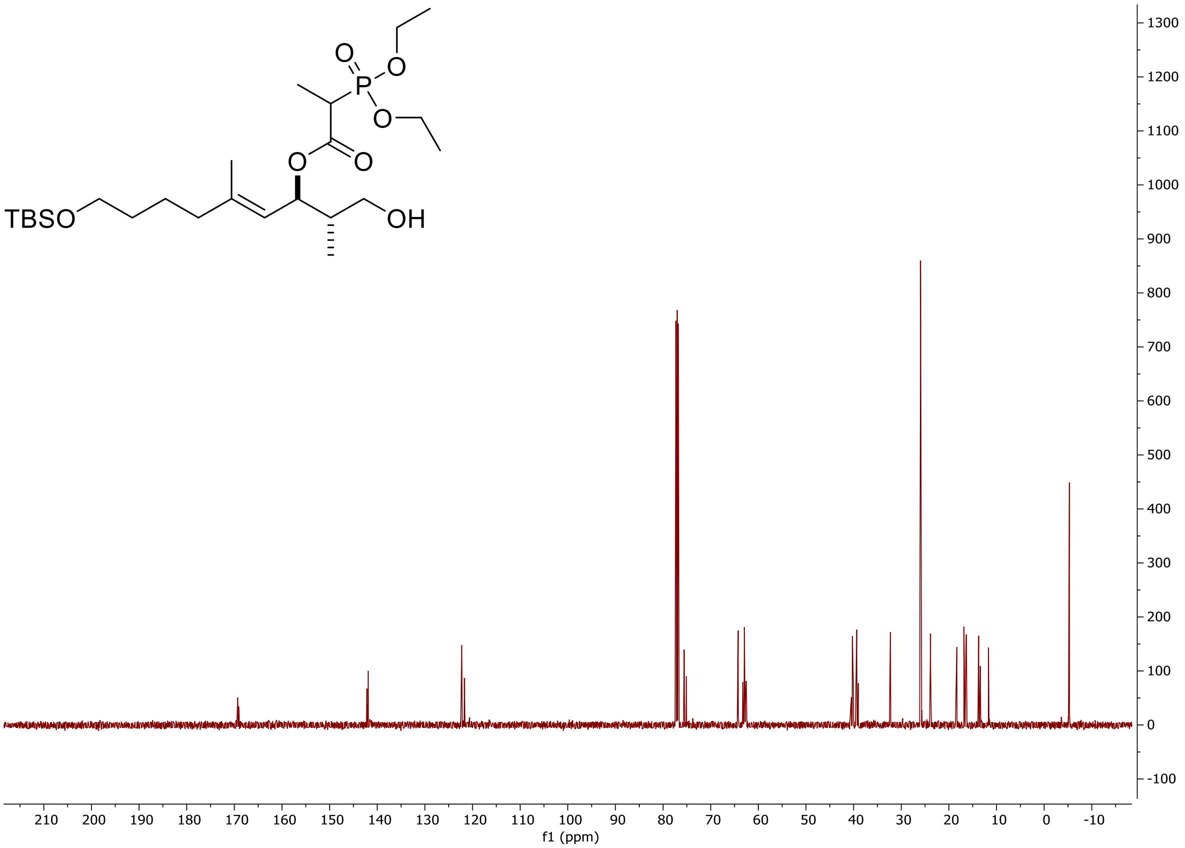
TBSO
OH
O
P
210 200 190 180 170 160 150 140 130 120 110 100 90 80 70 60 50 40 30 20 10 0 -10
f1 (ppm)
1300
1200
1100
1000
900
800
700
600
500
400
300
200
100
0
-100

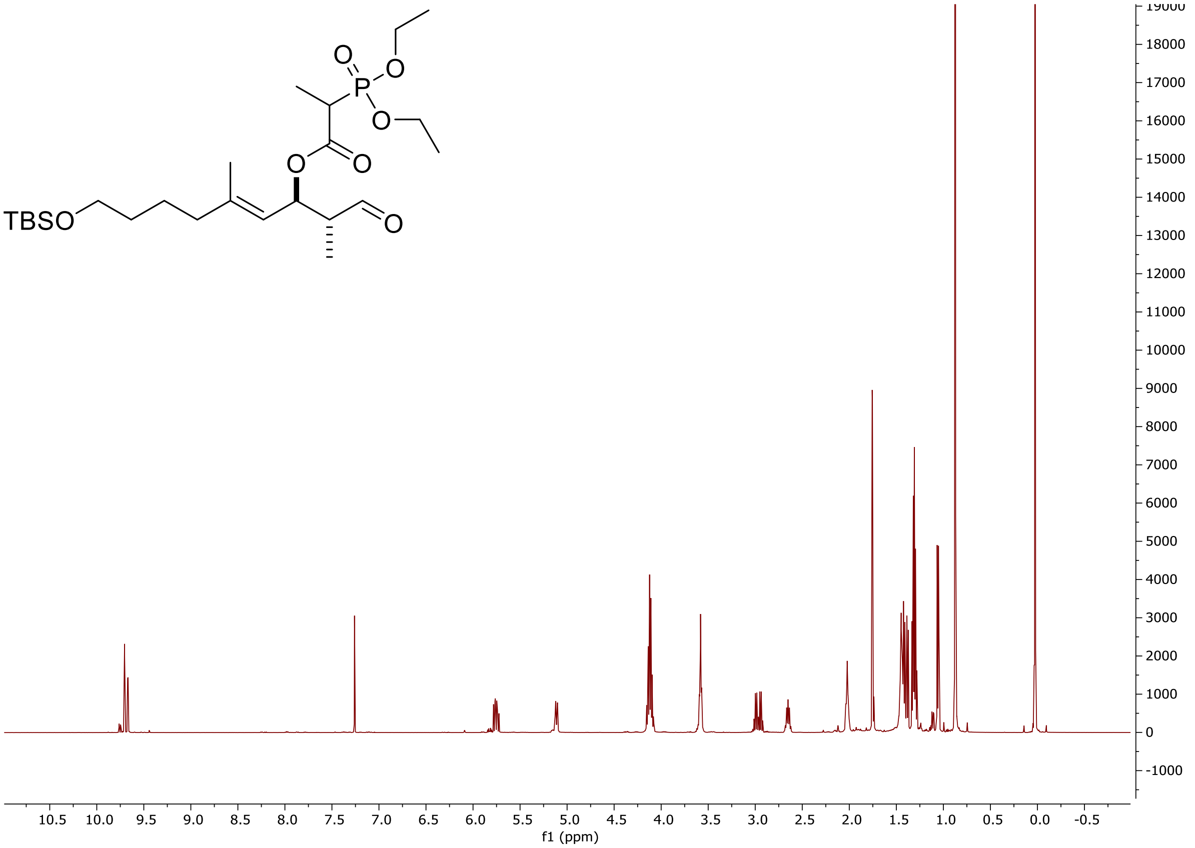
TBSO
O
P
O
O
O
O
O
10.5 10.0 9.5 9.0 8.5 8.0 7.5 7.0 6.5 6.0 5.5 5.0 4.5 4.0 3.5 3.0 2.5 2.0 1.5 1.0 0.5 0.0 -0.5
f1 (ppm)
19000 18000 17000 16000 15000 14000 13000 12000 11000 10000 9000 8000 7000 6000 5000 4000 3000 2000 1000 0 -1000

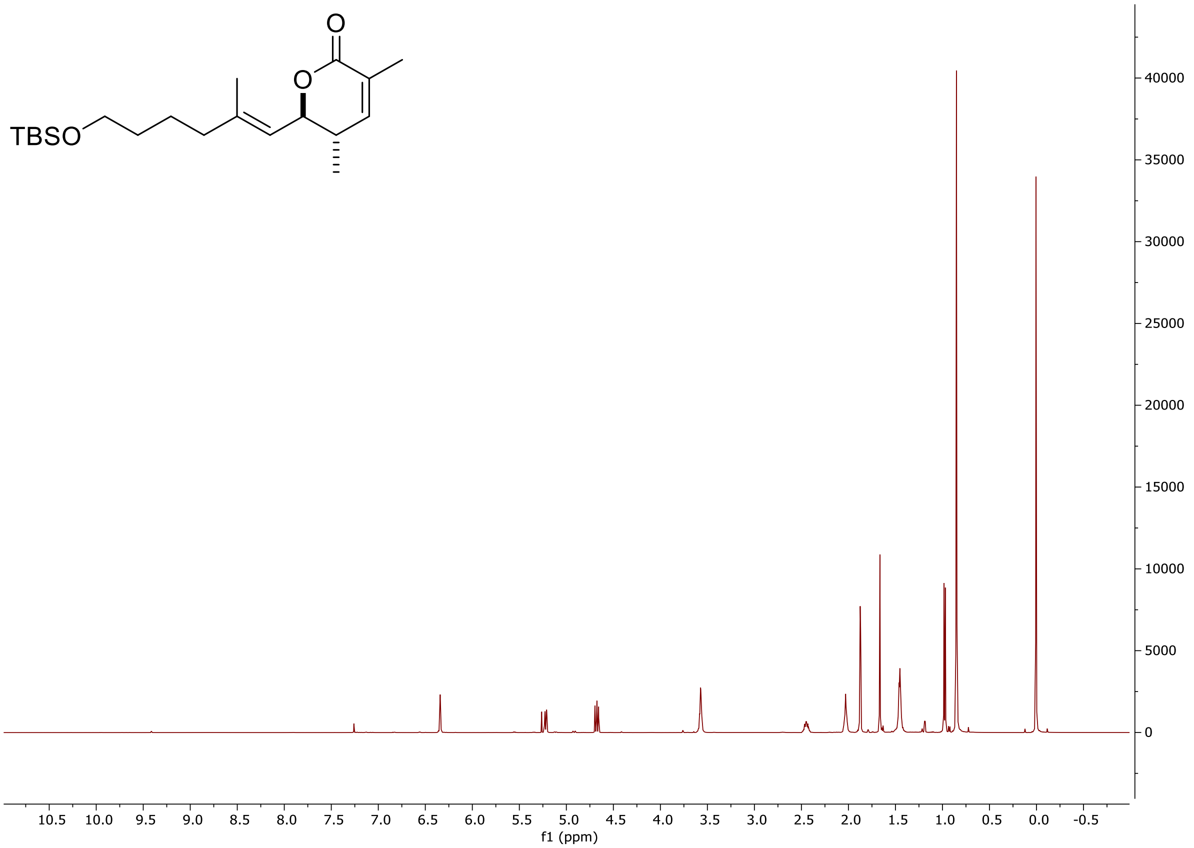
TBSO
O
O
10.5 10.0 9.5 9.0 8.5 8.0 7.5 7.0 6.5 6.0 5.5 5.0 4.5 4.0 3.5 3.0 2.5 2.0 1.5 1.0 0.5 0.0 -0.5
f1 (ppm)
40000 35000 30000 25000 20000 15000 10000 5000 0

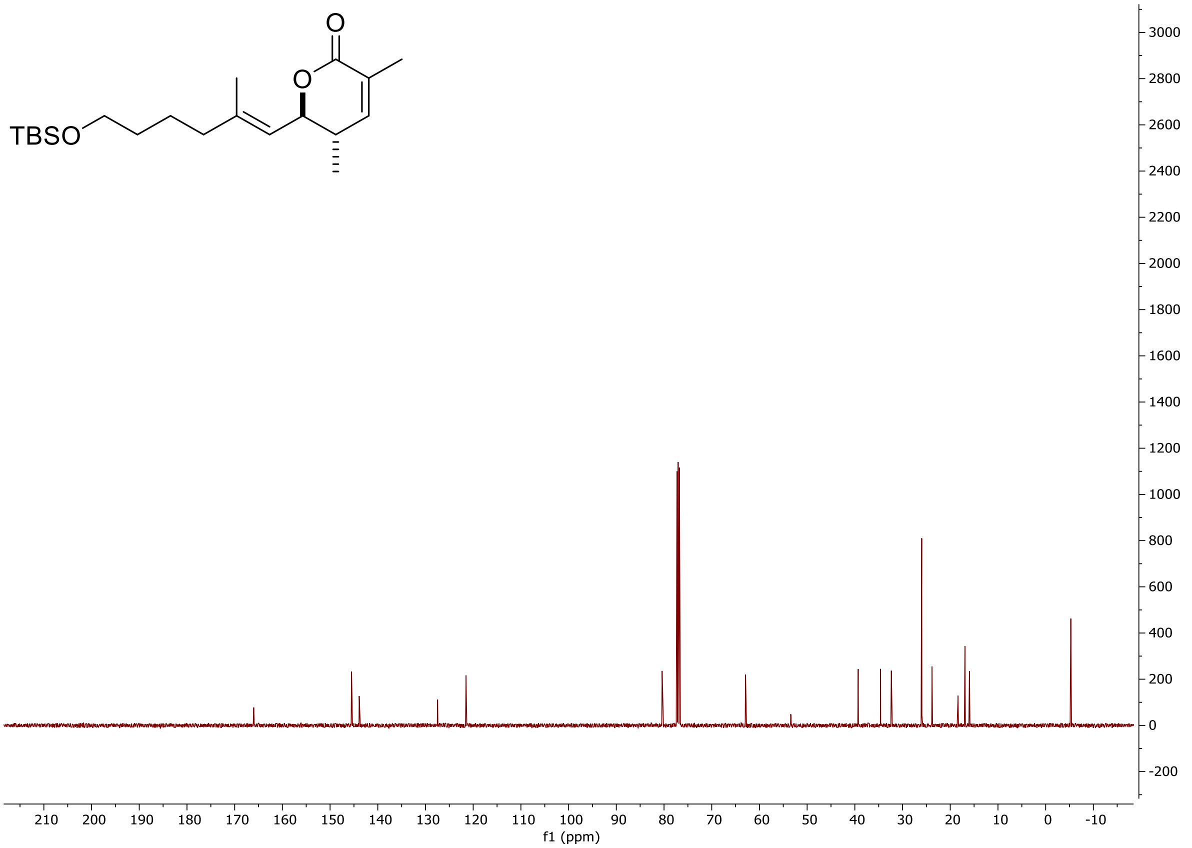
O
O
TBSO
3000
2800
2600
2400
2200
2000
1800
1600
1400
1200
1000
800
600
400
200
0
-200
210
200
190
180
170
160
150
140
130
120
110
100
90
80
70
60
50
40
30
20
10
0
-10
f1 (ppm)

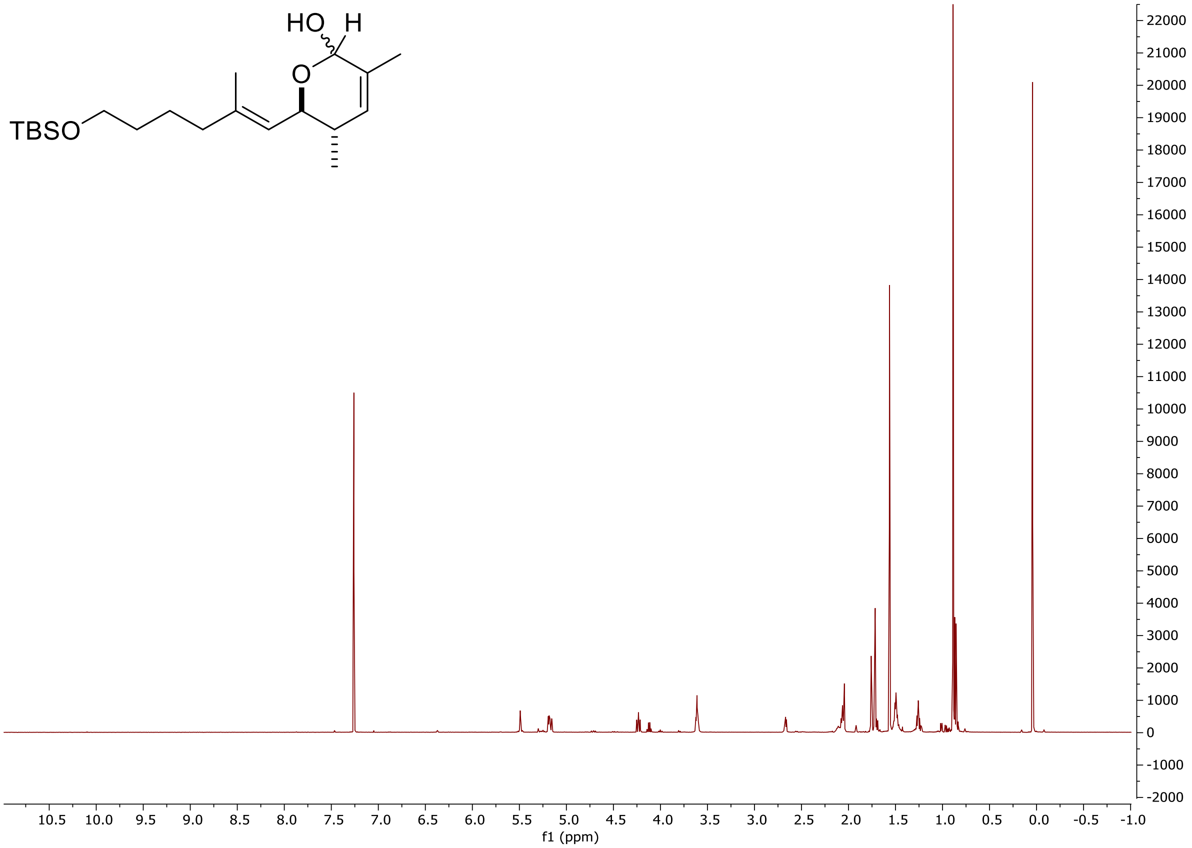
HO
H
O
TBSO
22000
21000
20000
19000
18000
17000
16000
15000
14000
13000
12000
11000
10000
9000
8000
7000
6000
5000
4000
3000
2000
1000
0
-1000
-2000
10.5
10.0
9.5
9.0
8.5
8.0
7.5
7.0
6.5
6.0
5.5
5.0
4.5
4.0
3.5
3.0
2.5
2.0
1.5
1.0
0.5
0.0
-0.5
-1.0
f1 (ppm)

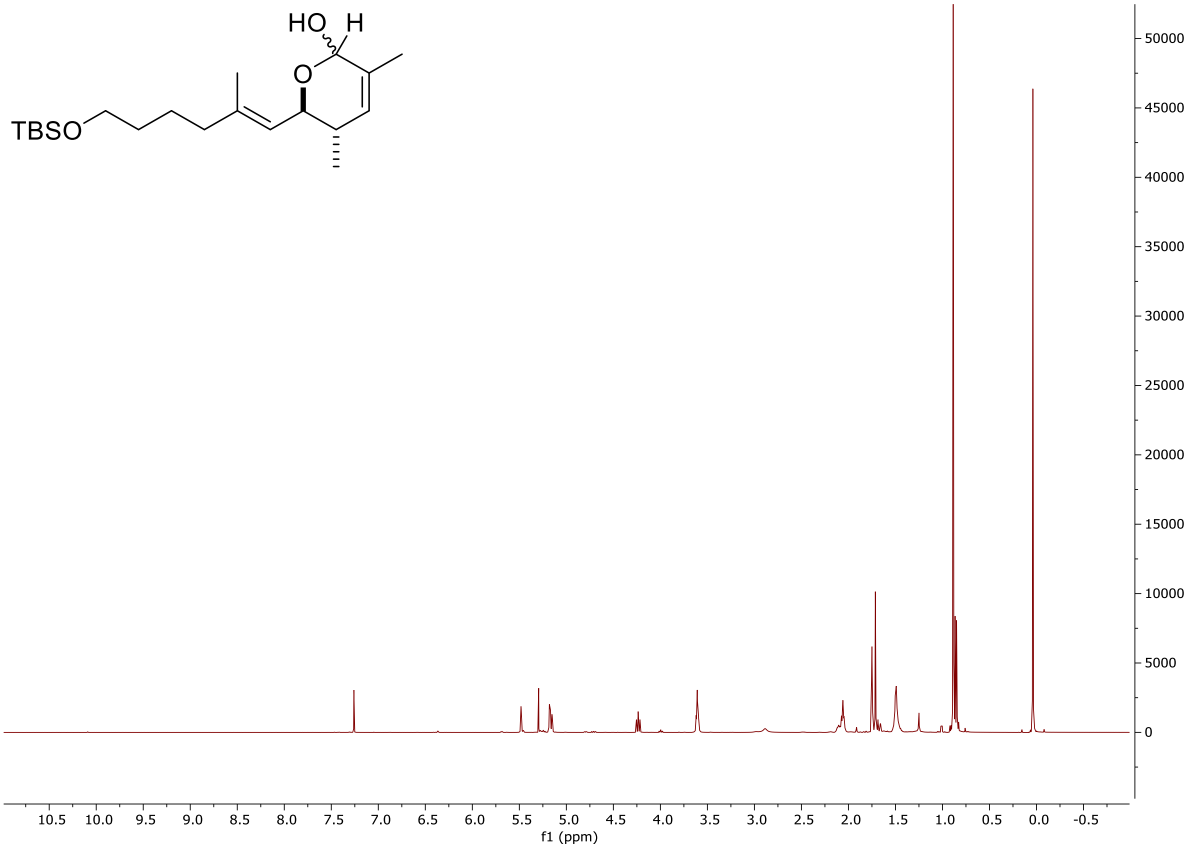
HO
H
O
TBSO
50000
45000
40000
35000
30000
25000
20000
15000
10000
5000
0
10.5 10.0 9.5 9.0 8.5 8.0 7.5 7.0 6.5 6.0 5.5 5.0 4.5 4.0 3.5 3.0 2.5 2.0 1.5 1.0 0.5 0.0 -0.5
f1 (ppm)

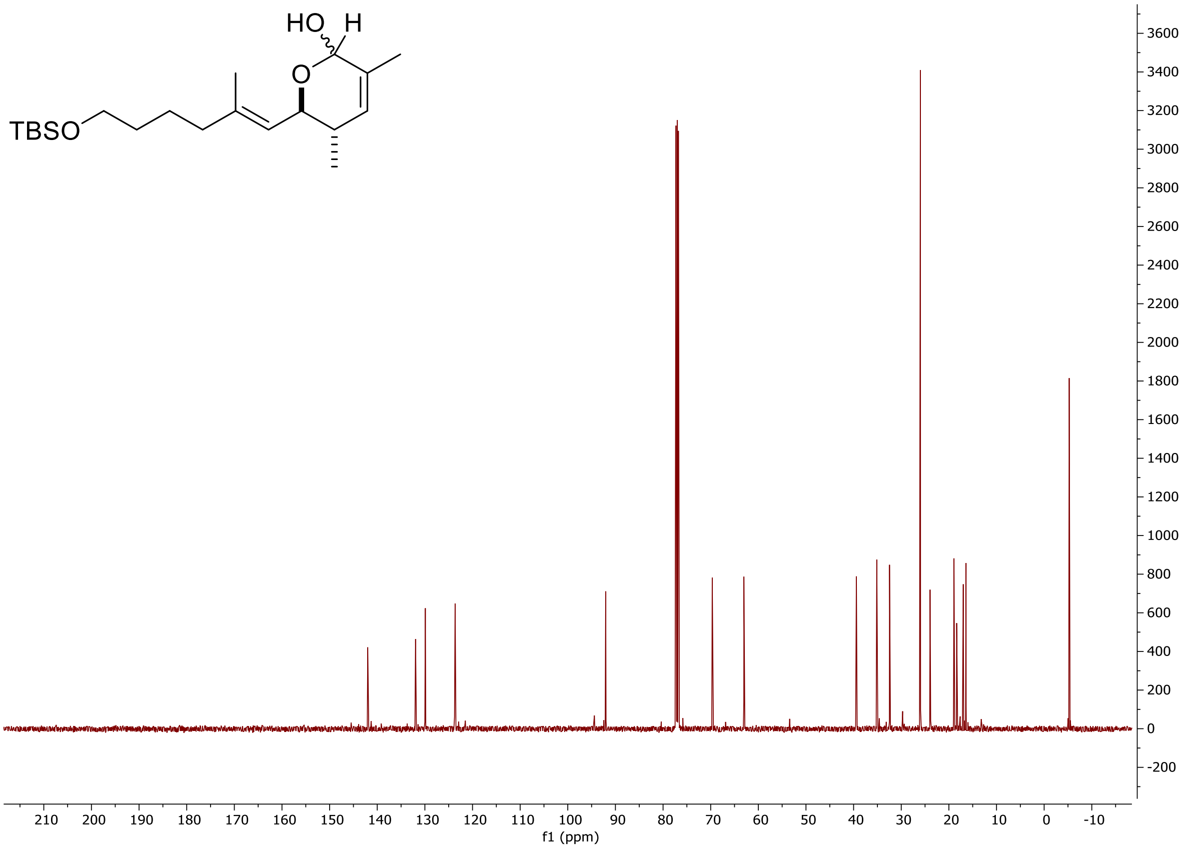
HO
H
O
TBSO
3600
3400
3200
3000
2800
2600
2400
2200
2000
1800
1600
1400
1200
1000
800
600
400
200
0
-200
210 200 190 180 170 160 150 140 130 120 110 100 90 80 70 60 50 40 30 20 10 0 -10
f1 (ppm)

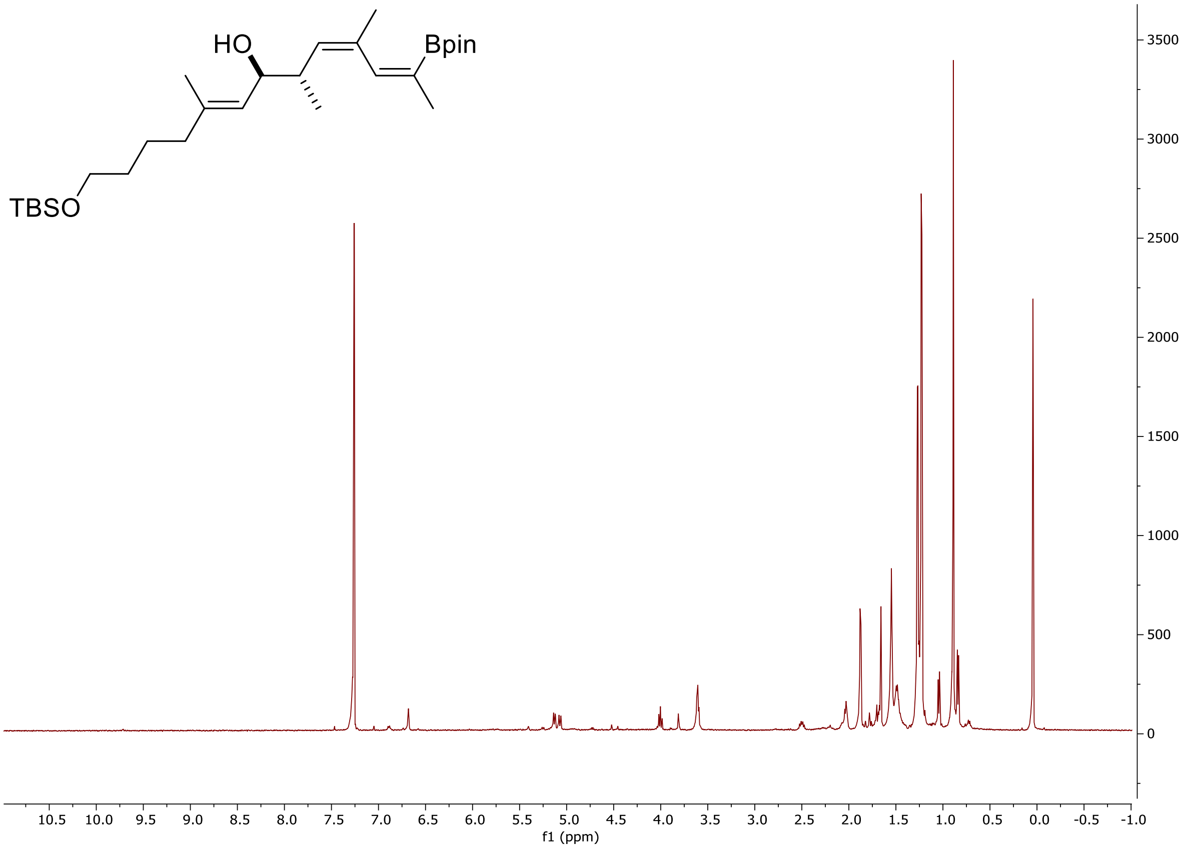
HO
Bpin
TBSO
3500
3000
2500
2000
1500
1000
500
0
10.5 10.0 9.5 9.0 8.5 8.0 7.5 7.0 6.5 6.0 5.5 5.0 4.5 4.0 3.5 3.0 2.5 2.0 1.5 1.0 0.5 0.0 -0.5 -1.0
f1 (ppm)

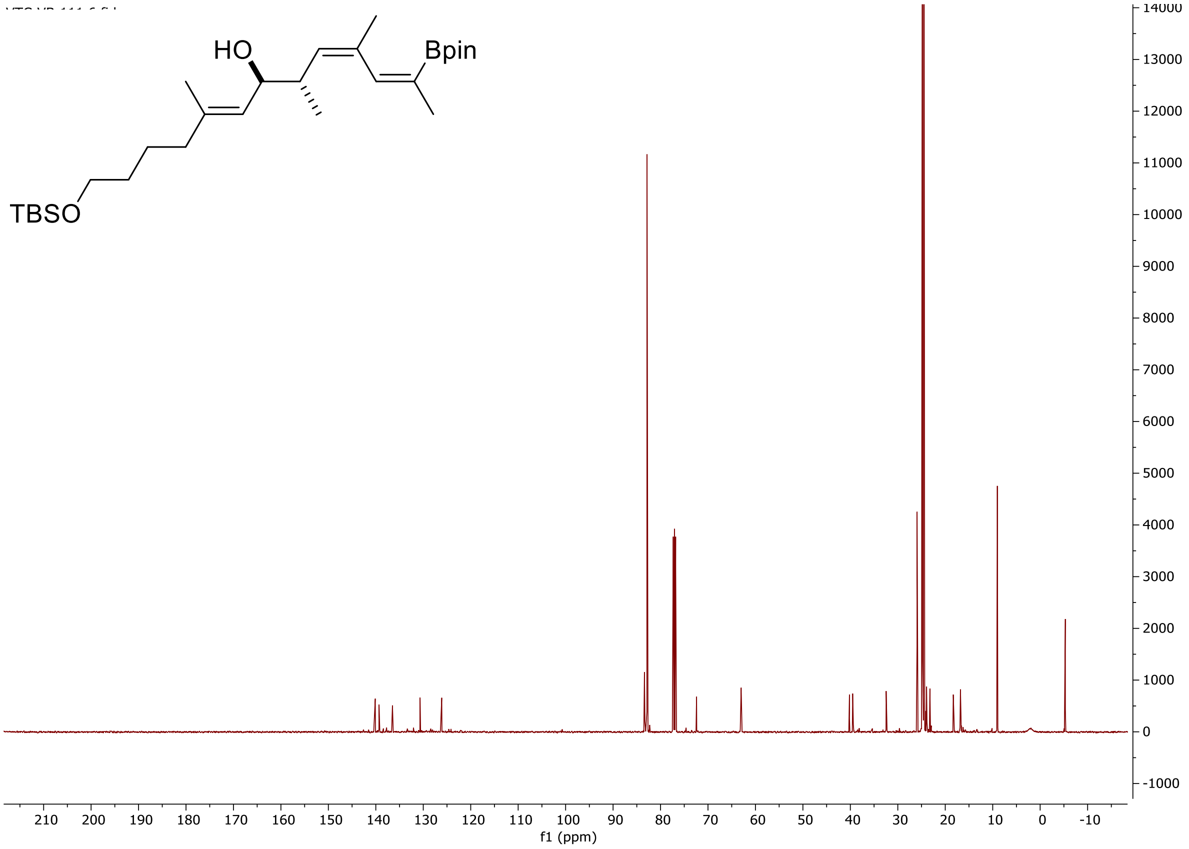
HO
Bpin
TBSO
14000
13000
12000
11000
10000
9000
8000
7000
6000
5000
4000
3000
2000
1000
0
-1000
210 200 190 180 170 160 150 140 130 120 110 100 90 80 70 60 50 40 30 20 10 0 -10
f1 (ppm)

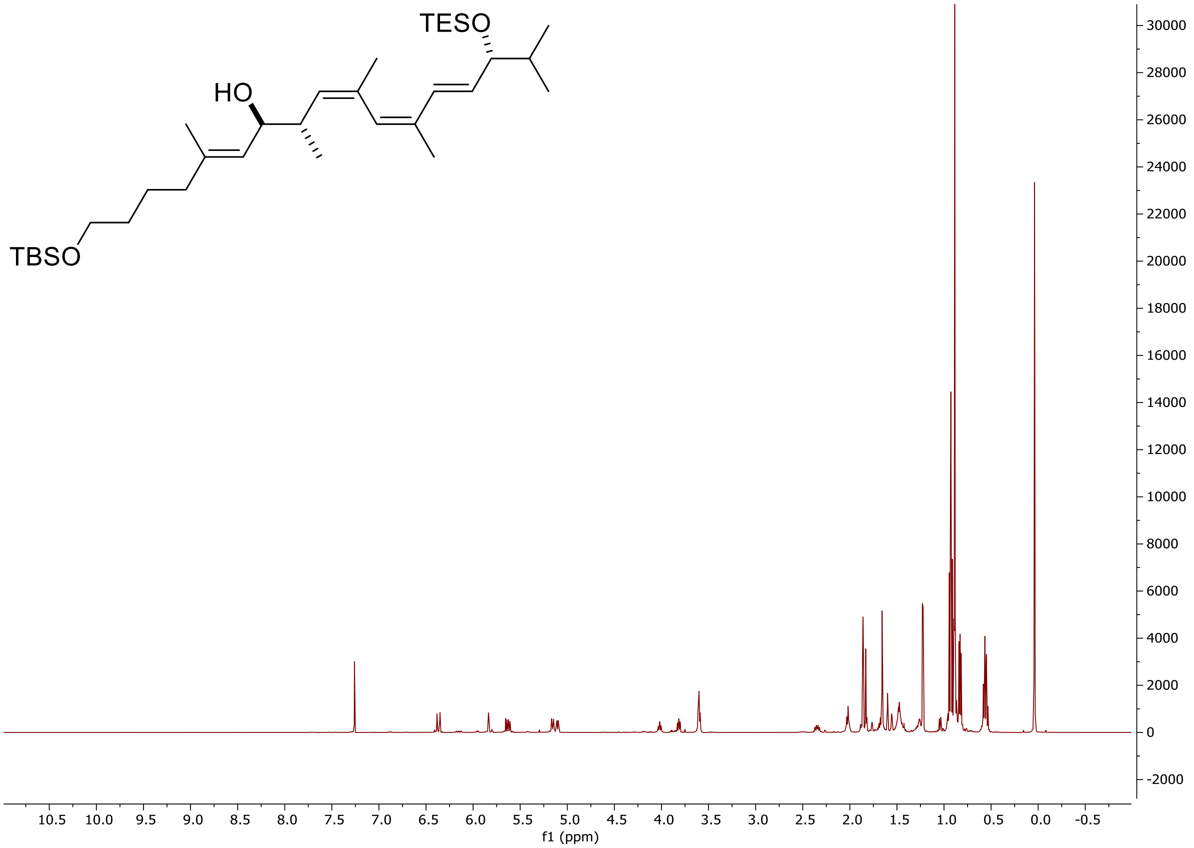
TESO
HO
TBSO
30000
28000
26000
24000
22000
20000
18000
16000
14000
12000
10000
8000
6000
4000
2000
0
-2000
10.5 10.0 9.5 9.0 8.5 8.0 7.5 7.0 6.5 6.0 5.5 5.0 4.5 4.0 3.5 3.0 2.5 2.0 1.5 1.0 0.5 0.0 -0.5
f1 (ppm)

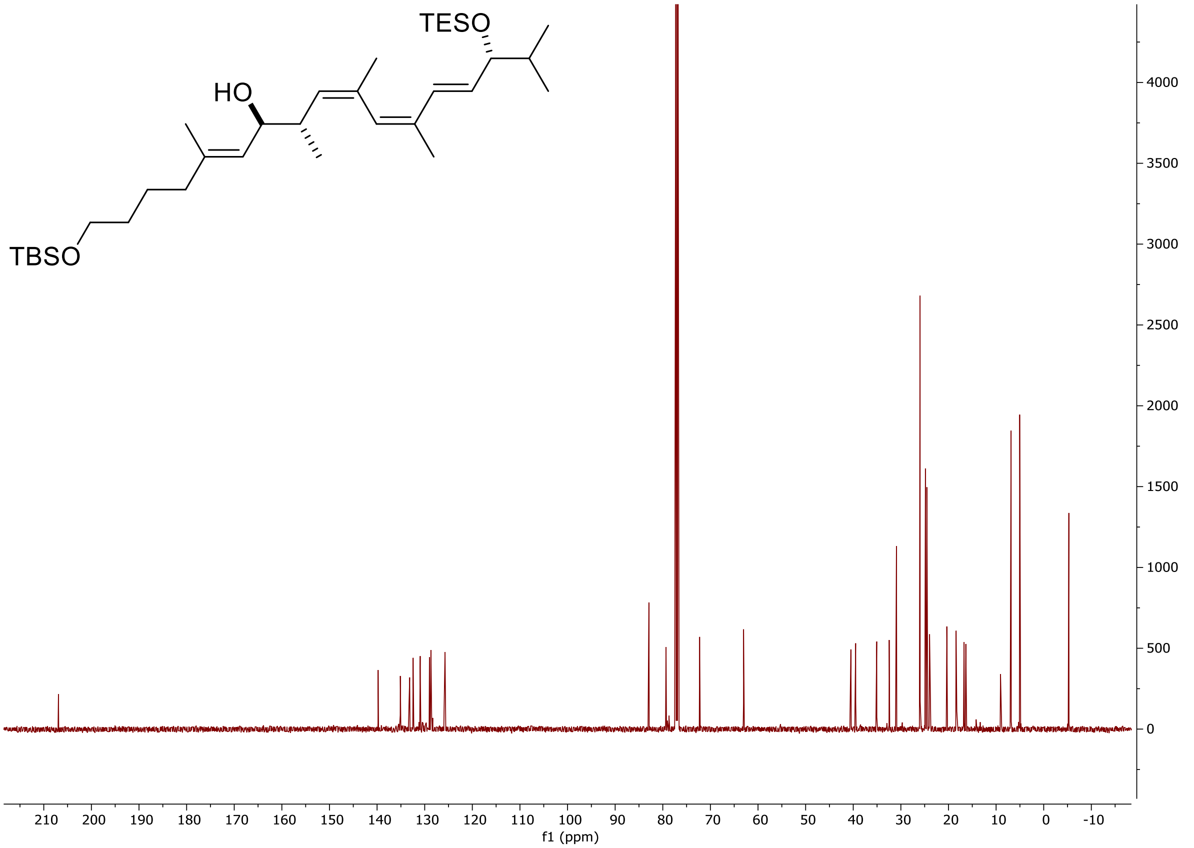
TESO
HO
TBSO
4000
3500
3000
2500
2000
1500
1000
500
0
210 200 190 180 170 160 150 140 130 120 110 100 90 80 70 60 50 40 30 20 10 0 -10
f1 (ppm)

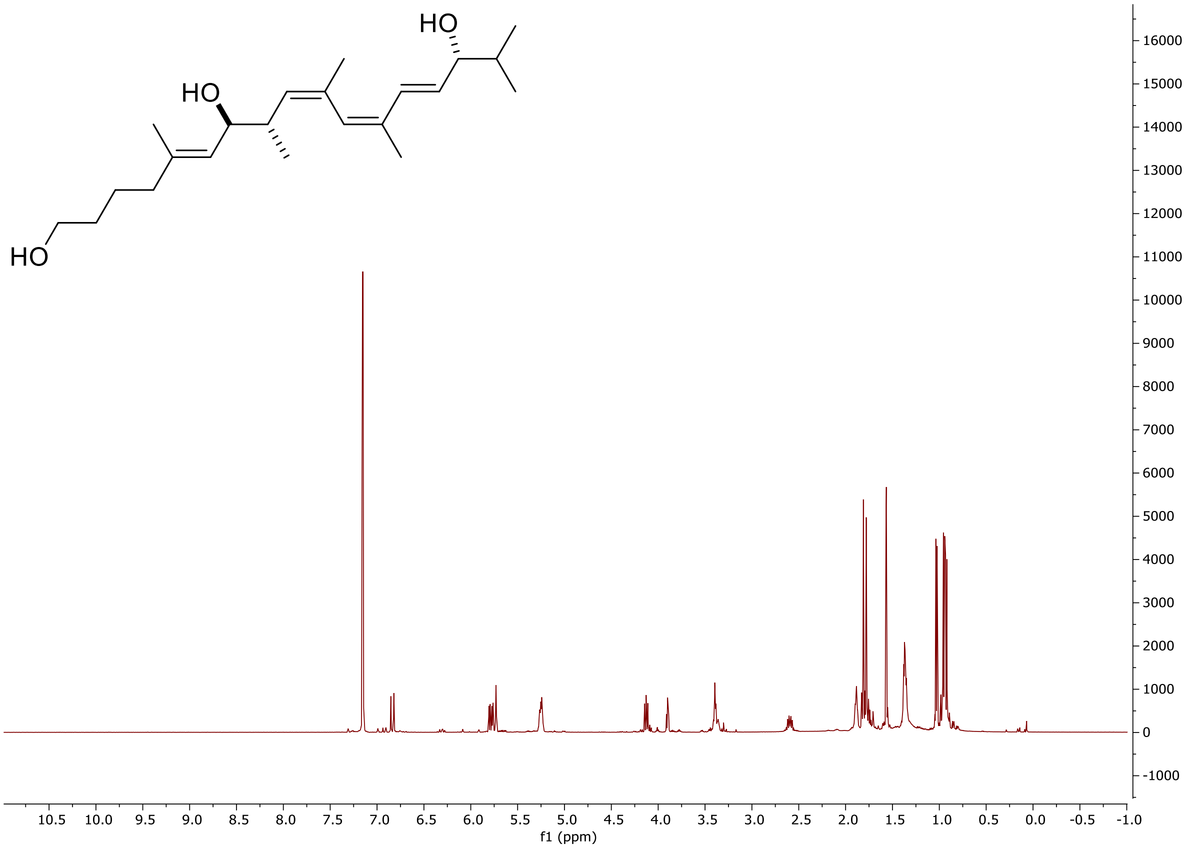
HO
HO
HO
16000
15000
14000
13000
12000
11000
10000
9000
8000
7000
6000
5000
4000
3000
2000
1000
0
-1000
10.5 10.0 9.5 9.0 8.5 8.0 7.5 7.0 6.5 6.0 5.5 5.0 4.5 4.0 3.5 3.0 2.5 2.0 1.5 1.0 0.5 0.0 -0.5 -1.0
f1 (ppm)

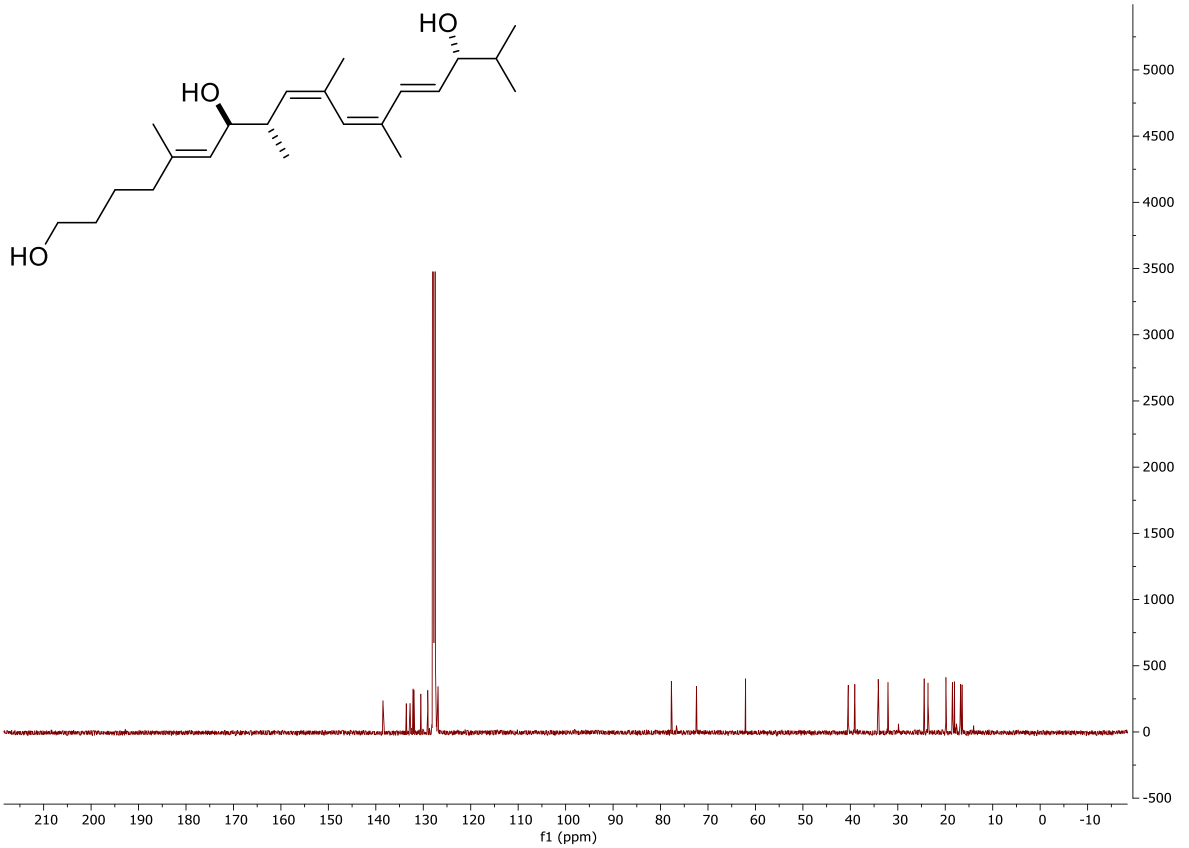
HO
HO
HO
5000
4500
4000
3500
3000
2500
2000
1500
1000
500
0
-500
210 200 190 180 170 160 150 140 130 120 110 100 90 80 70 60 50 40 30 20 10 0 -10
f1 (ppm)

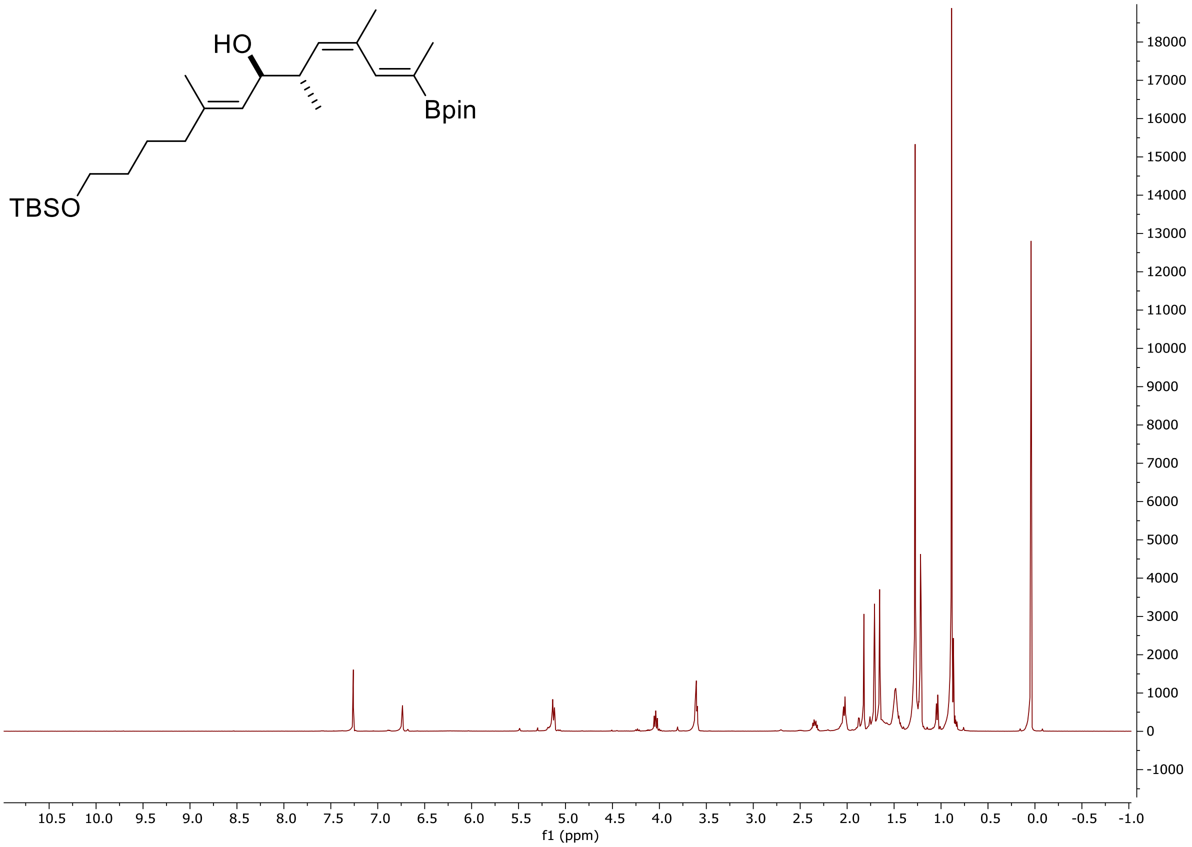

HO
Bpin
TBSO
18000
17000
16000
15000
14000
13000
12000
11000
10000
9000
8000
7000
6000
5000
4000
3000
2000
1000
0
-1000
10.5 10.0 9.5 9.0 8.5 8.0 7.5 7.0 6.5 6.0 5.5 5.0 4.5 4.0 3.5 3.0 2.5 2.0 1.5 1.0 0.5 0.0 -0.5 -1.0
f1 (ppm)

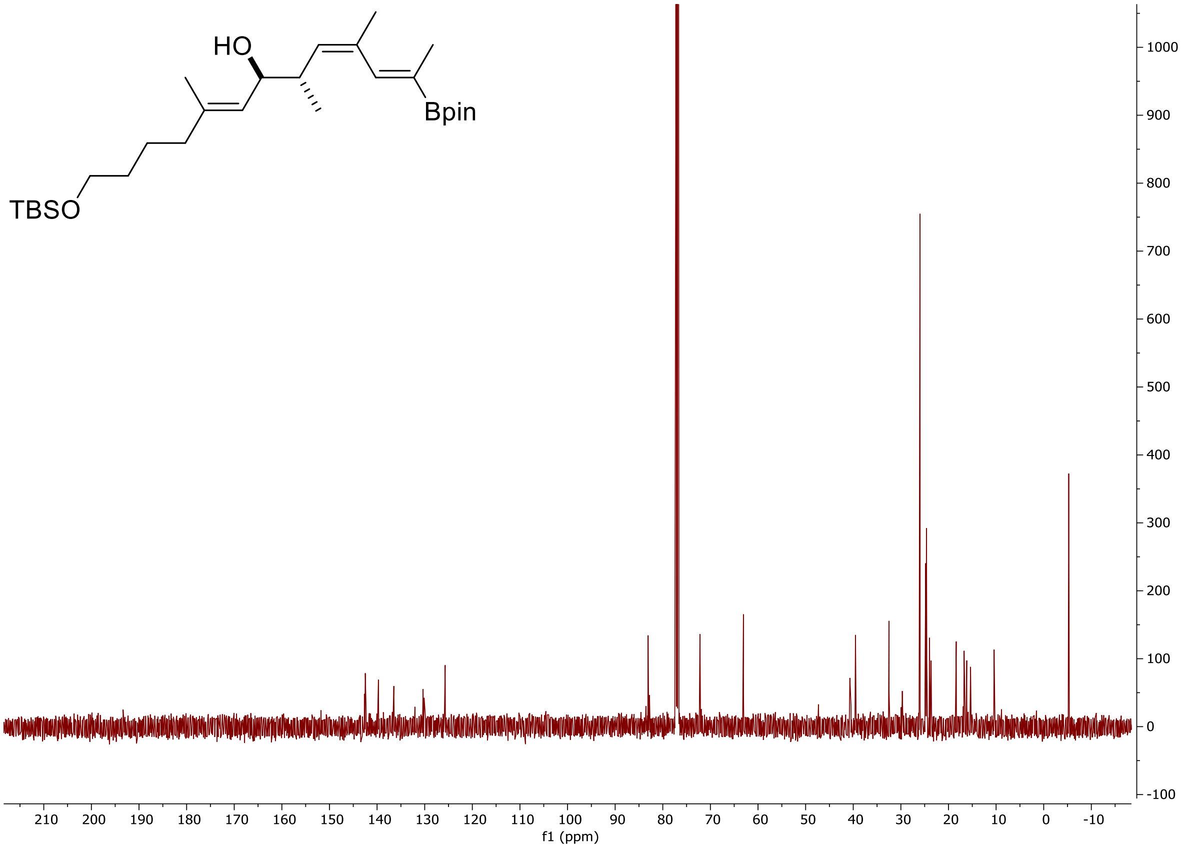

HO
Bpin
TBSO
1000
900
800
700
600
500
400
300
200
100
0
-100
210 200 190 180 170 160 150 140 130 120 110 100 90 80 70 60 50 40 30 20 10 0 -10
f1 (ppm)

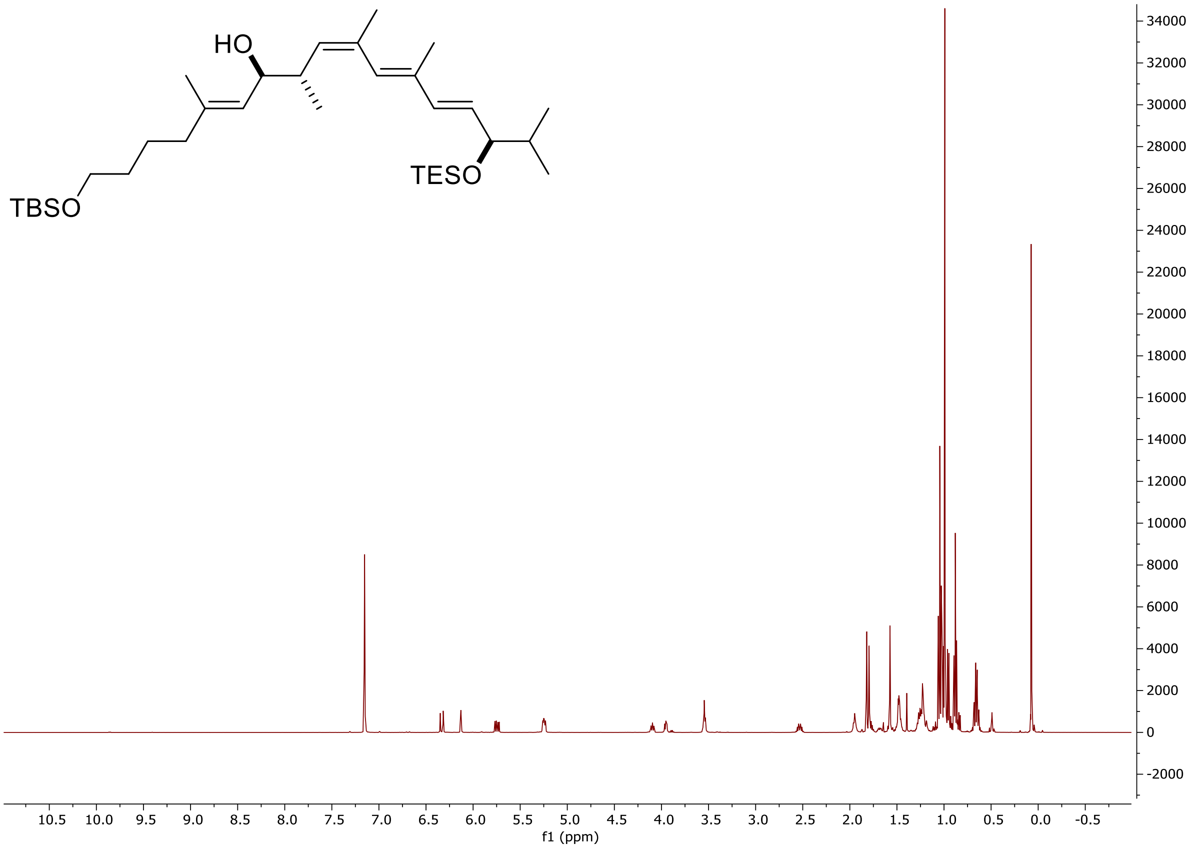
HO
TESO
TBSO
34000
32000
30000
28000
26000
24000
22000
20000
18000
16000
14000
12000
10000
8000
6000
4000
2000
0
-2000
10.5 10.0 9.5 9.0 8.5 8.0 7.5 7.0 6.5 6.0 5.5 5.0 4.5 4.0 3.5 3.0 2.5 2.0 1.5 1.0 0.5 0.0 -0.5
f1 (ppm)

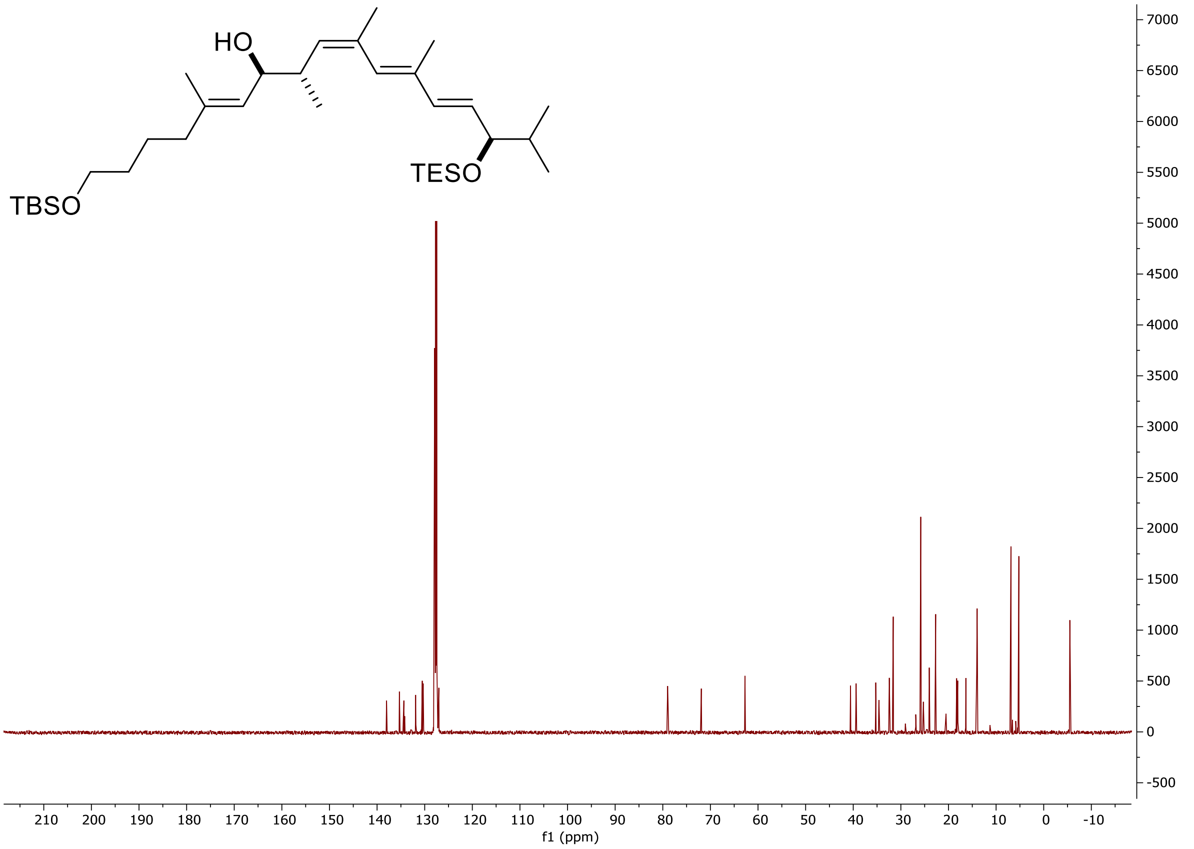
HO
TESO
TBSO
7000
6500
6000
5500
5000
4500
4000
3500
3000
2500
2000
1500
1000
500
0
-500
210 200 190 180 170 160 150 140 130 120 110 100 90 80 70 60 50 40 30 20 10 0 -10
f1 (ppm)

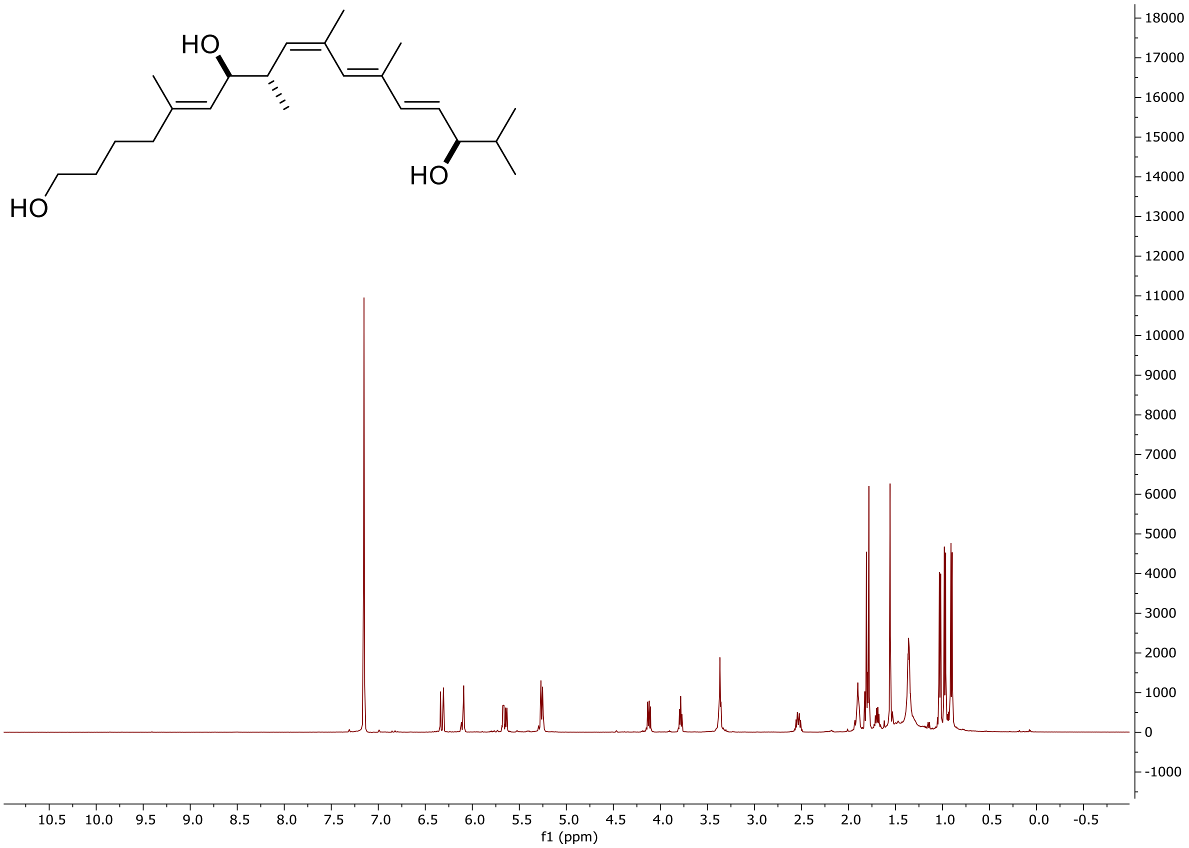
HO
HO
HO
18000
17000
16000
15000
14000
13000
12000
11000
10000
9000
8000
7000
6000
5000
4000
3000
2000
1000
0
-1000
10.5 10.0 9.5 9.0 8.5 8.0 7.5 7.0 6.5 6.0 5.5 5.0 4.5 4.0 3.5 3.0 2.5 2.0 1.5 1.0 0.5 0.0 -0.5
f1 (ppm)

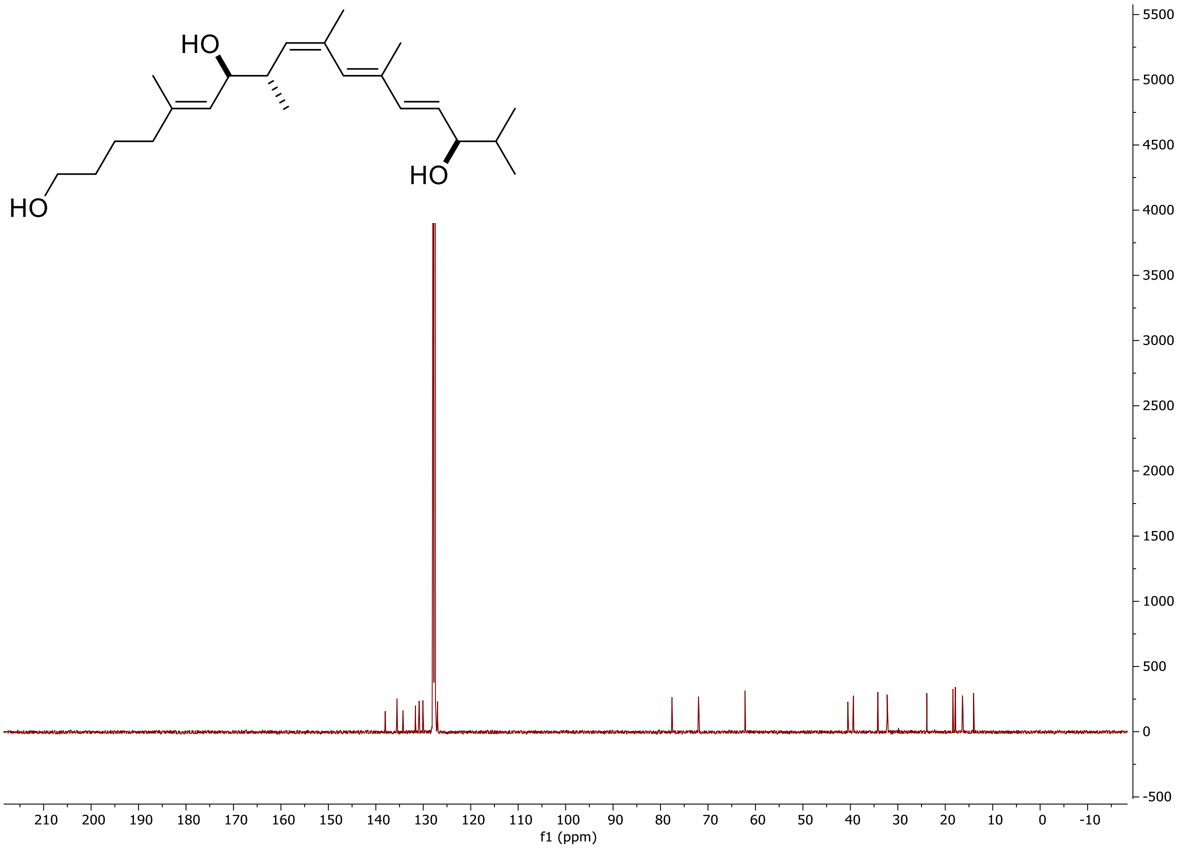
HO
HO
HO
5500
5000
4500
4000
3500
3000
2500
2000
1500
1000
500
0
-500
210 200 190 180 170 160 150 140 130 120 110 100 90 80 70 60 50 40 30 20 10 0 -10
f1 (ppm)

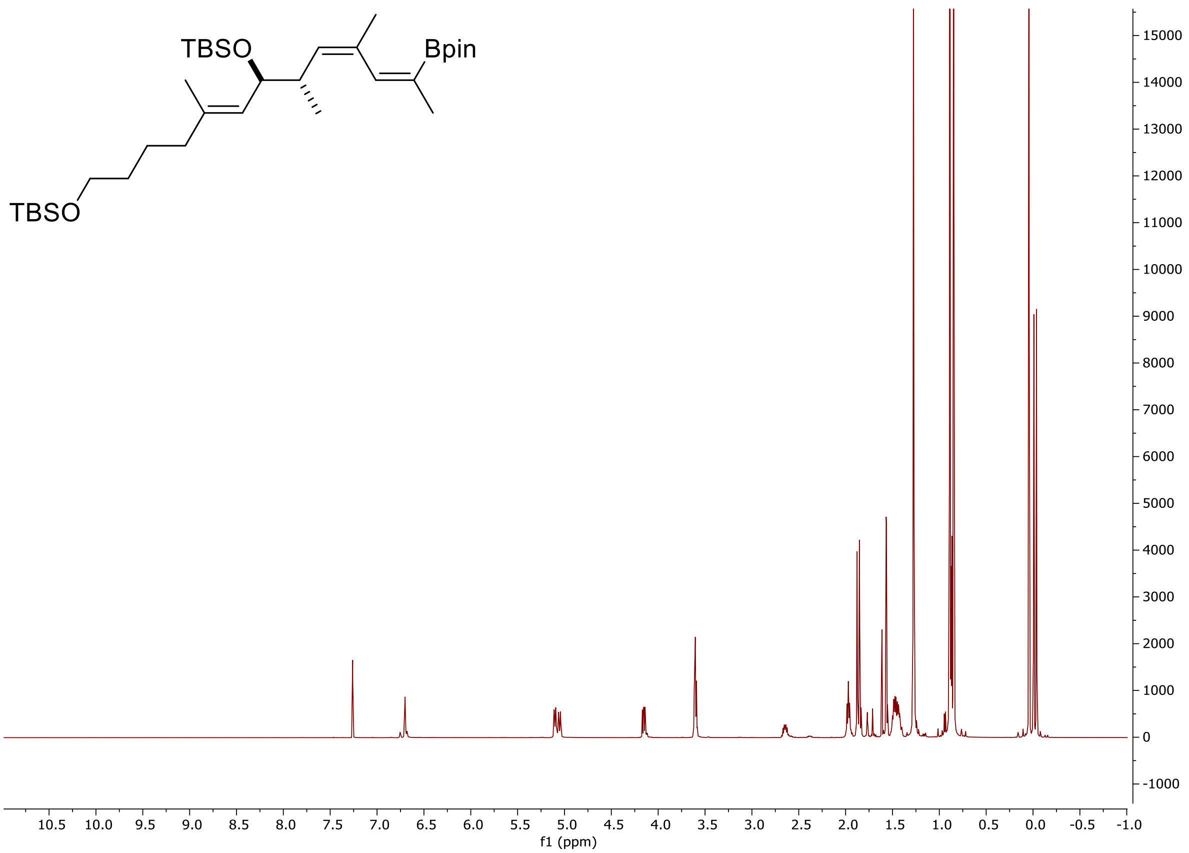
TBSO
Bpin
TBSO
15000
14000
13000
12000
11000
10000
9000
8000
7000
6000
5000
4000
3000
2000
1000
0
-1000
10.5 10.0 9.5 9.0 8.5 8.0 7.5 7.0 6.5 6.0 5.5 5.0 4.5 4.0 3.5 3.0 2.5 2.0 1.5 1.0 0.5 0.0 -0.5 -1.0
f1 (ppm)

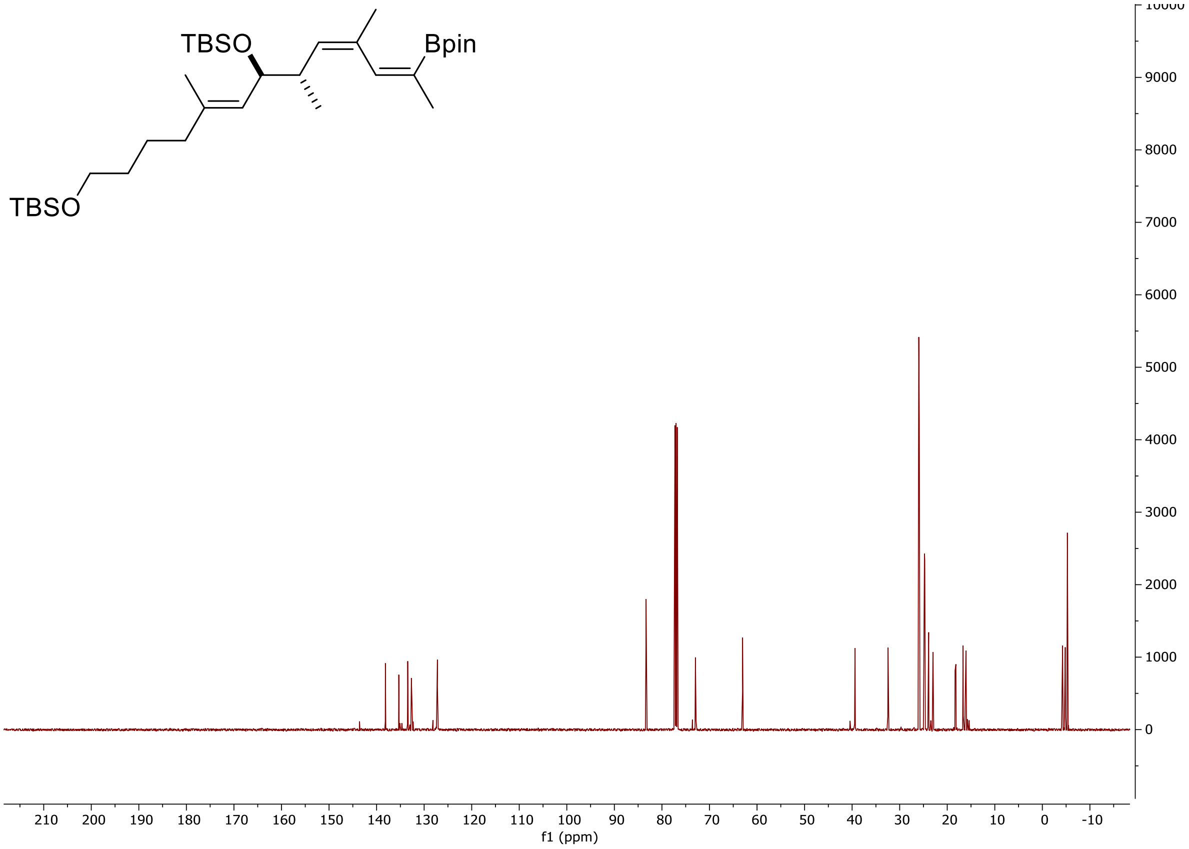
TBSO
Bpin
TBSO
10000
9000
8000
7000
6000
5000
4000
3000
2000
1000
0
210 200 190 180 170 160 150 140 130 120 110 100 90 80 70 60 50 40 30 20 10 0 -10
f1 (ppm)

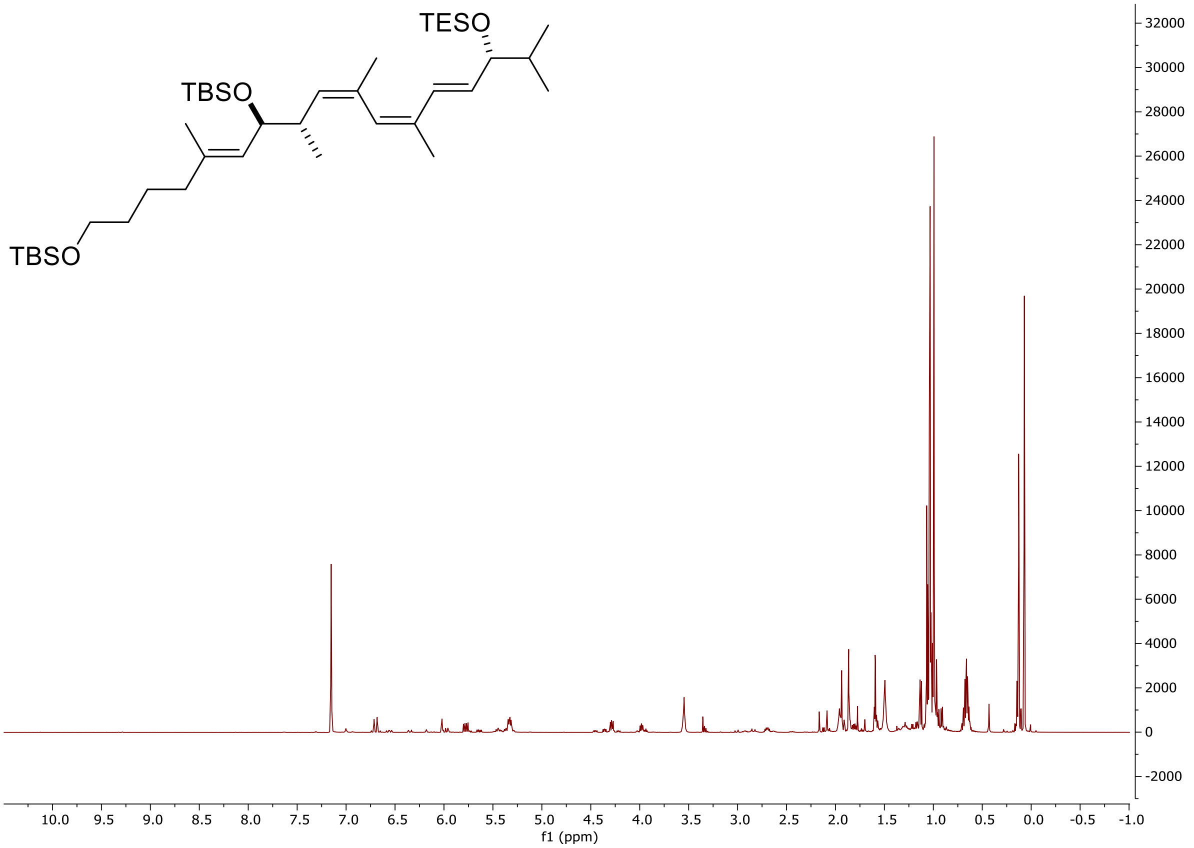
TESO
TBSO
TBSO
32000
30000
28000
26000
24000
22000
20000
18000
16000
14000
12000
10000
8000
6000
4000
2000
0
-2000
10.0 9.5 9.0 8.5 8.0 7.5 7.0 6.5 6.0 5.5 5.0 4.5 4.0 3.5 3.0 2.5 2.0 1.5 1.0 0.5 0.0 -0.5 -1.0
f1 (ppm)

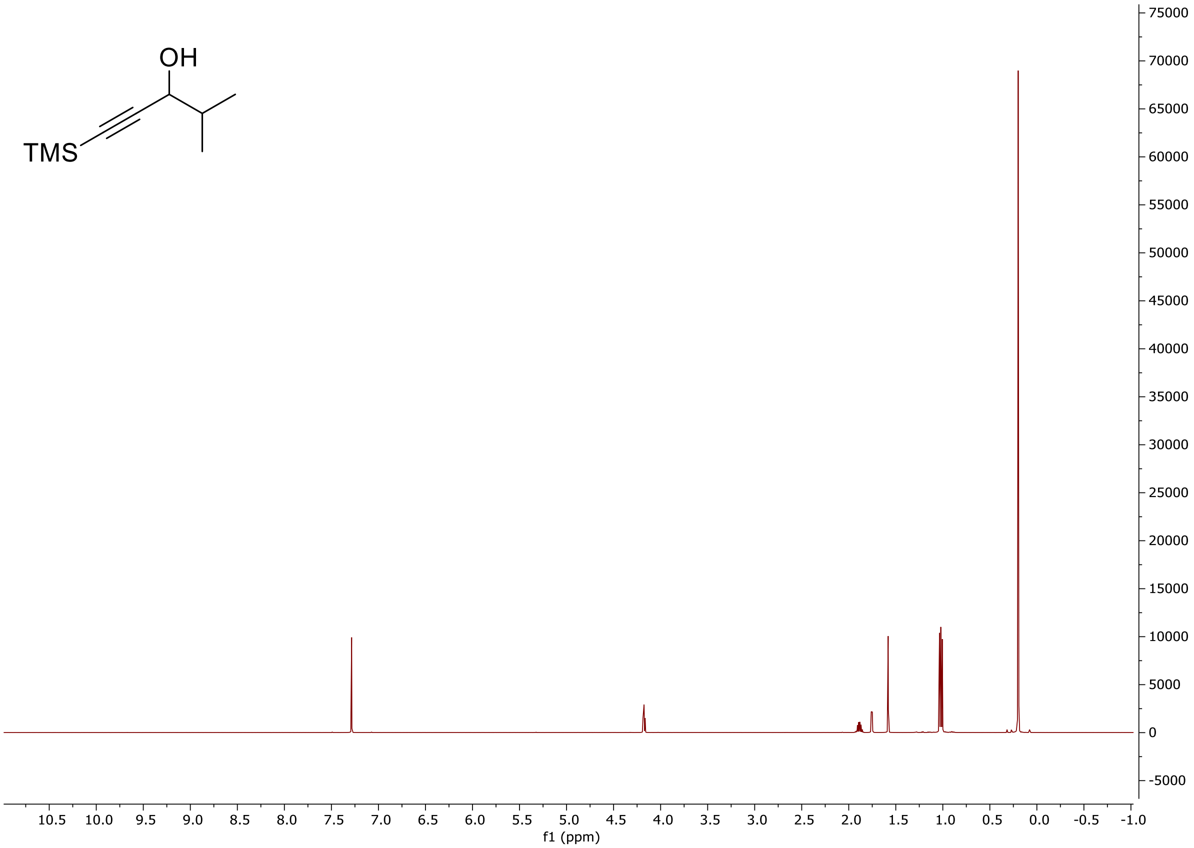
OH
TMS
75000
70000
65000
60000
55000
50000
45000
40000
35000
30000
25000
20000
15000
10000
5000
0
-5000
10.5 10.0 9.5 9.0 8.5 8.0 7.5 7.0 6.5 6.0 5.5 5.0 4.5 4.0 3.5 3.0 2.5 2.0 1.5 1.0 0.5 0.0 -0.5 -1.0
f1 (ppm)

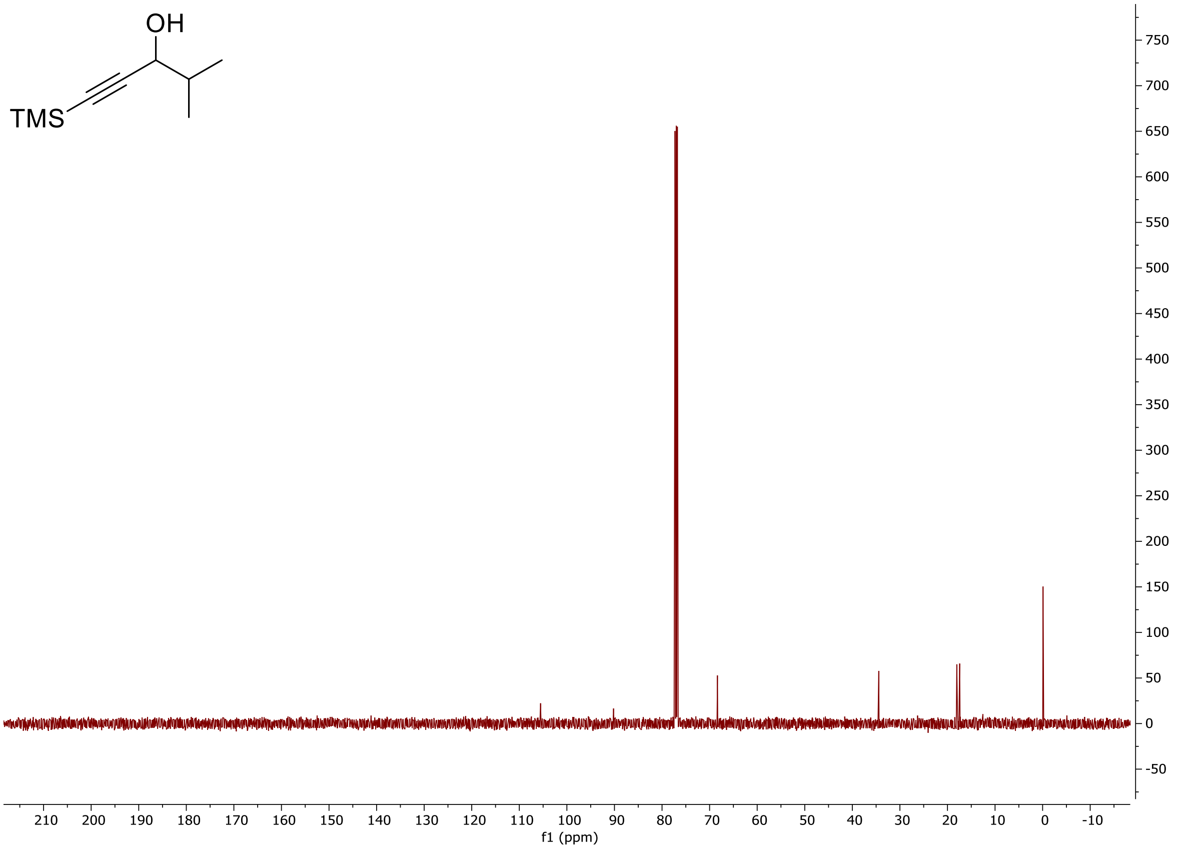
OH
TMS
750
700
650
600
550
500
450
400
350
300
250
200
150
100
50
0
-50
210 200 190 180 170 160 150 140 130 120 110 100 90 80 70 60 50 40 30 20 10 0 -10
f1 (ppm)

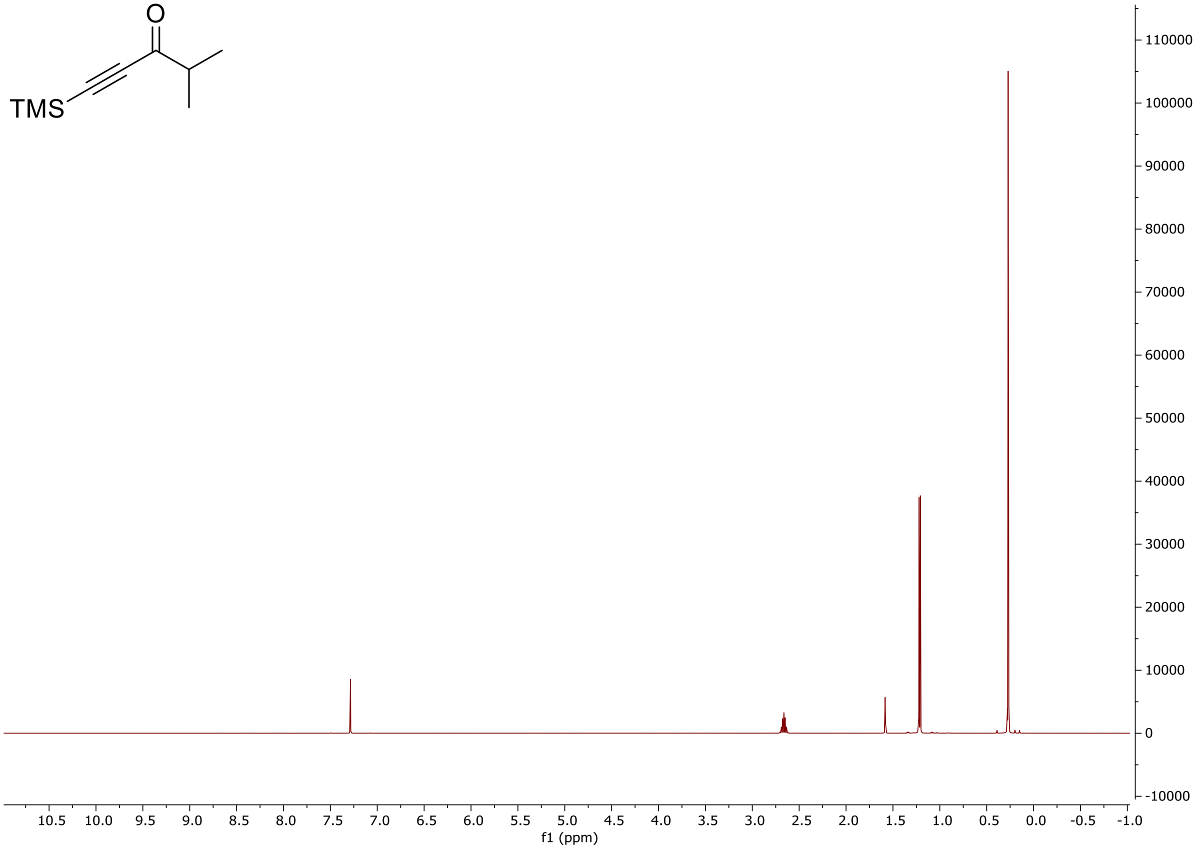
O
TMS
110000
100000
90000
80000
70000
60000
50000
40000
30000
20000
10000
0
-10000
10.5 10.0 9.5 9.0 8.5 8.0 7.5 7.0 6.5 6.0 5.5 5.0 4.5 4.0 3.5 3.0 2.5 2.0 1.5 1.0 0.5 0.0 -0.5 -1.0
f1 (ppm)

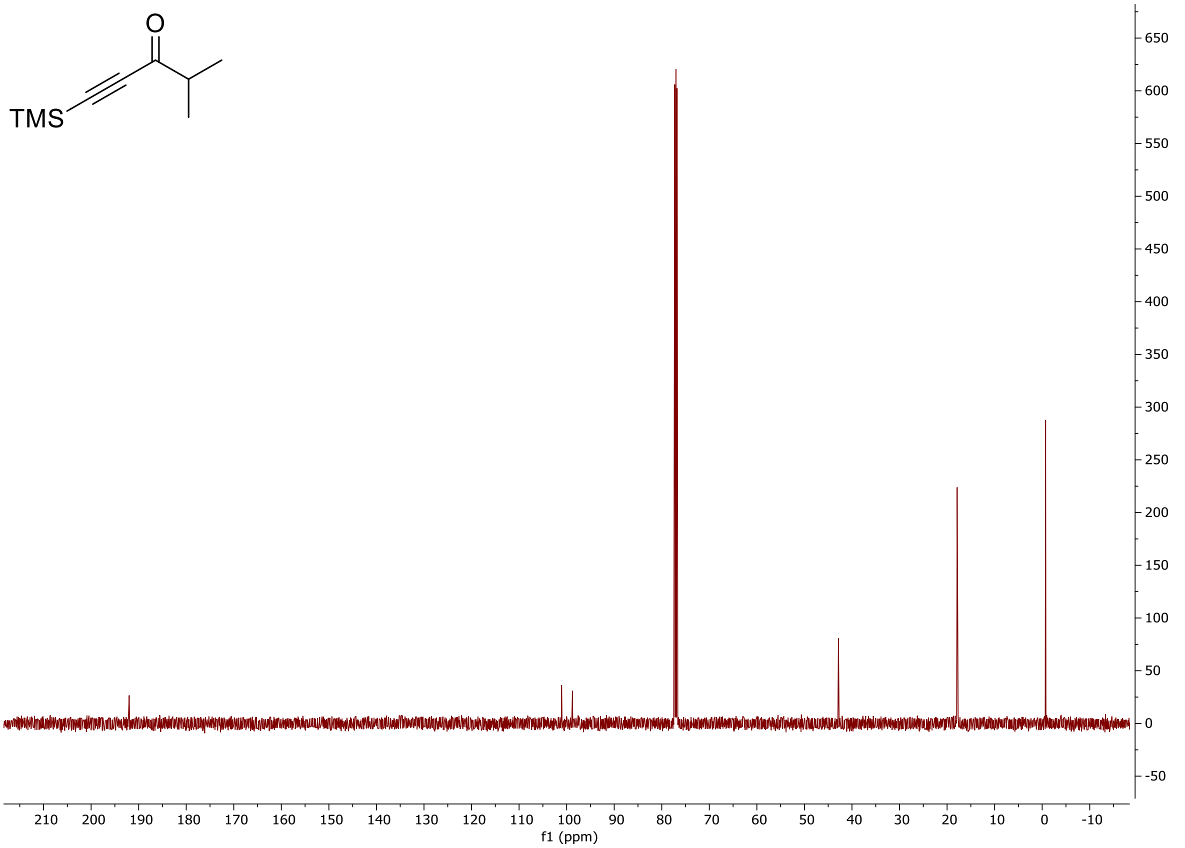
O
TMS
650
600
550
500
450
400
350
300
250
200
150
100
50
0
-50
210 200 190 180 170 160 150 140 130 120 110 100 90 80 70 60 50 40 30 20 10 0 -10
f1 (ppm)

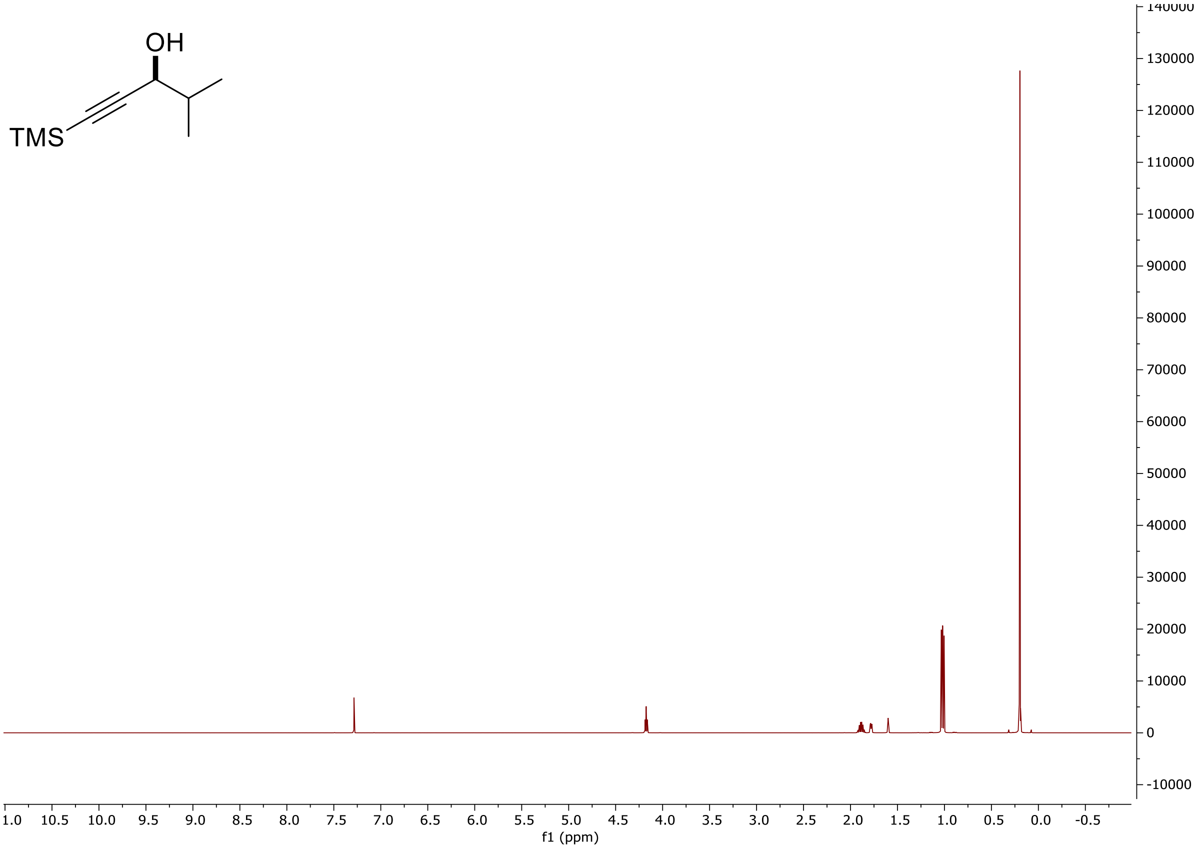
OH
TMS
140000
130000
120000
110000
100000
90000
80000
70000
60000
50000
40000
30000
20000
10000
0
-10000
1.0 10.5 10.0 9.5 9.0 8.5 8.0 7.5 7.0 6.5 6.0 5.5 5.0 4.5 4.0 3.5 3.0 2.5 2.0 1.5 1.0 0.5 0.0 -0.5
f1 (ppm)

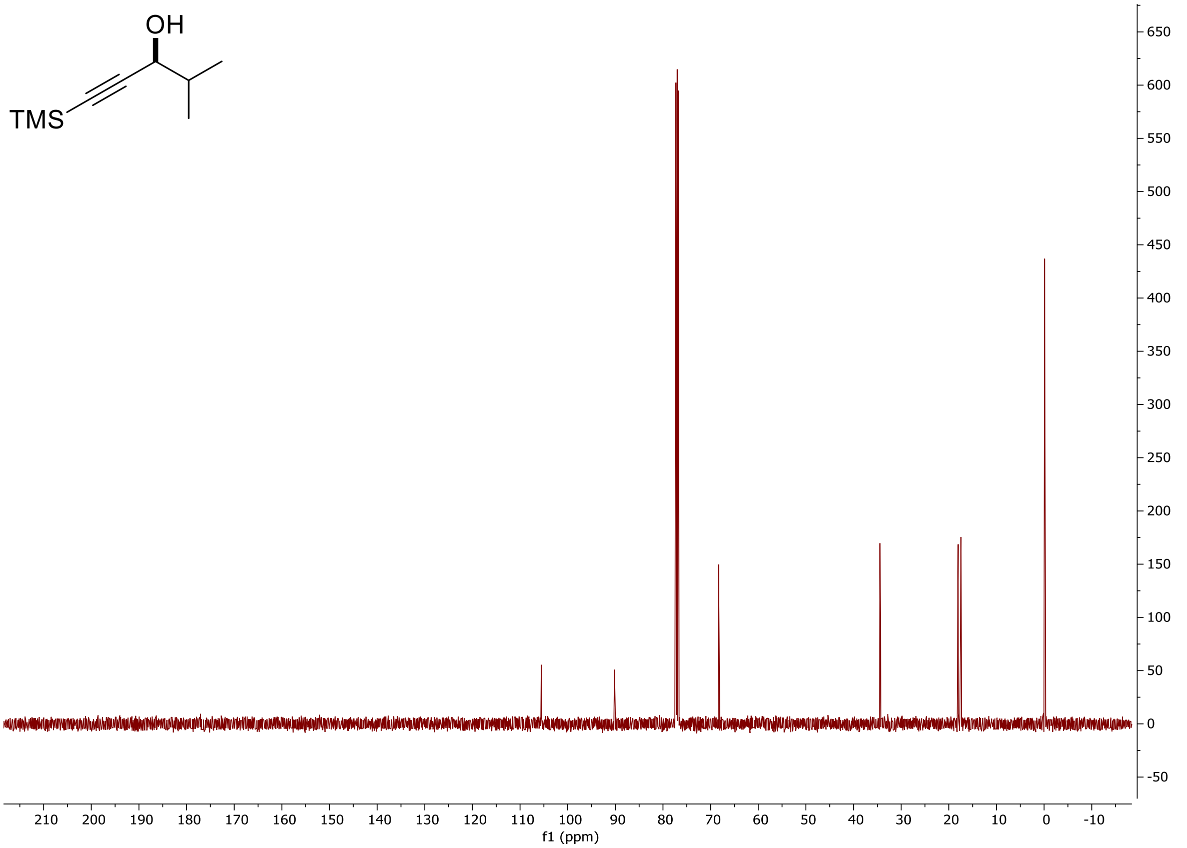

OH
TMS
650
600
550
500
450
400
350
300
250
200
150
100
50
0
-50
210 200 190 180 170 160 150 140 130 120 110 100 90 80 70 60 50 40 30 20 10 0 -10
f1 (ppm)

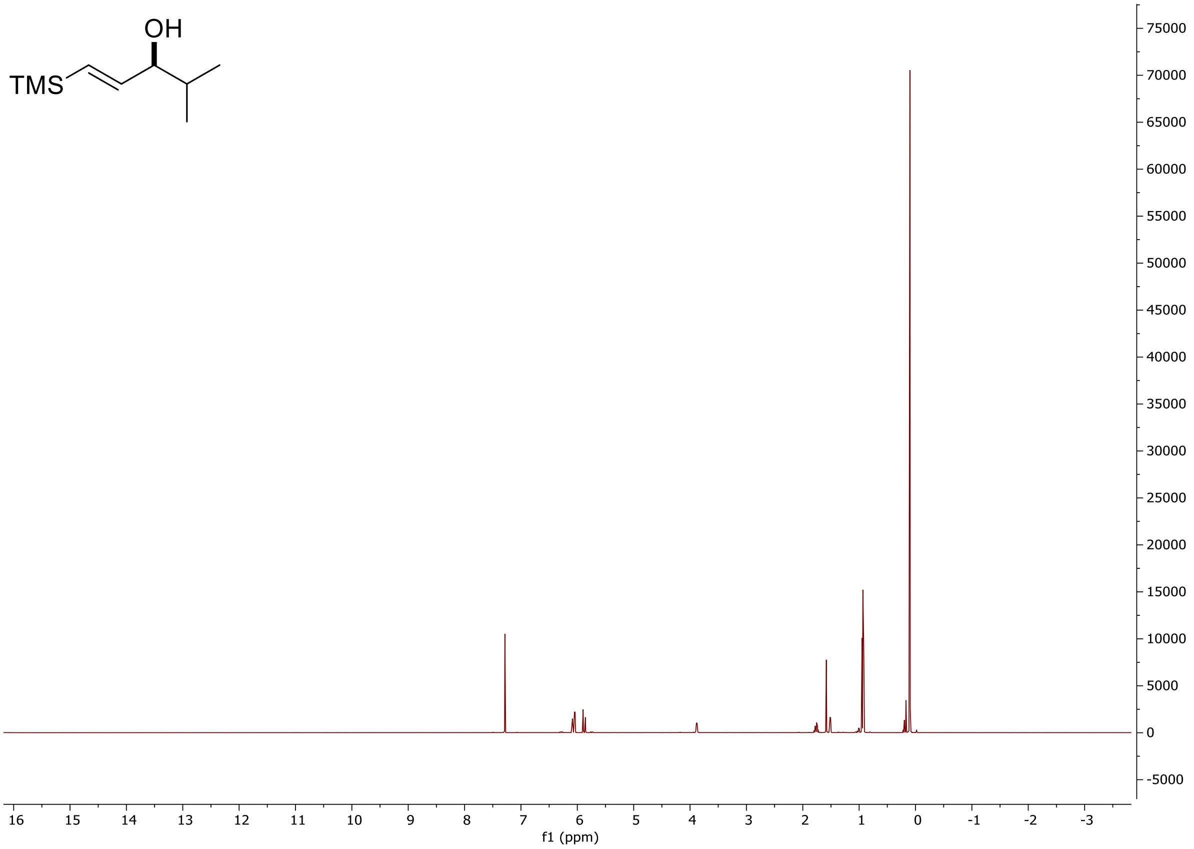

OH
TMS
75000
70000
65000
60000
55000
50000
45000
40000
35000
30000
25000
20000
15000
10000
5000
0
-5000
16 15 14 13 12 11 10 9 8 7 6 5 4 3 2 1 0 -1 -2 -3
f1 (ppm)

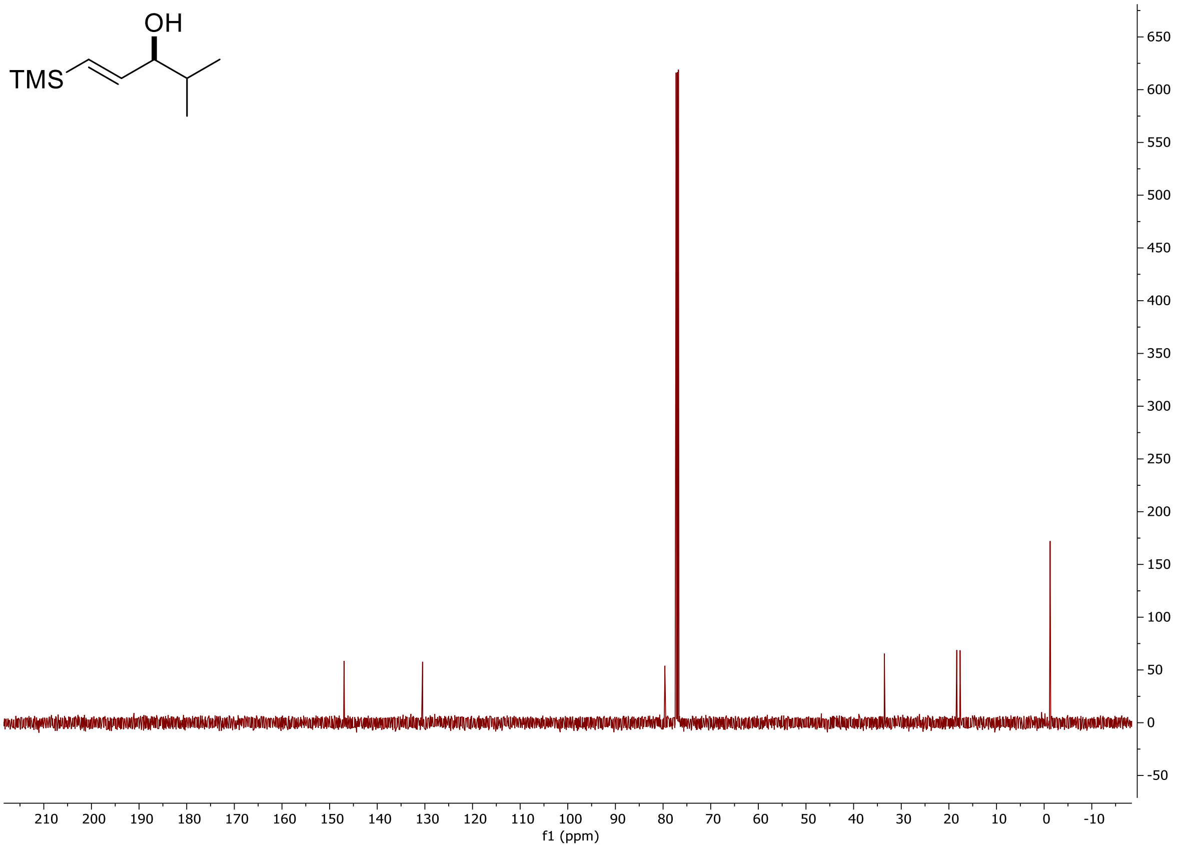
OH
TMS
650
600
550
500
450
400
350
300
250
200
150
100
50
0
-50
210 200 190 180 170 160 150 140 130 120 110 100 90 80 70 60 50 40 30 20 10 0 -10
f1 (ppm)

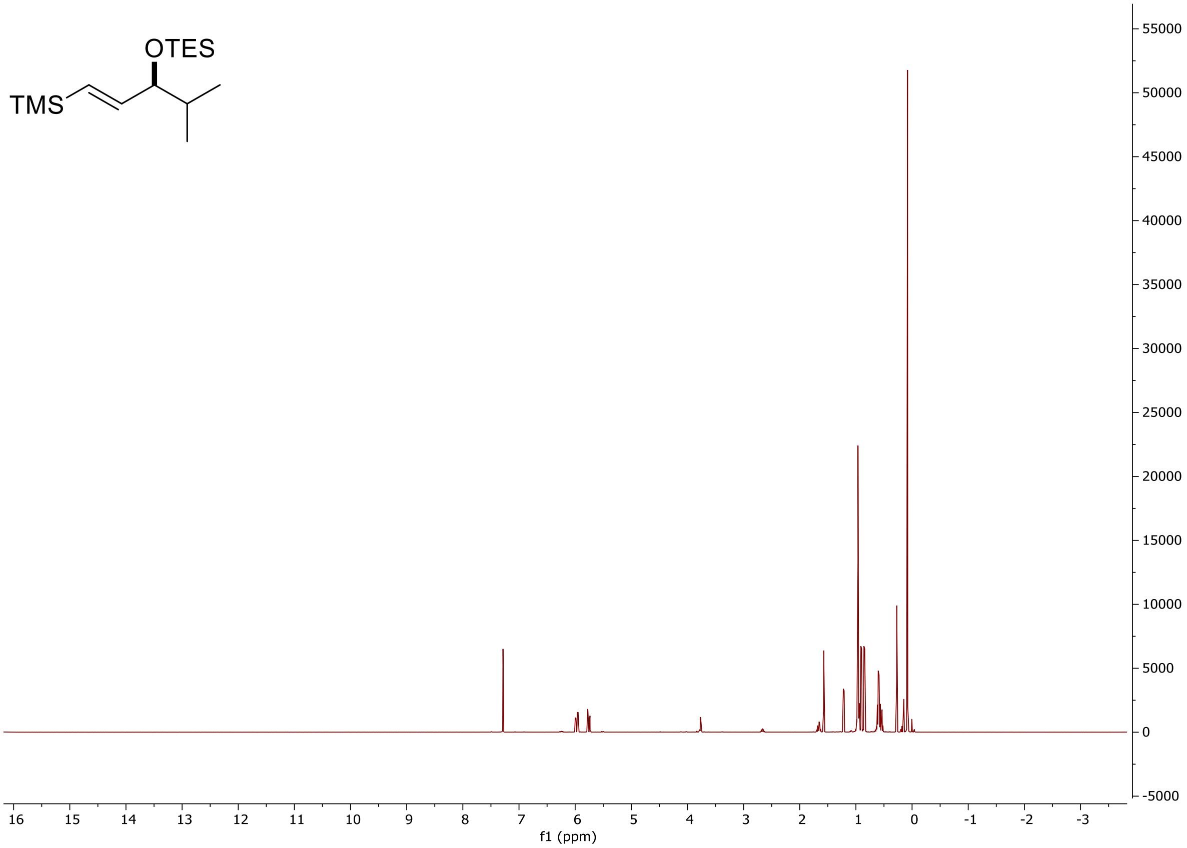
OTES
TMS
55000
50000
45000
40000
35000
30000
25000
20000
15000
10000
5000
0
-5000
16 15 14 13 12 11 10 9 8 7 6 5 4 3 2 1 0 -1 -2 -3
f1 (ppm)

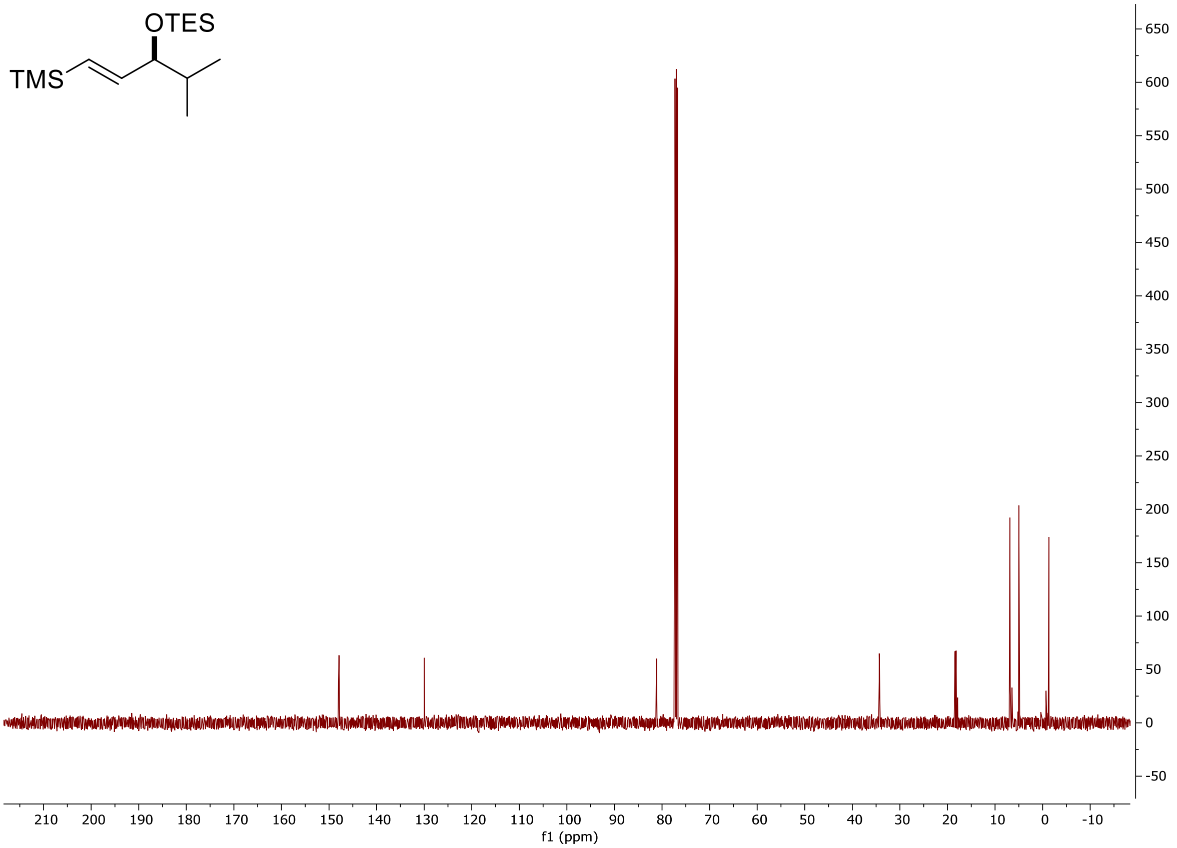
OTES
TMS
650
600
550
500
450
400
350
300
250
200
150
100
50
0
-50
210 200 190 180 170 160 150 140 130 120 110 100 90 80 70 60 50 40 30 20 10 0 -10
f1 (ppm)

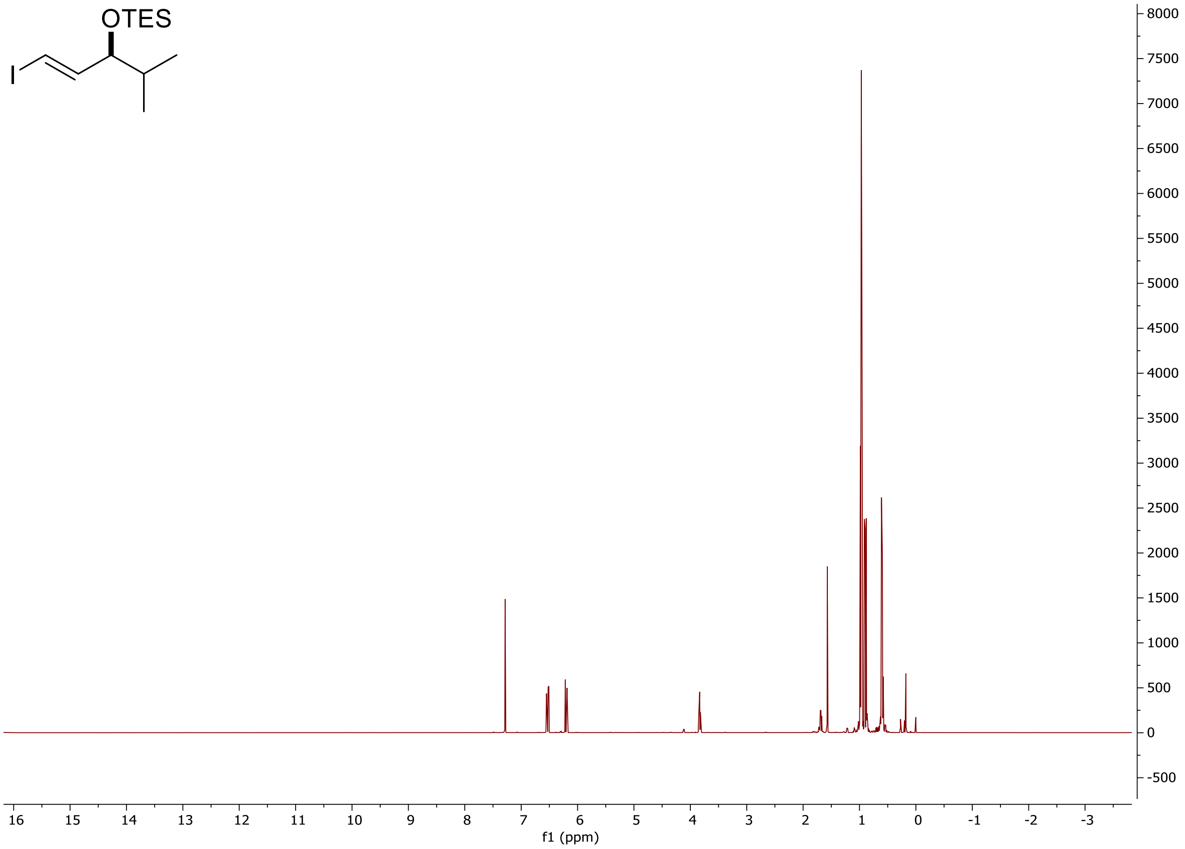
OTES
I
8000
7500
7000
6500
6000
5500
5000
4500
4000
3500
3000
2500
2000
1500
1000
500
0
-500
16 15 14 13 12 11 10 9 8 7 6 5 4 3 2 1 0 -1 -2 -3
f1 (ppm)

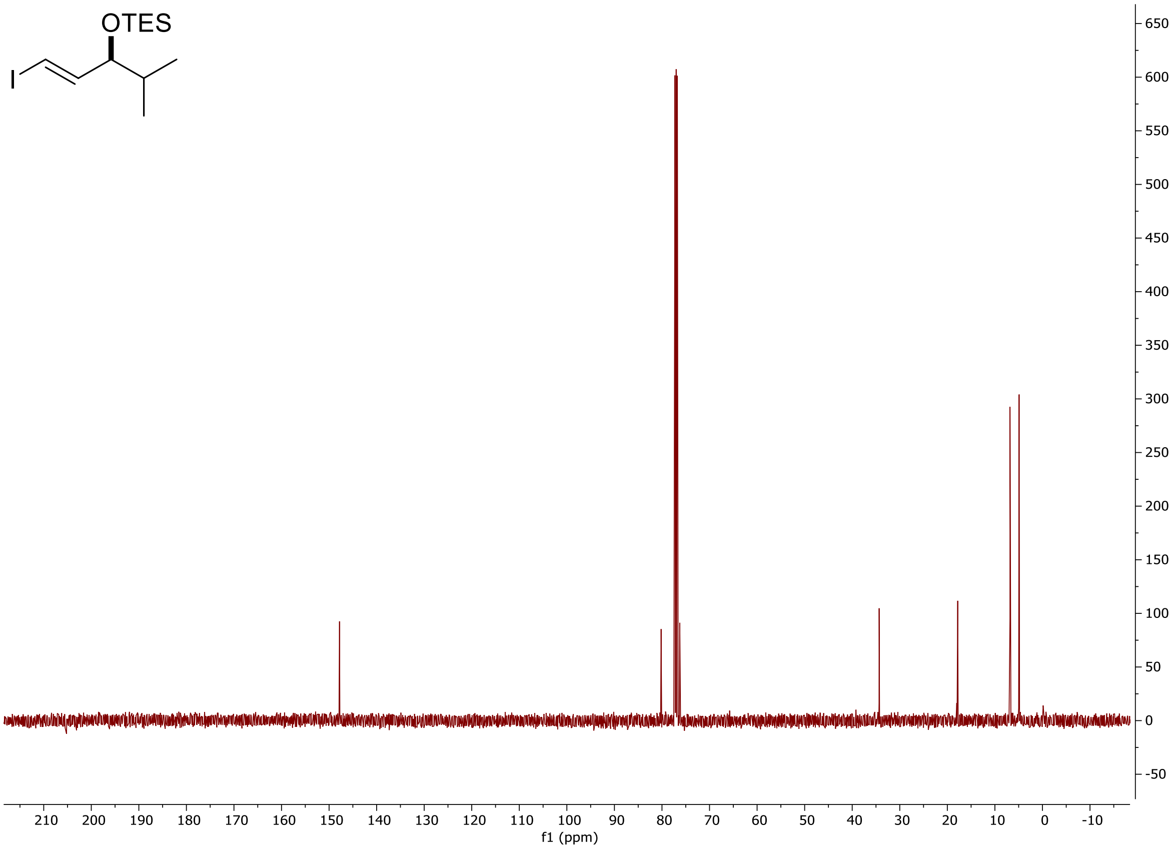
OTES
I
650
600
550
500
450
400
350
300
250
200
150
100
50
0
-50
210
200
190
180
170
160
150
140
130
120
110
100
90
80
70
60
50
40
30
20
10
0
-10
f1 (ppm)

References

Chapter 1:

1. F. Sasse, H. Steinmetz, *J. Antibiot. (Tokyo)* **2003**, *56*, 520-525.

2. G. Höfle, H. Reichenbach, F. Sasse, H. Steinmetz. German Patent DE 41 42 951 C1, df **1993**.

3. D. Menche, J. Hassfeld, H. Steinmetz, *Organic Letters*, **2006**, *8,* 4751-4754.

4. D. Menche, J. Hassfeld, J. Li, S. Rudolph, *J. Am. Chem. Soc.* **2007**, *129*, 6100-6101.

5. P.A. Roethle, I.T. Chen, D. Trauner, *J. Am. Chem. Soc.* **2007**, *129*, 8960-8961.

6. D. Menche, *Eur. J. Org. Chem.* **2007**, 1196-1202.

7. D. Menche, *J. Antibiot.* **2007**, *60,* 328-331.

8. D. Menche, *J. Nat. P.* **2011,** *74*, 1100-1105

9. S. Saroussi, N. Nelson, *J. Exp. Biol.* **2009**, *212*, 1604-1610.

10. Proteolytic Networks in Cancer

11. R.M. Weidmann, A.M. Vollmar, *Cancer Res.* **2012**, *72*, 5976-5987.

12. S.D. Mason, J.A. Joyce, *Trends. Cell. Biol.* **2011**, *21*, 228-237.

13. Kai U. Bindseil, Axel Zeeck, *Eur. J. Org. Chem.* **1994**, *11*, 305-312.

14. M. Perez-Sayans, *Canc. Treat. Rev.* **2009**, *35*, 707-713.

15. D. Mence, S. Bockelmann, *J. Biol. Chem.* **2010**, *285*, 38304-38314.

16. Merk, H., Messer, P., Ardelt, M. A., Lamb, D. C., Zahler, S., Müller, R., Vollmar, A. M.; Pachmayr, J. *Molecular Cancer Therapeutics.* **2017**, *16(11), 2329–2339.*

Chapter 2:

1. D. Menche; J. Hassfeld, *J. Am. Chem. Soc.* **2007**, *129*, 6100-6101.

2. Baker, R.; Castro, J. L. *J.Chem. Soc., Perkin Trans. 1* **1990**, 47.

3. A. Abiko; S. Masamune, *J. Am. Chem. Soc.* **1997**, *119*, 2586.

4. C.J. Cowden; I. Paterson, *Org. React.* **1997**, *51*, 1.

5. W.C. Still; C. Gennari, *Tetrahedron Lett.* **1983**, *24*, 4405.

6. H.C. Brown; S.K. Bhat, *J. Org. Chem.* **1989**, *54*, 1570.

7. E.J. Corey; C.J. Helal, *Angew. Chem., Int. Ed.* **1998**, *37*, 1986.

8. G, Höfle; F. Sasse, German Patent DE 41 42 951 C1, 1993.

9. P.A. Roethle; I.T. Chen; D. Trauner, *J. Am. Chem. Soc.* **2007**, *129*, 8960-8961.

10. B.M. Trost; J.L. Gunzer, *J. Am. Chem. Soc.* **2001**, *123*, 9449-9450.

11. K. Tanino; K. Arakawa, *Tetrahedron Lett.* **2006**, *47*, 861-864.

12. B.m. Trost; F.D. Toste, *Tetrahedron Lett.* **1999**, *40*, 7739-7743.

13. Beaudry, C. M.; Trauner, D. *Org. Lett.* **2002**, *4*, 2221-2224.

14. Schmidt, U.; Gleich, P.; Griesser, H.; Utz, R. *Synthesis* **1986**, *12*, 992-998.

15. D. Menche, *J. Nat. P.* **2011,** *74*, 1100-1105.

16. Y. Kita; H. Maeda, *Synlett* **1993**, *1*, 273-274.

17. Inanaga, J.; Hirata, K.; Saeki, H.; Katsuki, T.; Yamaguchi, M. *Bull. Chem. Soc. Jpn.* **1979**, 52, 1989-1993.

18. L.S. Liebeskind; C. Wang, *J. Org. Chem.* **1994**, *59*, 5905-5911.

19. D. Menche, *J. Antibiot.* **2007**, *60*, 328-331.

20. E. Negishi; Z. Huang, *J. Am. Chem. Soc.* **2007**, *129*, 14788-14792.

21. Menche, D., Hassfeld, J., Li, J., Mayer, K., & Rudolph, S. (**2009**). *The Journal of Organic Chemistry, 74(19), 7220–7229.*

22. Horstmann, N., Essig, S., Bockelmann, S., Wieczorek, H., Huss, M., Sasse, F., & Menche, D. (**2011**). *Journal of Natural Products, 74(5), 1100–1105.*

23. For an example of how simplification from a synthesis standpoint leads to valuable SAR information, see the following article about devazepide, simplified from asperlicin: J. Carillo, N Agra, *Anticancer Drugs*, **2009**, *7*, 527-533.

24. Cram, D. J.; Kopecky, K. R. *J. Am. Chem. Soc*. **1959**, 81, 2748. (b) Reetz, M. T. *Acc. Chem. Res*. **1993**, 26, 462.

25. Hudrlik, P. F.; Peterson, D. *J. Am. Chem. Soc.* **1979**, *97*, 1464

26. J-A. Funel and J. Prunet, *J. Org. Chem*., **2004**, 69, 4555.

27. (a) W. S. Wadsworth, Jr., *Org. React*., **1977**, 25, 73; (b) J. Boutagy and R. Thomas, *Chem. Rev*., **1974**, 74, 87; (c) B. E. Maryanoff and A. B. Reitz, *Chem. Rev*., **1989**, 89, 863; (d) S. E. Kelly, *In Comprehensive Organic Synthesis*, B. M. Trost and I. Fleming Ed., Pergamon, Oxford, **1991**, Vol. 1, pp. 729–817.

28. A. K. Mandal, J. S. Schneekloth, K. Kuramochi and C. M. Crews, *Org. Lett*., **2006**, 8, 427.

29. D. B. Dess and J. C. Martin, *J. Org. Chem*., **1983**, 48, 4155.

30. O. Muller, E. Moulin, C. Nevado, J. Gagnepain, G. Kelter, F. Heinz-Helbert and A. Furstner, *Tetrahedron,* **2010**, 66, 6421–6428.

31. Review: E. J. Corey and C. Helal, *Angew. Chem., Int. Ed.,* **1998**, 37, 1986.

32. (a) M. Cherest, H. Felkin and N. Prudent, *Tetrahedron Lett.*, **1968**, 9, 2199; (b) M. Cherest and H. Felkin, *Tetrahedron Lett*., **1968**, 9, 2205.

33. Swick, S. M.; Schaefer, S. L.; O'Neil, G. W. *Tetrahedron Lett*. **2015**, 56, 4039–4042.

34. Swick, S. M., Schaefer, S. L., & O'Neil, G. W. (**2015**). *Tetrahedron letters*, *56*(26), 4039–4042.

35. Drouet, K.E.; Theodorakis, E. A. *J. Am. Chem. Soc.* **1999** (121) 456.

36. Dineen, T. A.; Roush, W. R. *Org. Lett*. **2004**, 6, 1523.

37. Fürstner, A.; Funel, J.-A.; Tremblay, M.; Bouchez, L. C.; Nevado, C.; Waser, M.; Ackerstaff, J.; Stimson, C. *Chem. Commun.* **2008**, 2873.

38. O'Neil, Gregory & M. Craig, Alexander & R. Williams, John & Young, Jeffery & Spiegel, Paul. **2017** *Synlett*. 28.

39. Reker, D.; Perna, A. M.; Rodrigues, T.; Schneider, P.; Reutlinger, M.; Mönch, B.; Koeberle, A.; Lamers, C.; Gabler, M.; Steinmetz, H.; Müller, R.; Schubert-Zsilavecz, M.; Werz, O.; Schneider, G. *Nat. Chem.* **2014**, 6, 1072.

40. Zarghi, A.; Arfaei, S.; *Iranian Journal of Pharmaceutical Research* (**2011**), 10 (4): 655-683.

Chapter 3:

1. N. Miyaura, A. Suzuki, J. Chem. Soc. *Chem. Commun*. **1979**, 866.

2. N. Miyaura, A. Suzuki, K. Yamada, *Tetrahedron Lett*. **1979**, 20,3437.

3. Hooshmand, S. E., hiedari, bahreh, Sedghi, R., & Varma, R. S. (**2018**). *Green Chemistry.*

4. Taheri Kal Koshvandi, A, Heravi, MM, Momeni, T. *Appl Organometal Chem*. **2018**, *32,* 4210.

5. Johansson Seechurn, C. C. C., Kitching, M. O., Colacot, T. J., & Snieckus, V. (**2012**). *Angewandte Chemie International Edition*, 51(21), 5062–5085.

6. Brown, D. G., & Boström, J. (**2015**). *Journal of Medicinal Chemistry*, 59(10), 4443–4458.

7. Taheri Kal Koshvandi, A, Heravi, MM, Momeni, T. Current Applications of Suzuki–Miyaura Coupling Reaction in The Total Synthesis of Natural Products: An update. *Appl Organometal Chem*. **2018**, *32*, 4210.

8. Lloyd-Jones, G. C.; Lennox, A. J. J. *Chem. Soc. Rev.*, **2014**, 43, 412.

9. McCluskey, A.; Holdsworth, C.; Zayas, H.; Bowyer, M.; Gordon, C.; *Tetrahedron Letters*. **2009**, *50***,** 5894-5895

10. B. Karimi, F. Mansouri and H. Vali, *Green Chem*., **2014**, 16, 2587–2596.

11. Miyaura, N., & Suzuki, A. (**1995**). *Chemical Reviews, 95(7), 2457–2483.*

12. H. Toya, T. Satoh, K. Okano, K. Takasu, M. Ihara, A. Takahashi, H. Tanaka, H. Tokuyama, *Tetrahedron* **2014**, 70, 8129.

13. Menche, D.; Irschik, H.; Sasse, F.; Raja, A.; Altendorfer, M. *Org. Biomol. Chem.*, **2013**, *11*, 2116.

14. Still, W. C.; Gennari, C. *Tetrahedron Lett*. **1983**, 24, 4405.

15. Sakai, T.; Blanchette, M.; Choy, W.; Davis, J.; Essenfeld, A.; Masamune, S.; Roush, W. *Tetrahedron Letters*, **1984**, *25*, 2183-2186.

16. Endo, K.; Hirokami, M.; Shibata, T. *J. Org. Chem*. **2010**, 75, 3469.

17. Morken, J.; Zhang, L.; Coombs, J.; *Org. Lett*. **2015**, *17*, 1708−1711.